

UNCLASSIFIED

AD **428905**

DEFENSE DOCUMENTATION CENTER

FOR

SCIENTIFIC AND TECHNICAL INFORMATION

CAMERON STATION, ALEXANDRIA, VIRGINIA



UNCLASSIFIED

NOTICE: When government or other drawings, specifications or other data are used for any purpose other than in connection with a definitely related government procurement operation, the U. S. Government thereby incurs no responsibility, nor any obligation whatsoever; and the fact that the Government may have formulated, furnished, or in any way supplied the said drawings, specifications, or other data is not to be regarded by implication or otherwise as in any manner licensing the holder or any other person or corporation, or conveying any rights or permission to manufacture, use or sell any patented invention that may in any way be related thereto.

⑤ 691300

14



THE PENNSYLVANIA STATE UNIVERSITY  
INSTITUTE FOR SCIENCE & ENGINEERING  
UNIVERSITY PARK, PENNSYLVANIA

AD No. \_\_\_\_\_  
DDC FILE COPY

428905

## Solid Glass and Ceramic External-Pressure Vessels

January 15, 1964

SERIAL NO. NOW 63-0209-c-2 ✓



Copy No. 23

NAVY DEPARTMENT • BUREAU OF NAVAL WEAPONS • CONTRACT NOW 63-0209-c

\$ 7.60

(3) 671300

*Upper Case*

(6) Solid Glass and Ceramic External-Pressure Vessels,

(10) By J. D. Stachiw.

The Pennsylvania State University  
Institute for Science & Engineering  
ORDNANCE RESEARCH LABORATORY  
University Park, Pennsylvania

(11) January 15, 1964,

APPROVED FOR DISTRIBUTION

*Lance L. Keph.*

ASSISTANT DIRECTOR

APPROVED FOR DISTRIBUTION

*John C. Johnson*

DIRECTOR

(15) Contract

SERIAL NO. NOW 33-0209-C-2

## Distribution List


Chief, Bureau of Naval Weapons (RU-2) Department of the Navy Washington 25, D. C.	1 copy	Commander U. S. Naval Ordnance Laboratory White Oak Silver Spring 19, Maryland Attn: Dr. S. J. Raff	1 copy
Chief, Bureau of Naval Weapons (RUTO-33) Department of the Navy Washington 25, D. C.	2 copies	Commander U. S. Naval Ordnance Test Station 3202 East Foothill Boulevard Pasadena Annex Pasadena 8, California	2 copies
Chief, Bureau of Naval Weapons (RUDC) Department of the Navy Washington 25, D. C.	1 copy	Commanding Officer U. S. Naval Underwater Ordnance Station Newport, Rhode Island	2 copies
Chief, Bureau of Naval Weapons (RUSD) Department of the Navy Washington 25, D. C.	1 copy	Commanding Officer U. S. Naval Torpedo Station Keyport, Washington	1 copy
Chief, Bureau of Naval Weapons (DL1-3) Department of the Navy Washington 25, D. C.	2 copies	Commanding Officer U. S. Naval Torpedo Station Quality Evaluation Technical Library Keyport, Washington	1 copy
Chief, Naval Operations (OP 721) Department of the Navy Washington 25, D. C. For: IEP ABC 28	5 copies	Officer in Charge U. S. Naval Underwater Weapons Systems Engineering Center Newport, Rhode Island	1 copy
Chief, Naval Operations (OP 31) Department of the Navy Washington 25, D. C.	1 copy	Director (Code 2021) U. S. Naval Research Laboratory Washington 25, D. C.	3 copies
Chief, Naval Operations (OP 312) Department of the Navy Washington 25, D. C.	1 copy	Director (Code 2027) U. S. Naval Research Laboratory Washington 25, D. C.	1 copy
Chief, Naval Operations (OP 71) Department of the Navy Washington 25, D. C.	1 copy	Commanding Officer and Director U. S. Navy Electronics Laboratory San Diego 52, California	1 copy
Chief, Naval Operations (O3EG) Department of the Navy Washington 25, D. C.	1 copy	Commanding Officer and Director David Taylor Model Basin Washington 7, D. C.	1 copy
Chief, Naval Operations (OPO7TC) Technical Analysis and Advisory Group Rm5E613, Pentagon Washington 25, D. C.	1 copy	Commanding Officer U. S. Navy Mine Defense Laboratory Panama City, Florida	1 copy
Chief, Naval Operations (OPO9B5) Department of the Navy Washington 25, D. C.	1 copy	Commanding Officer and Director U. S. Navy Underwater Sound Laboratory Fort Trumbull New London, Connecticut	1 copy
Chief, Bureau of Ships Department of the Navy Washington 25, D. C.	3 copies	Commander U. S. Naval Missile Center Point Mugu Port Hueneme, California	1 copy
Commander Defense Documentation Center Attention TIPDR Cameron Station Alexandria, Virginia 22314	10 copies	Officer in Charge Naval Aircraft Torpedo Unit Naval Air Station Quonset Point, Rhode Island	1 copy
Commander U. S. Naval Ordnance Laboratory White Oak Silver Spring 19, Maryland	2 copies		

Commander U. S. Naval Air Development Center Johnsville, Pennsylvania	1 copy	Commander, Test and Evaluation Force U. S. Atlantic Fleet U. S. Naval Base Norfolk 11, Virginia	1 copy
Hudson Laboratories Dobbs Ferry, New York	1 copy	Vitro Corporation of America 14,000 Georgia Avenue Silver Spring, Maryland	1 copy
Scientific and Technical Information Facility P. O. Box 5700 Bethesda, Maryland Attn: NASA Representative (S-AK/DL)	1 copy	Westinghouse Electric Corporation Landsdowne Plant Baltimore, Maryland	1 copy
Director, Applied Physics Laboratory University of Washington Seattle, Washington	2 copies	Woods Hole Oceanographic Institution Woods Hole, Massachusetts	1 copy
Director, Marine Physical Laboratory Scripps Institution of Oceanography San Diego 52, California	1 copy	Aerojet General Corporation Azusa, California Attn: G. M. McRoberts	1 copy
Clevite Ordnance 540 East 105th Street Cleveland, Ohio	1 copy	Institute for Defense Analyses 1666 Connecticut Avenue, N. W. Washington 9, D. C.	1 copy



### Abstract

**SOLID** glass or ceramic hulls provide the maximum buoyancy and internal useful volume for underwater vehicles. This material displays low creep characteristics and withstands external pressure cycling and mild underwater dynamic pressures. Scratches on the exterior surfaces do not decrease appreciably the compressive and elastic strength of such vessels when exposed to either static or cycling pressure. Connectors have been devised that enable glass cylinders to be joined into a monolithic structure that is resistant to both pressure and flexure.



*a-*

## Table of Contents

Solid Glass and Ceramic External-Pressure Vessels	.	.	1
Introduction	.	.	1
The Test Models	.	.	2
The Tests	.	.	4
Evaluation of Test Results	.	.	5
Summary	.	.	6
Appendix	.	.	7
A. Uses of Glass for Pressure-Vessel Construction	.	.	7
B. Experimental Data	.	.	9
References	.	.	11
Illustrations	.	.	Following the colored divider



## Solid Glass and Ceramic External-Pressure Vessels

### Introduction

IN THE quest for construction materials with high compressive-strength-to-weight ratios, glass and ceramics show great promise. Although these materials have been used for several thousand years, their application has been limited largely to items such as jewelry, bottles, jars, windows, lenses, mirrors, prisms, and drinking glasses. Only very recently has their use been extended to laboratory ware, oven-proof kitchenware, and structural brick. Now, because of the demands of aerospace and hydrospace, the astounding mechanical properties of glass and ceramics are being utilized.

These materials are characterized primarily by their hardness and brittleness - only a few precious stones excel them in hardness; and very few materials, if any, exceed them in brittleness. But beyond this superficial characterization of their mechanical properties are many unique properties (1,2).\*

The properties that make glass and ceramics valuable for structural uses are: compressive strength in excess of 300,000 psi (see Table I); tensile strength in excess of 100,000 psi (for finely drawn fibers); densities ranging between 0.08 and 0.15 lb per cu in.; moduli of elasticity varying from  $8 \times 10^6$  to  $50 \times 10^6$ ; linear elastic behavior; impermeability to water; heat conductivity of 7 to 600 Btu/h/sq ft/deg F/in.; thermal expansion rates of  $6 \times 10^{-7}$  to  $75 \times 10^{-7}$  per deg F; and working temperatures in excess of 1000 deg F. The properties that make the design of glass and ceramic structures difficult are: low tensile strengths of 10,000 to 50,000 psi and flexural strengths of 15,000 to 75,000 psi for cross sections larger than a fiber; decrease of tensile and flexural strength with the duration of loading; extreme sensitivity to imperfections on surfaces under tension; and low resistance to mechanical shock.

When competing with metals and plastics for application in structures that are primarily loaded in tension or in bending, the glass and ceramic structural members (except for extremely fine fibers) are at a disadvantage because of their low tensile and flexural strengths, which decrease with time under load. However, in structures that are subjected primarily to compressive loads (such as external-pressure vessels), glass and ceramics show a favorable comparison (Fig. 1).\*\*

As a logical first step in this research program, a literature search was made of the various ways in which glass has been used in external-pressure vessels (in forms other than solid). These uses are described in Section A of the Appendix.

Only recently has serious thought - H. A. Perry (3) at the U. S. Naval Ordnance Laboratory and C. L. Key at the Ordnance Research Laboratory - been given to the use of solid glass construction for external-pressure vessels. The brittleness of the material and the absence of any need to penetrate abyssal depths of the oceans made its use questionable; however, recent interest in the mysteries of the ocean depths and the resultant need for high-strength, low-weight, external-pressure vessels have brought attention to solid glass and ceramics. Before any design of solid glass or ceramic vessels could be contemplated, a pilot experimental program had to be instituted to answer questions concerning the design of external-pressure vessels:

1. Are the elastic stability formulas for metallic vessels under external hydrostatic pressure applicable to glass and ceramic shells?

\* Numbers in parentheses refer to References on last numbered page of this report.

\*\*Illustrations will be found at the end of the report, following the colored divider.

TABLE I  
COMPRESSIVE-STRENGTH-TO-WEIGHT RATIO  
OF SEVERAL GLASS AND CERAMIC MATERIALS

Material	Ratio (psi/lb/cu in.)
Solid glasses and ceramics	1,500,000 to 4,000,000
Fiber-glass-and-epoxy laminates	600,000 to 2,000,000
Fiber-glass- or flake-glass-and-epoxy laminates	400,500 to 900,000
Rod-glass-and-cast-aluminum composites	400,000 to 800,500
Sphere-glass-and-epoxy composites	200,500 to 700,000
Sphere-glass-and-cast-aluminum composites	200,000 to 300,500

2. Do stress raisers (such as the sharp fillets at the roots of stiffeners), when located only in areas where compressive stresses occur, cause a measurable decrease in the implosion strength of the vessel?

3. Is there any measurable creep of the material when the vessel is subjected to high compressive biaxial stress for short periods of time?

4. How resistant are glass and ceramic vessels to underwater hydrodynamic shock generated by explosives detonated near the vessel?

5. What decrease in the implosion pressure of the vessel can be expected if it is subjected to external-pressure cycles that induce fatigue stresses in the material?

6. What is the actual biaxial compressive strength of some representative glass and ceramics, such as Pyroceram 9606, Pyrex, and 99 per cent alumina oxide ceramic?

7. Can pressure hulls for large underwater vehicles be fabricated from small structural components without recourse to welding or bonding and yet retain the elastic stability and strength inherent to monolithic shells?

8. How can brittle glass and ceramic shells be prevented from fracturing as a result of impacts?

For at least tentative answers to these questions, the author designed glass, ceramic, and plastic vessels for implosion and impact testing. The design, fabrication, and testing of these vessels is described in this report. Capital letters are used to identify the test models, and numerical subscripts are used to differentiate between models of identical design and material.

## The Test Models

### STABILITY THEORY

To determine the applicability of stability theories to glass and ceramic pressure vessels and to determine their creep, fatigue strength, and resistance to underwater shock, a series of rib-stiffened Pyroceram and alumina oxide cylinders were designed. The conventional design theories of R. von Mises and Kendrick were followed to design cylinders with an 8-in. outer diameter for critical hydrostatic pressures above 10,000 psi. Since present fabrication methods had to be utilized, the ratio of wall thickness to diameter had to be kept above 0.015 for Pyroceram cylinders and 0.035 for alumina oxide cylinders. The four Pyroceram cylinders were designed with both three

stiffening ribs (Models  $I_1$  and  $I_2$ ) with 14,000-psi critical pressure (Figs. 2 and 3), and with five stiffening ribs (Models  $J_1$  and  $J_2$ ) with 10,000-psi critical pressure (Figs. 4 and 5). The three alumina cylinders, Models  $K_1$ ,  $K_2$ , and  $K_3$  (Figs. 6 and 7), had two stiffening ribs and a 10,000-psi critical pressure. Except for the difference in length between the Pyroceram and alumina oxide cylinders, the major difference was that the alumina shells had small fillet radii and the Pyroceram shells had large radii.

#### UNDERWATER SHOCK

A series of high-strength aluminum cylinders were made to provide a yardstick with which to compare the underwater-shock resistance of glass and ceramics. The dimensions of the high-strength aluminum cylinders, Models  $L_1$  and  $L_2$  (Figs. 8 and 9), with a 2400-psi critical design pressure were identical to alumina oxide Model  $K$ ; whereas the aluminum cylinders, Models  $M_1$  and  $M_2$ , with a 4500-psi critical design pressure (Fig. 10) were identical (dimensionally) to Pyroceram cylinder Model  $I$ .

#### COMPRESSIVE STRENGTH

Hollow spheres (Fig. 11) were used to determine the ultimate biaxial compressive strength of glass and ceramics. These spheres consisted of two hemispheres bonded together with epoxy resin. The ratio of wall thickness to diameter was such that failure resulting from elastic instability could not occur at hydrostatic pressures below 100,000 psi - the operating pressure of the hydrostatic testing tank. The hollow spheres were selected for the determination of the compressive strength of the material because only in the spherical shell is it possible to obtain uniform distribution of pure, biaxial compressive stress.

#### SURFACE COATINGS

To evaluate various surface coatings for protecting glass or ceramics from shock, 4-in.-OD Pyrex and alumina ceramic tubes were first coated and then fractured using a simple pendulum as an impact generator. Pendulum weights of 1, 5, and 9 lb were used. The kinetic energy or velocity of the pendulum provided a comparison of the effectiveness of coatings. Some shock tests were also performed on coated and uncoated Pyroceram hemispheres (Fig. 12) by subjecting them to impacts with a 1/2-lb ball. A detailed description of these tests is presented in ref. 4.

#### STRUCTURAL SEAMS

The experimental study of structural seams for spherical and cylindrical pressure vessels was limited to models made of acrylic resin because of its availability. Beveled, longitudinal staves were used in the construction of Model  $JC$  cylinders (Fig. 13a), and spherical polygons were used in the construction of Model  $JS$  spheres (Fig. 14b). The yardstick of comparison was the static collapse pressure, under hydrostatic loading, of the monolithic Models  $MC$  (Fig. 13b) and  $MS$  (Fig. 14a).

#### JOINTS

An investigation was conducted to determine whether the joints used to connect metallic cylinders were adequate for glass and ceramic shells that, although possessing very high compressive strength, have very low tensile and shear strengths. The external Marman clamp, the internal Marman clamp, and the interrupted-screw breech-type lock were evaluated. The external Marman clamp and the breech-type lock were tested on glass Models  $XXX$  and  $XXX_2$  (Figs. 15 through 21);

the internal Marman clamp was tested on acrylic resin Model IMC (Figs. 22 and 23). The three types of joint fasteners were evaluated by their ability to withstand external hydrostatic pressure and bending moments applied across the two halves of the models.

## The Tests

### STATIC PRESSURE

Static-pressure tests of the glass and ceramic models were performed at the Southwest Research Institute and the Naval Ordnance Laboratory. The spherical models were placed in an oil-filled tank, the tank was sealed, and the hydrostatic pressure was raised until the model imploded. The open ends of the cylindrical models were sealed with two flat aluminum plates connected by tie rods; thus, the ends of the shells were free to contract during the application of external pressure. No gaskets were used between the end plates and the shells; sealing was accomplished by a layer of heavy grease. The hydrostatic pressure was increased at a rate of approximately 1000 psi per min. At designated intervals, the pressure was held constant during the reading of strains on the automatic Gilmore strain recorder.

To determine creep characteristics, the pressure was raised slowly, until a given external pressure was reached. This pressure was maintained for a prolonged period, and strain was measured at regular intervals.

### FATIGUE

For the fatigue test, the pressure was cycled rapidly between a pressure of 100 psi and a pressure equal to 80, 85, or 90 per cent of the nominal static critical pressure. The pressure cycles were continued for either a fixed number of cycles or until implosion occurred. No strain measurements were made during the fatigue tests.

### FLEXURE

For the flexure test of joints, the joined sections were subjected to four-point loading and kept under load for several minutes. For application of forces, nylon ribs were employed. The hydrostatic-pressure tests of the joints were conducted in the same manner as the implosion tests; however no strains were recorded and, since all models were equipped with integral hemispherical ends, no end plates were required.

### UNDERWATER SHOCK

The underwater-shock tests were of two types: low-static-pressure shock tests and high-static-pressure shock tests. Both types of tests were performed in tanks completely filled with water. For the low-static-pressure shock tests, static pressure was provided by a 5-ft head of water. For the high-static-pressure tests, the hydrostatic pressure was 50 per cent of the static critical pressure for each model. Shock loads were produced by Pentolite explosive mounted at varying distances below the center of the shell. The distance between the explosive and the shell was decreased until the brittle vessels were fractured or until large-scale plastic deflection occurred in the ductile models. For the underwater-shock tests, water was used for the pressurizing medium; all other tests were conducted in oil. In all tests, resistance strain gages, Type BLH-AFX-7, were mounted on the inside of the shells.

## Evaluation of Test Results

On the basis of the test results, which are listed in Section B of the Appendix, it can be concluded that:

1. The elastic-shell-stability and elastic-strain-distribution formulas for metallic external-pressure vessels are also applicable to solid Pyroceram and alumina oxide vessels.

2. Stress raisers such as sharp radii at the root of stiffeners and deep scratches on surfaces, if located in areas where only resultant compressive stresses occur, cause no significant decrease in the stability or compressive strength of the solid Pyroceram or alumina oxide ceramic vessels when subjected to external hydrostatic pressure.

3. The fatigue strength of solid Pyroceram shells is very high; no failure occurred when the material was cycled over a range of compressive stresses extending from approximately 1000 to 180,000 psi for 3000 cycles. However, the areas stressed to a compressive fatigue stress of 180,000 psi for 3000 cycles showed some signs of deterioration: flaking of the external shell surface at mid-bays (Figs. 24 and 25); and flaking of the internal shell surface at the stiffeners (Figs. 26 and 27).

4. The resistance of the Pyroceram and alumina oxide ceramic vessels to underwater shock waves, when tested at an ambient pressure of 3 to 5 psi, was several orders of magnitude less than that of 7075-T6 aluminum shells with identical dimensions (Table II); and alumina ceramic was found to be less shock resistant than Pyroceram. The resistance of Pyroceram to underwater shock waves seemed to increase with an increase in the ambient pressure, whereas that of the 7075-T6 aluminum markedly decreased (Table II). The limited number of alumina ceramic models precluded the possibility of determining whether their shock resistance increases with an increase in ambient pressure; however, since alumina ceramic is much like Pyroceram, it can be postulated with considerable certainty that the shock resistance of alumina ceramic also increases with increasing ambient hydrostatic pressure. To summarize: when comparing the resistance to underwater shock of 7075-T6 aluminum external-pressure vessels to that of identical Pyroceram vessels on the basis of dynamic pressure required to collapse them (Table II) at the ocean surface, Pyroceram vessels are considerably less resistant to underwater shock waves than aluminum vessels; but, as the depth increases, the Pyroceram vessels become more shock resistant, whereas the aluminum vessels become less shock resistant.

5. Over 30-min periods, the test models have shown very little creep when subjected to hydrostatic pressure great enough to produce a compressive stress of 150,000 psi.

6. At implosion, the maximum compressive stresses in the spherical models were 364,000 psi for Pyroceram, 368,000 psi for alumina oxide ceramic, and 152,000 psi for Pyrex. These

TABLE II  
EFFECT OF IMMERSION DEPTH ON THE DYNAMIC-PRESSURE  
RESISTANCE OF PYROCERAM AND ALUMINUM MODELS

Material	Model	Immersion Depth (ft)	Dynamic Pressure (psi)	Extent of Failure
Pyroceram	I <sub>1</sub>	0	11,000	Complete
	I <sub>2</sub>	13,000	22,500	Complete
Aluminum	M <sub>1</sub>	0	31,000	11 per cent damage
	M <sub>2</sub>	5000	31,000	45 per cent damage

stresses do not indicate, necessarily, the maximum compressive strength of the material because failure could have been initiated by imperfect matching of joint surfaces between individual hemispheres.

7. The elastic stability and compressive strength of segmented cylinders and spherical shells assembled with taped rather than bonded seams (Figs. 13a and 14b) are identical to the elastic stability and compressive strength of monolithic vessels of identical dimensions and material (5). On the basis of tests performed on acrylic resin models, the diameter of glass or ceramic pressure vessels need not be limited by the current production facilities for the casting of monolithic vessels. They may be assembled from relatively small segments, as described above, and still retain their elastic stability and compressive strength under external pressure if the ground-joint surfaces match perfectly or if proper gaskets are used.

8. There appear to be two promising approaches to increase the resistance of brittle pressure vessels to point-impact loading. One approach relies on protective coatings that will absorb some of the kinetic energy of the impacting body and, at the same time, spread the contact pressure over a greater surface area of the vessel. The other approach applies, by chemical or mechanical means, compressive stresses in the surface of the vessel that exceed those produced by the tensile-stress component produced by point impact. The protective coatings of neoprene, glass-fiber and epoxy laminates, and aluminum have been found to give appreciable protection to glass and ceramic cylinders against point impact of 10-lb objects only if the coatings are more than 1-in. thick. Coatings of even 1/8-in. thickness are effective against 1/2-lb objects (Fig. 12).

Generally speaking, it appears that, for underwater vehicles with limited outer and inner diameters, the best protection is afforded by mechanical or chemical means that put the outer shell surface under compression or impart greater tensile strength. This has been accomplished by reinforcing glass and ceramics with metallic fibers; by use of glass heat treatments; by applications of the Chemcor process to glass; and by the shrinkage of metallic cylinders on the glass and ceramic shells. When composite rather than monolithic glass or ceramic vessels are used, the gasket material between individual segments may serve as fracture-propagation barriers (4).

9. Cylinders of brittle materials such as glass or ceramic can be successfully joined to withstand external hydrostatic pressure and bending moments if a specially designed joint is employed that takes the low tensile strength of brittle materials into consideration. A breech-type joint (Figs. 18 and 19) meets this requirement.

## Summary

Glass and ceramics have already found some application in the construction of underwater vehicles, either as fibers, flakes, or spheres in an epoxy or aluminum matrix. It is anticipated that, in the near future, glass and ceramics also will be employed as tubes and rods in an aluminum matrix or as the sole load-carrying members of rib-stiffened or sandwich-type cylinders, with or without the added reinforcement of metallic fibers. The selection of particular construction techniques must be governed by the desired structural and volumetric efficiencies of the proposed vessel, the cost of fabrication, and the depth of operation. There is no one best fabrication technique for glass or ceramic vessels; but, if structural efficiency and volumetric efficiency are the most desirable attributes of a proposed deep-submergence hull, then solid glass and ceramics are the best materials.

The compressive-strength-to-weight ratio of these materials is unexcelled and, combined with their intrinsic high moduli of elasticity, they appear to be obvious choices for transparent (or opaque) load-carrying underwater domes or as the main structural members of oceanographic probes and vehicles.

## Appendix

### A. Uses of Glass for Pressure-Vessel Construction

#### FIBER-GLASS-AND-EPOXY LAMINATES

GLASS was first used in external-pressure vessels as fine fibers of very high tensile strength imbedded in an epoxy matrix. Fiber-glass-and-epoxy laminates were being used quite extensively in the aerospace industry as construction material for internal-pressure containers, and the application of the same construction techniques to external-pressure vessels seemed very natural. Although compressive strengths as high as 120,000 psi were obtained in vessels of laminated fiber glass and epoxy resin, this construction proved to be less reliable and more costly than expected. The average compressive strength was only 80,000 psi (6) and, to obtain even this compressive strength, very elaborate equipment was necessary to wind a continuous glass fiber at a constant, predetermined tension and in the desired direction while applying a resin coating to the fiber. In the experimental testing programs, the external-pressure vessels made of fiber-glass-and-epoxy laminates displayed several shortcomings: low fatigue strength, considerable permanent creep when exposed to 50 or 60 per cent of critical pressure, some deterioration of the matrix strength after immersion in sea water under pressure for long periods of time, and a small but noticeable absorption of water. Still, in structural members of vessels where only modest compressive stresses and short-duration, high tensile stresses are encountered, the fiber-glass-and-epoxy laminates are very desirable.

#### FLAKE-GLASS-AND-EPOXY LAMINATES

To simplify the fabrication of glass-reinforced epoxy shells, to decrease the permeability to water, and to decrease the notch sensitivity of the laminates, a new laminate was developed (7) in which, instead of glass fibers, glass flakes of 10 to 35 mesh and approximately  $2\mu$  thickness were used. This material results in an average compressive strength of 50,000 psi, a tensile strength of 20,000 psi, a flexural strength of 30,000 psi, and a modulus of elasticity of 5 or 6 million psi. Although weaker than fiber-glass-and-epoxy laminates, the notch sensitivity and the permeability to water were much lower than those of fiber-glass laminates. It is thought that the lower permeability to water is due to the much longer and more tortuous path that the water must traverse from the outside to the inside surface of the vessel. The low notch sensitivity of flake-glass laminates, on the other hand, has been postulated to be due to inherent stress raisers within the flake laminates that already have a stress-concentration factor of at least 1.5. Perhaps the most promising application of glass flakes is in flake-fiber-epoxy laminations, which have slightly lower strength than fiber-glass-and-epoxy laminates but considerably lower water permeability, lower notch sensitivity at surface discontinuities, and much better machinability of external surfaces. For better quality control and higher mechanical properties, some cylinders have been made in which the glass flakes were replaced by a 2- to 10-mil-thick, epoxy-coated, continuous glass tape wound in a helix on a cylindrical mandrel.

#### SPHERE-GLASS-AND-EPOXY COMPOSITES

Because of the increased compressive strength, fiber-glass- and flake-glass-epoxy laminates have been used to decrease the weight of underwater vessels since a smaller amount of structural



material is used than would be the case if epoxy resin alone were to be utilized in the fabrication. To achieve the same goal, the over-all density was reduced by adding minute, hollow glass spheres ( $2\text{-}\mu$  wall thickness) to the epoxy (8). By selecting the size of glass spheres (30 to  $300\mu$  in diameter) and using them in proper proportion with epoxy resins, it was possible to achieve composite material densities of 22 to 45 lb per cu ft with corresponding compressive strengths of approximately 2500 to 20,000 psi. Although these compressive strengths are low, the material is lighter than water; therefore, the wall of a pressure vessel can be made the desired thickness without decreasing appreciably the buoyancy of the submerged structure. This approach to pressure-vessel design is advantageous as long as no limit is placed on the external diameter of the vessel, and protection from water permeability is provided by an external impervious layer. The material, being epoxy, will also creep some under prolonged exposure to high external pressure.

The addition of glass spheres to epoxy reduces the tensile strength of the composite material to about 3000 psi; however, this disadvantage can be overcome by adding glass fibers. If the fibers are placed on the external and internal surfaces of the vessel, they will effectively carry all of the tensile stresses generated by bending moments that otherwise would tend to fracture the low-strength sphere-glass-and-epoxy composite.

This material will find widespread application as a low-density potting compound for the internal components of unmanned, underwater oceanographic probes. The large bulk and the fair compressive strength of such a potting compound filling all the voids in the vehicle will make it sufficiently rigid to eliminate the need for a shell structure to carry all the compressive stresses generated by external hydrostatic pressure.

Attempts are also being made to utilize the hollow glass spheres with a metallic instead of an epoxy matrix (9). A metallic matrix should eliminate - or at least decrease considerably - the creep, strength deterioration, and water permeability. The fatigue strength of the structure will also increase substantially. The metallic matrix that is most compatible with the glass spheres is cast aluminum. So far, only flat plates have been cast of sphere glass and aluminum composites, but no great difficulties exist for applying the same construction techniques to cylindrical pressure vessels. A compressive strength of 22,000 psi and a tensile strength of 2700 psi have been obtained with sphere-glass-and-aluminum composites with a density of 0.058 lb per cu in.

#### TUBE-GLASS AND ROD-GLASS STIFFENERS FOR CASTINGS

Some attempts have also been made to reinforce metals with glass fibers. So far, the results have not been too encouraging; the entrapment of gas bubbles between fibers and the nonwettability of glass surfaces present major obstructions to achieving uniform, nonpermeable castings with improved compressive strength-to-weight ratios. However, experiments by the author have shown that if, instead of many fine glass fibers in an aluminum casting, a smaller number of  $1/4$ - to 1-in. heat-resistant glass rods or tubes is substituted, then the compressive strength of cast aluminum pressure vessels can be increased without any increase in weight. To attain the increase in compressive strength, however, the glass rods and tubes must be located selectively, depending upon the magnitude of expected compressive stresses; and sufficient space must be provided for molten metal to flow freely between the rods during the casting operation. The analogy of steel-reinforced concrete may be used here except that, in concrete, the steel rods are located in areas of maximum tensile stress whereas, in metallic castings, the glass rods and tubes are located in regions of maximum compressive stress. When the proper heat-resistant glass was used, no fractures in the glass rods and tubes occurred. The combination of glass reinforcements with a metallic matrix gives the glass rods and tubes the much-needed protection against point impacts. The metallic matrix, besides providing impermeable barriers to water, permits ready incorporation of tapped holes for internal fastenings in the vessel.



## B. Experimental Data

### RESULTS OF STATIC-PRESSURE TESTS

- Model I<sub>1</sub> - Three-ribbed Pyroceram cylinder (Fig. 2); design critical pressure, 14,000 psi. This model was tested to 10,000 psi without implosion; measured strains shown in Figs. 28, 29, and 30; no creep detected after 30 min at 10,000 psi.
- Model J<sub>1</sub> - Five-ribbed Pyroceram cylinder (Fig. 4); design critical pressure, 10,000 psi. This model failed at 10,000 psi; measured strains shown in Figs. 31 through 40.
- Model J<sub>2</sub> - After being subjected to a fatigue test (see below) the model was scratched to a depth of 1/64 in. as shown in Fig. 41 and subjected to a static-pressure test. Failure occurred at 11,500 psi; no strains were recorded.
- Model K<sub>1</sub> - Two-ribbed alumina ceramic cylinder (Fig. 6); design critical pressure, 10,000 psi. This model failed at 12,700 psi; measured strains shown in Figs. 42 through 47.
- Model K<sub>2</sub> - Prior to test, this model was scratched to a depth of 1/64 in. as shown in Fig. 48. Failure occurred at 14,200 psi; measured strains are shown in Figs. 49 through 53.
- Model L<sub>1</sub> - Two-ribbed high-strength aluminum cylinder (Fig. 8); design critical pressure, 2400 psi. Failure occurred at 2400 psi; measured strains are shown in Figs. 54 through 58. Strain gage location is the same as that for Model K (see Fig. 42).
- Model L<sub>2</sub> - After being damaged severely (Fig. 59) in underwater shock testing, failure occurred at 1950 psi (Fig. 60).
- Model M<sub>1</sub> - Three-ribbed high-strength aluminum cylinder (Fig. 10); design critical pressure, 4500 psi. After being severely damaged in underwater shock testing, failure occurred at 4000 psi (Fig. 61).
- Model M<sub>2</sub> - After being severely damaged (Fig. 62) in underwater shock testing, failure occurred at 2500 psi (Fig. 63).
- Model A - The sphere (Fig. 11) of 99 per cent alumina oxide ceramic, with a design critical pressure of 365,000 psi, imploded at a hydrostatic pressure of 55,000 psi.
- Model P<sub>x</sub> - The sphere (Fig. 11) of Pyrex glass, with a design critical pressure of 217,000 psi, imploded at a hydrostatic pressure of 35,000 psi.
- Model P<sub>m</sub> - The sphere (Fig. 11) of 9606 Pyroceram, with a critical design pressure of 203,000 psi, imploded at a hydrostatic pressure of 72,000 psi.
- Model XXX - The 9606 Pyroceram model (Fig. 15), with a design critical pressure of 15,000 psi, imploded at a hydrostatic pressure of 14,800 psi.
- Model XXX<sub>2</sub> - The 9606 Pyroceram model (Fig. 18), with a design critical pressure of 15,000 psi and a breech-type lock, was subjected to pressures up to 16,000 psi. Implosion did not occur.
- Model JC - The segmented acrylic resin cylinder, shown in Fig. 13a, with a design critical pressure of 760 psi, imploded at a hydrostatic pressure of 780 psi.
- Model MC - The monolithic acrylic resin cylinder, shown in Fig. 13b, with a design critical pressure of 760 psi, imploded at a hydrostatic pressure of 780 psi.

Model JS - The acrylic resin sphere assembled from unbonded spherical polygons (Fig. 14b), with a design critical pressure of 1150 psi, imploded at a hydrostatic pressure of 1140 psi.

Model MS - The acrylic resin sphere assembled from bonded spherical polygons (Fig. 14a), with a design critical pressure of 1150 psi, imploded at a hydrostatic pressure of 1120 psi.

#### RESULTS OF FATIGUE TEST

Model J<sub>2</sub> - The five-ribbed Pyroceram cylinder (Fig. 4), with a design critical pressure of 10,000 psi, was subjected to 1000 cycles of 100- to 8000-psi pressure, 1000 cycles of 100- to 8500-psi pressure, and 1000 cycles of 100- to 9000-psi pressure. Some of the shell material was observed to flake off at the completion of the test (Figs. 24 through 27); however, no implosion occurred.

#### RESULTS OF UNDERWATER SHOCK TESTS

Model I<sub>1</sub> - Three-ribbed Pyroceram cylinder (Fig. 2); design critical pressure, 14,000 psi. At a static pressure of 2 psi, this model was imploded by a 7-gm Pentolite charge detonated 5.75 in. below the model after withstanding an identical charge set off at a distance of 10.75 in.

Model I<sub>2</sub> - At a static pressure of 5500 psi, this cylinder was imploded by an 8.3-gm Pentolite charge detonated 3 in. below the model after withstanding identical charges set off at distances of 10, 8, and 5 in.

Model M<sub>1</sub> - Three-ribbed high-strength aluminum cylinder (Fig. 10); design critical pressure, 4500 psi. At a static pressure of 2 psi, this model was severely damaged by a 16-gm Pentolite charge detonated 3 in. below the model after withstanding an identical charge set off at distances of 8 and 5 in. The permanent deformation of the model occurred solely between the stiffeners, and the magnitude of the indentation was 1/8 in.

Model M<sub>2</sub> - At a static pressure of 2250 psi, this cylinder was severely damaged (Fig. 62) by a 16-gm Pentolite charge detonated 3 in. below the model after withstanding identical charges set off at distances of 8 and 5 in. The permanent deformation or indentation of the model was 0.11 in. on the stiffener and 0.15 in. midway between the stiffeners.

Model K<sub>3</sub> - Two-ribbed alumina ceramic cylinder (Fig. 6); design critical pressure, 10,000 psi. At a static pressure of 2 psi, this model was imploded (Fig. 64) by a 9.6-gm Pentolite charge detonated 8 in. below the model.

Model L<sub>2</sub> - Two-ribbed high-strength aluminum cylinders (Fig. 8); design critical pressure, 2400 psi. At a static pressure of 2 psi, this model was severely damaged (Fig. 58) by a 16-gm Pentolite charge detonated 3 in. below the model after withstanding 7-gm Pentolite charges set off at distances of 24, 14 1/2, 9 1/2, 5 3/4, and 3 in.

#### RESULTS OF FLEXURE TEST

Model IMC - This acrylic resin shell, equipped with the internal Marman clamp (Fig. 23), was subjected to a tensile load of 50,000 lb without failure. Subsequently, the model failed when subjected to a bending moment of 30,000 lb-in. applied by the four-point loading method.

## References

1. Staff Report, "Engineering with Glass, Part One: What Is Glass?" and "Engineering with Glass, Part Two: What Can Glass Do?" Mechanical Engineering, Vol. 85, Nos. 3 and 4, March and April 1963.
2. Staff Report, "Alumina Ceramics," Industrial and Engineering Chemistry, December 1962.
3. H. A. Perry, Structural Value Analysis of Unyielding Materials for Pressure Hulls, U. S. Naval Ordnance Laboratory, Silver Spring, Maryland, December 1962.
4. J. D. Stachiw, Protection of Glass Shells against Point Impact Fracturing by the Use of Metallic and Non-Metallic Coatings, Ordnance Research Laboratory Technical Memorandum, TM 6.3112-05, July 9, 1963.
5. J. D. Stachiw, Elastic Stability of Segmented Cylinders and Spheres under External Hydrostatic Pressure, Ordnance Research Laboratory Technical Memorandum, TM 26.3111-03, February 5, 1963.
6. Staff Report, "What Every Engineer Should Know about Reinforced Plastics," Metal Progress, June - July 1962.
7. Staff Report, Establishment of the Potential of Flake Reinforced Laminates as Engineering Structural Materials, Final Report, Narmco Research & Development Division of Telecomputing Corporation, San Diego, California, March 1962.
8. Inlyte Float Materials, Inland Manufacturing Division of the General Motors Corporation Technical Information Bulletin, TIB-4, Dayton, Ohio, August 5, 1963.
9. Eccofoam MD, Dielectric Materials Division of Emerson & Cuming, Inc., Preliminary Technical Bulletin 6-2-14, Canton, Massachusetts, February 1962.

**Illustrations**

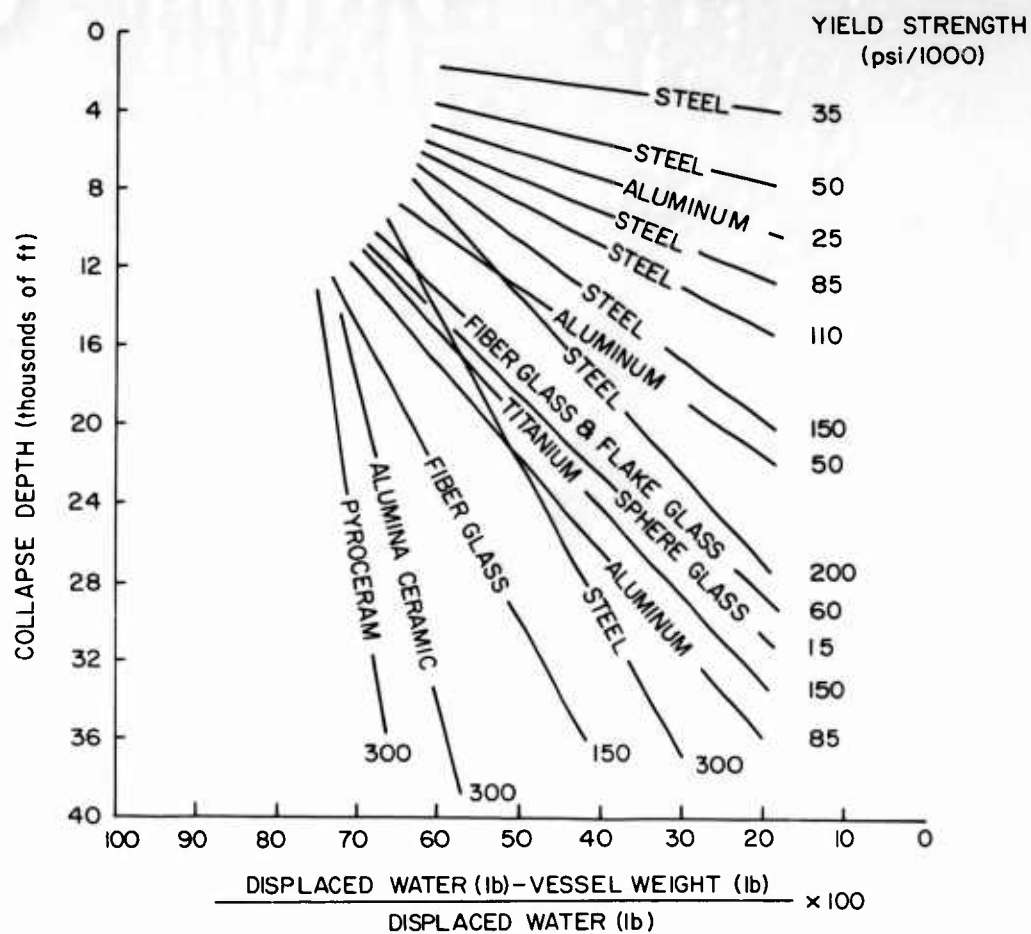


Fig. 1 - Relative Strength of Rib-Stiffened Cylinders Made of Various Materials





Fig. 3 - Three-Ribbed Pyroceram Cylinder, Model I

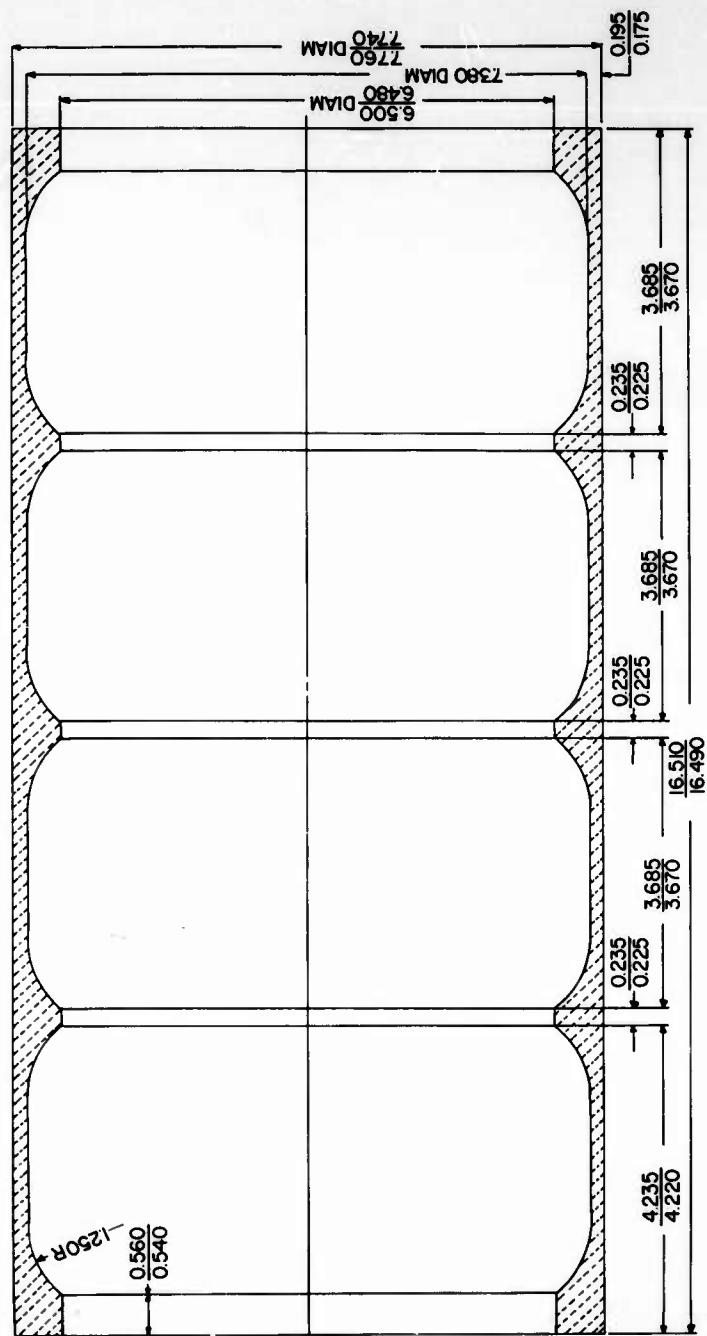


Fig. 4 - Dimensions of Five-Ribbed Pyroceram Cylinders, Model J



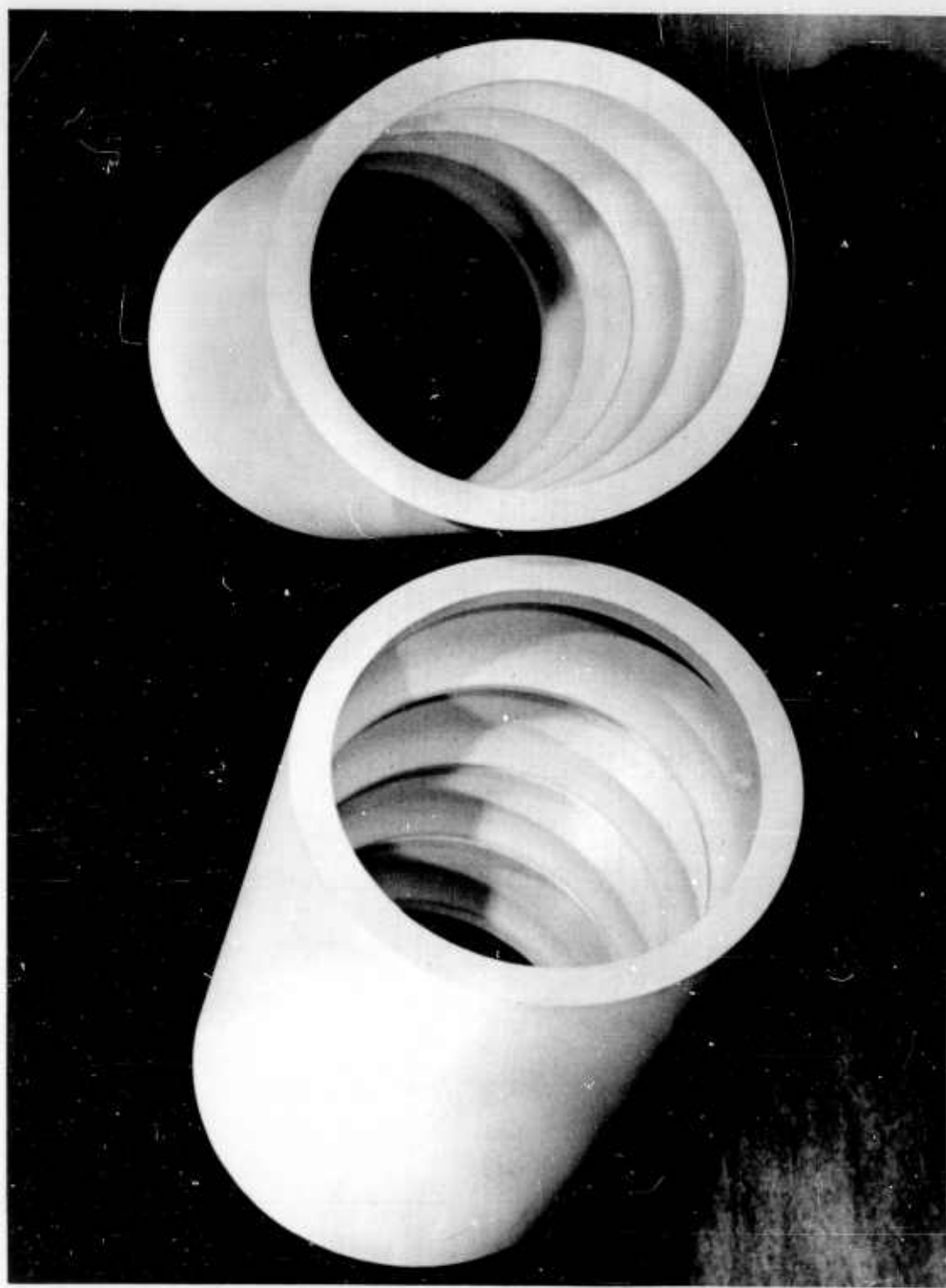


Fig. 5 - Five-Ribbed Pyroceram Cylinders, Model J

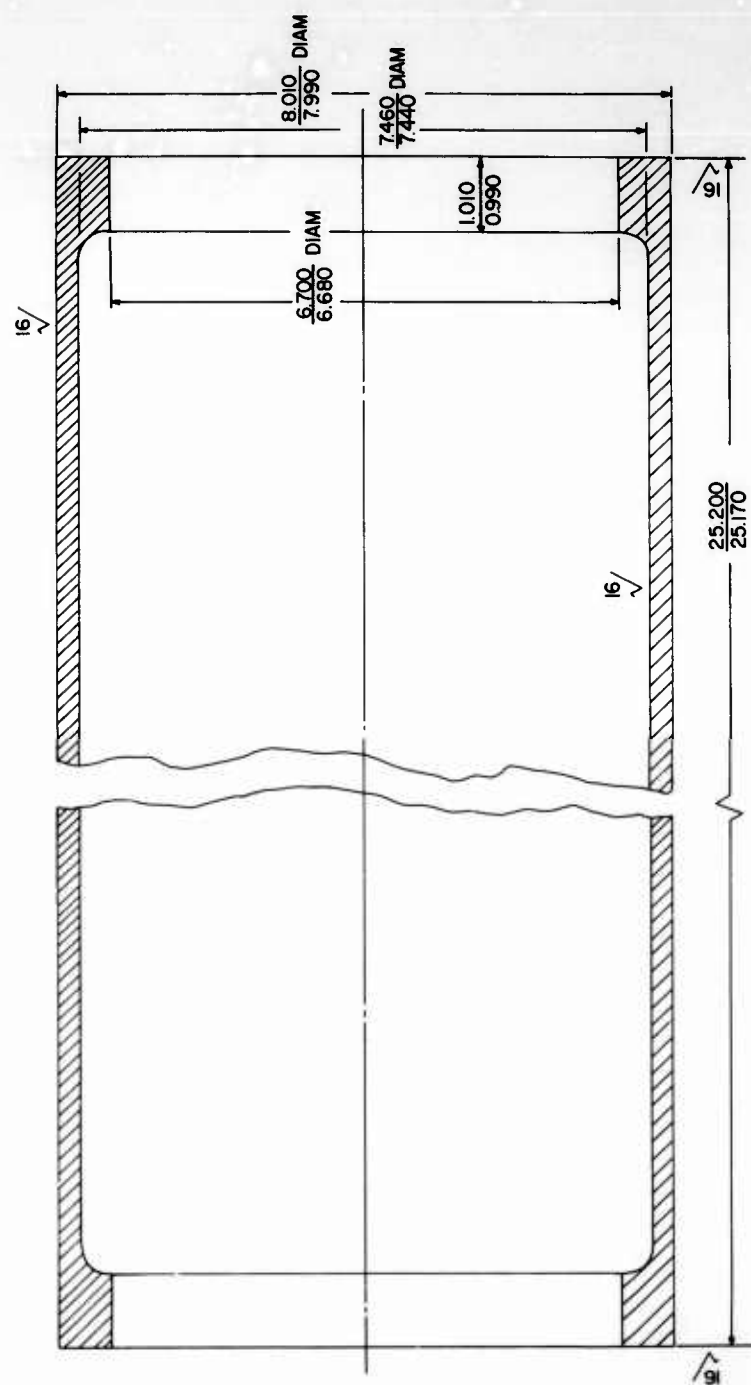


Fig. 6 - Dimensions of Two-Ribbed Alumina Ceramic Cylinders, Model K

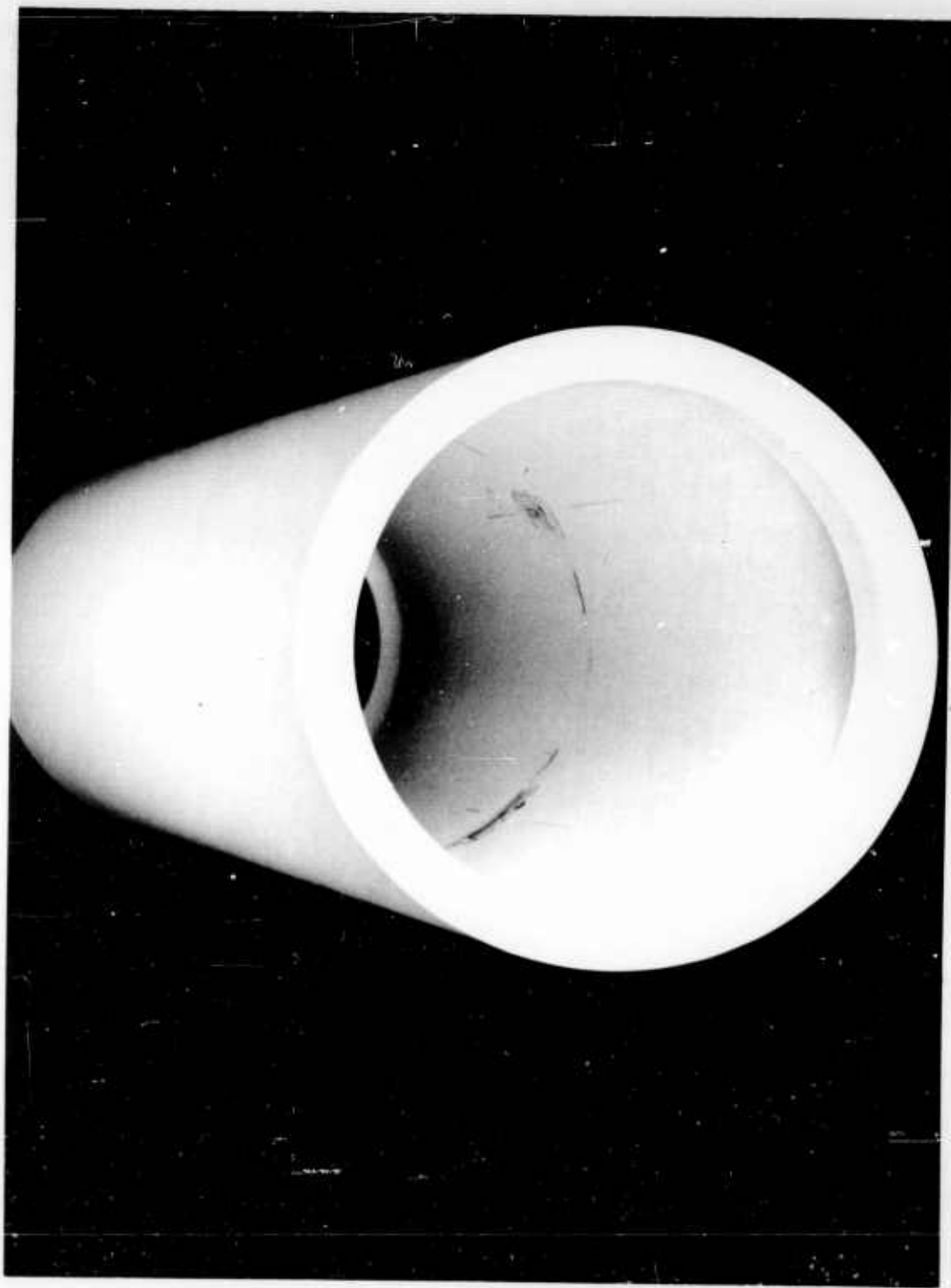


Fig. 7 - Two-Ribbed Alumina Ceramic Cylinder, Model K

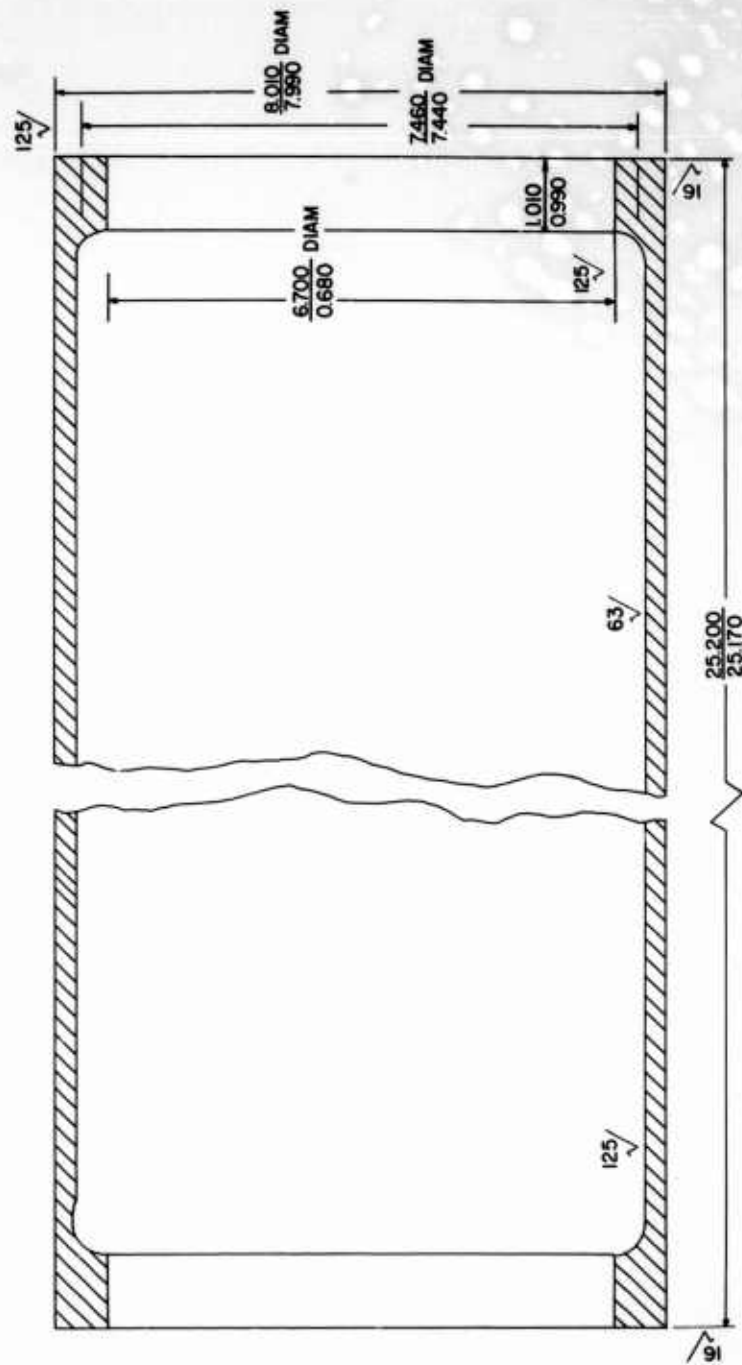


Fig. 8 - Dimensions of Two-Ribbed High-Strength Aluminum Cylinder, Model L

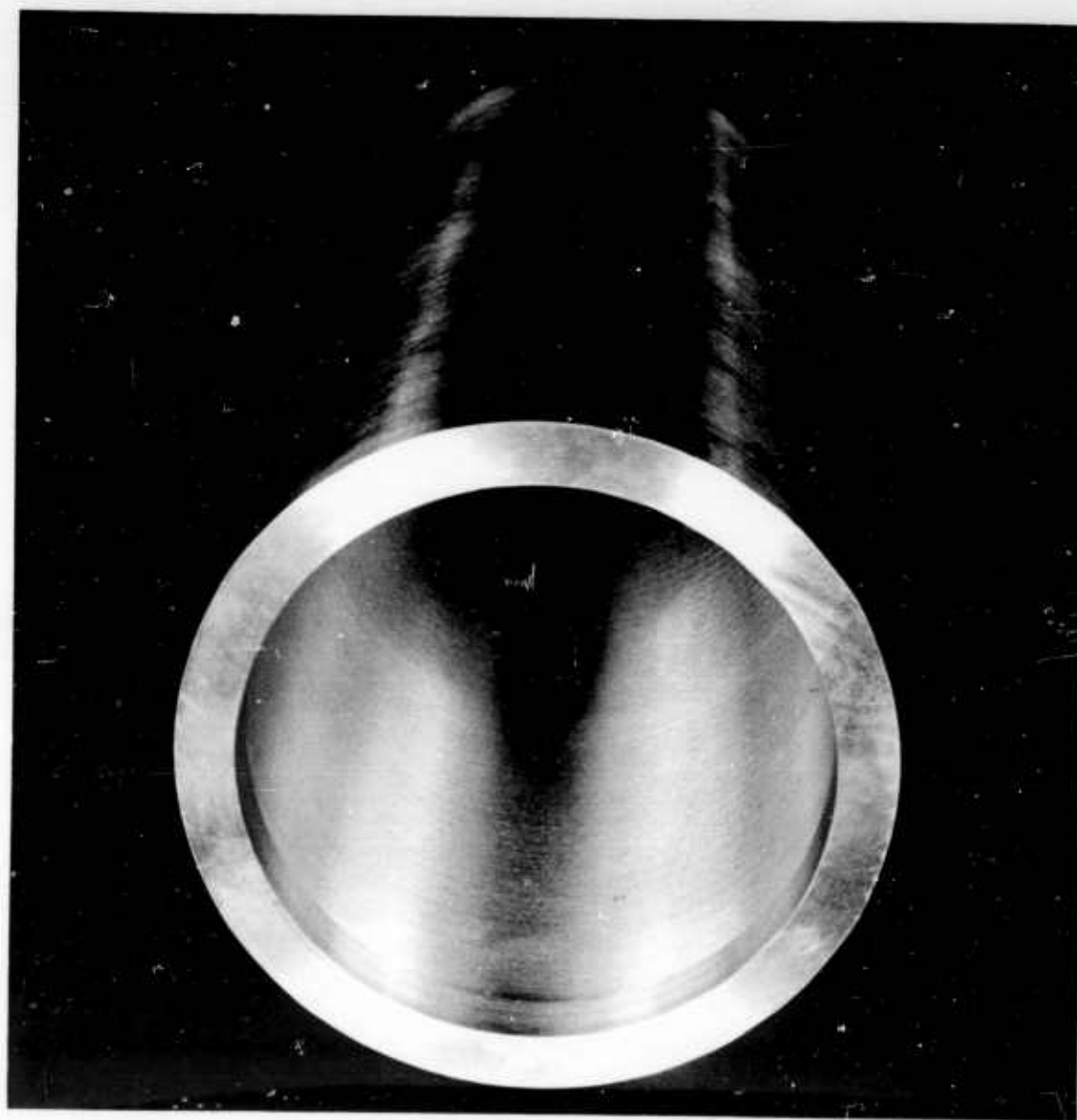


Fig. 9 - Two-Ribbed High-Strength Aluminum Cylinder, Model L

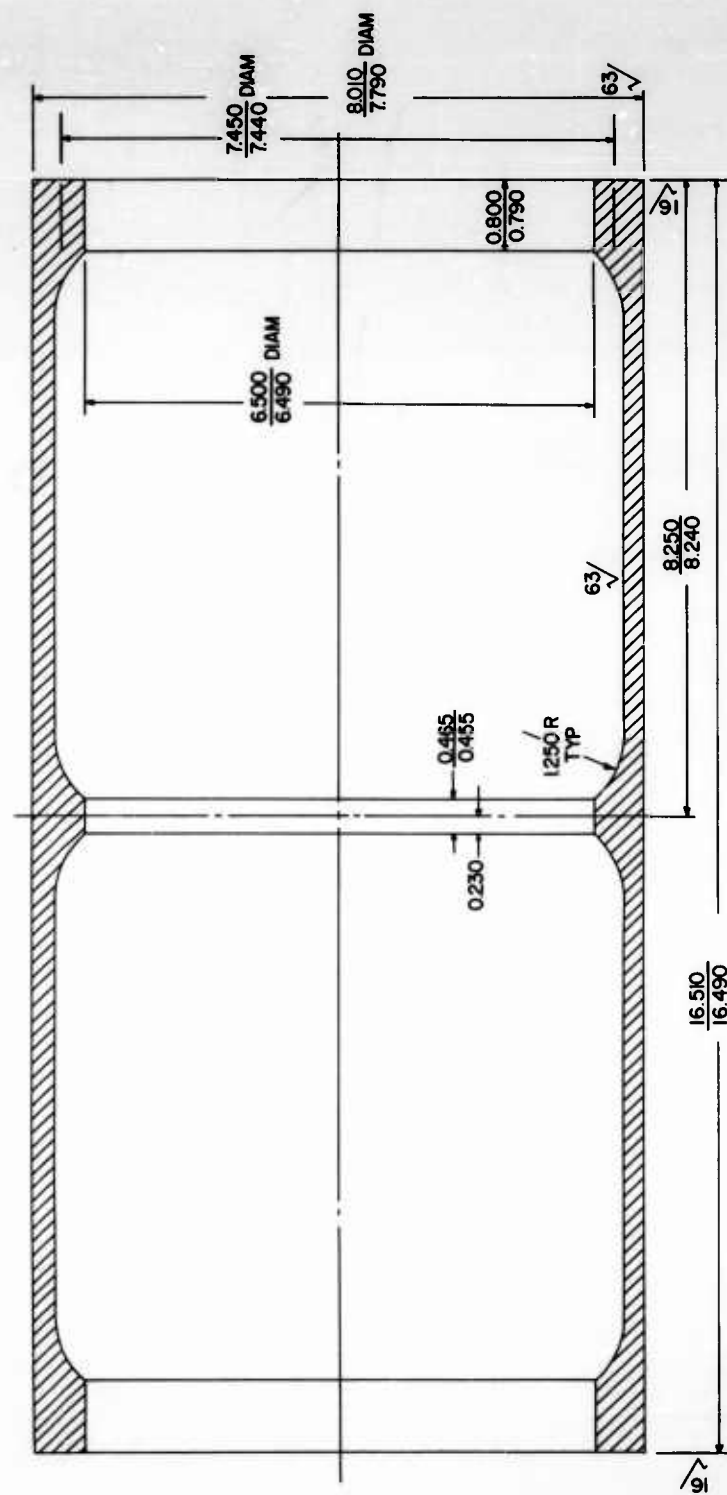
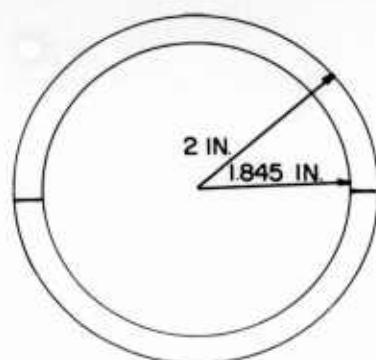
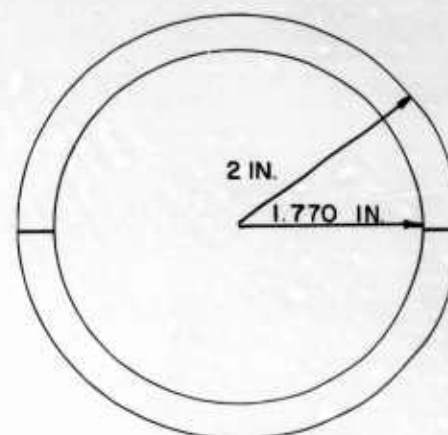


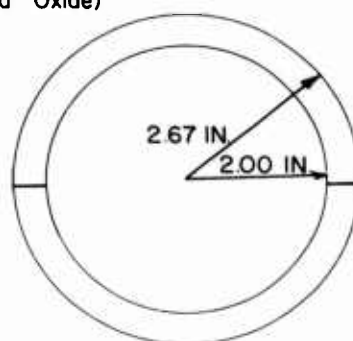
Fig. 10 - Dimensions of Three-Ribbed High-Strength Aluminum Cylinder, Model M



MODEL A  
(99% Alumina Oxide)



MODEL  $P_x$   
(Pyrex Glass)



MODEL  $P_m$   
(No. 9606 Pyroceram)

Fig. 11 - Dimensions of Hollow Spheres Used to Determine Biaxial Compressive Strength, Models A,  $P_x$ , and  $P_m$



Fig. 12 - Pyroceram Hemispheres after Point-Impact Tests



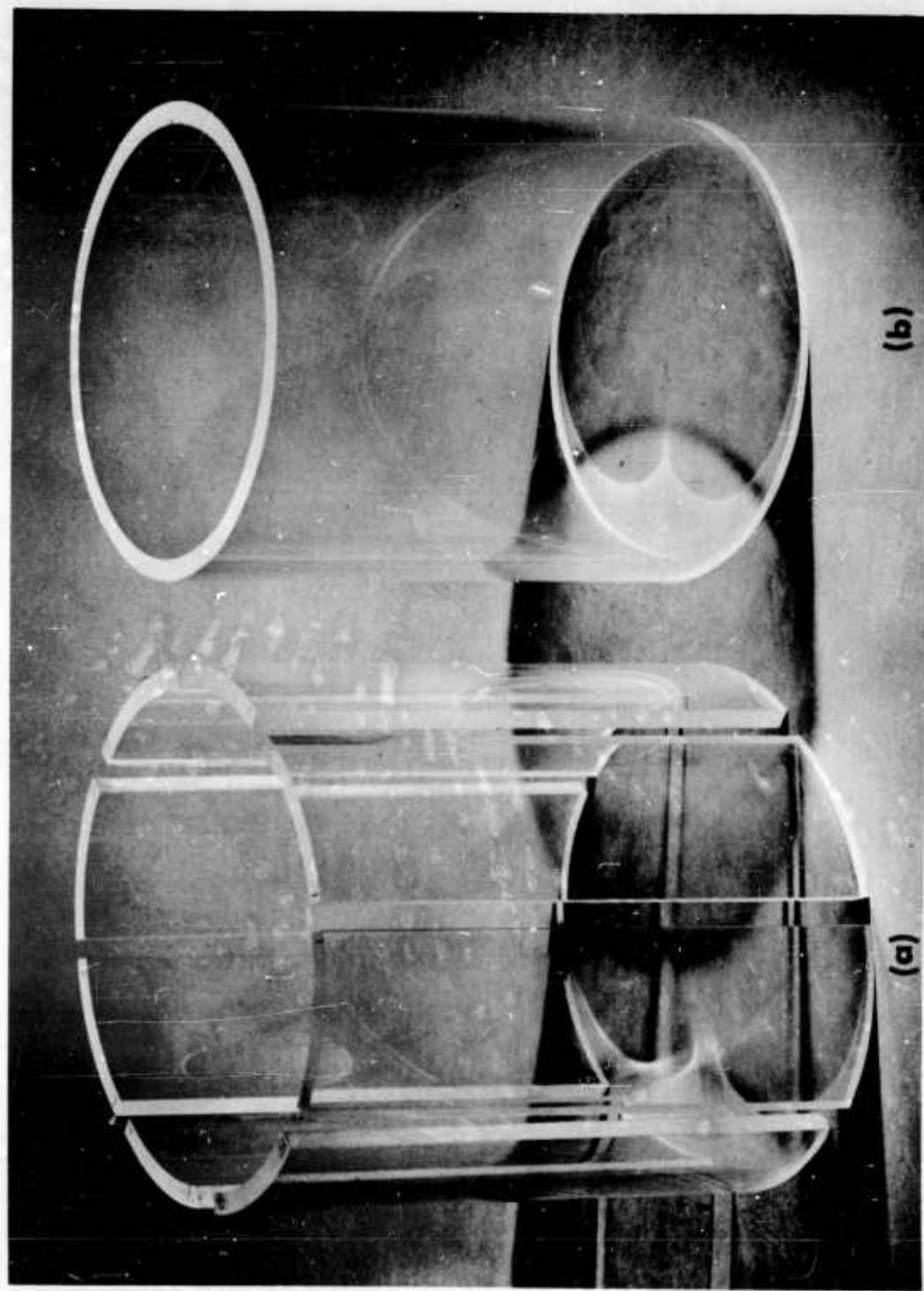


Fig. 13 - Acrylic Resin Cylinders for Tests of Seams: Model JC (a) Is a Segmented Cylinder with Taped Seams (see Ref. 5); Model MC (b) Is a One-Piece (Monolithic) Cylinder

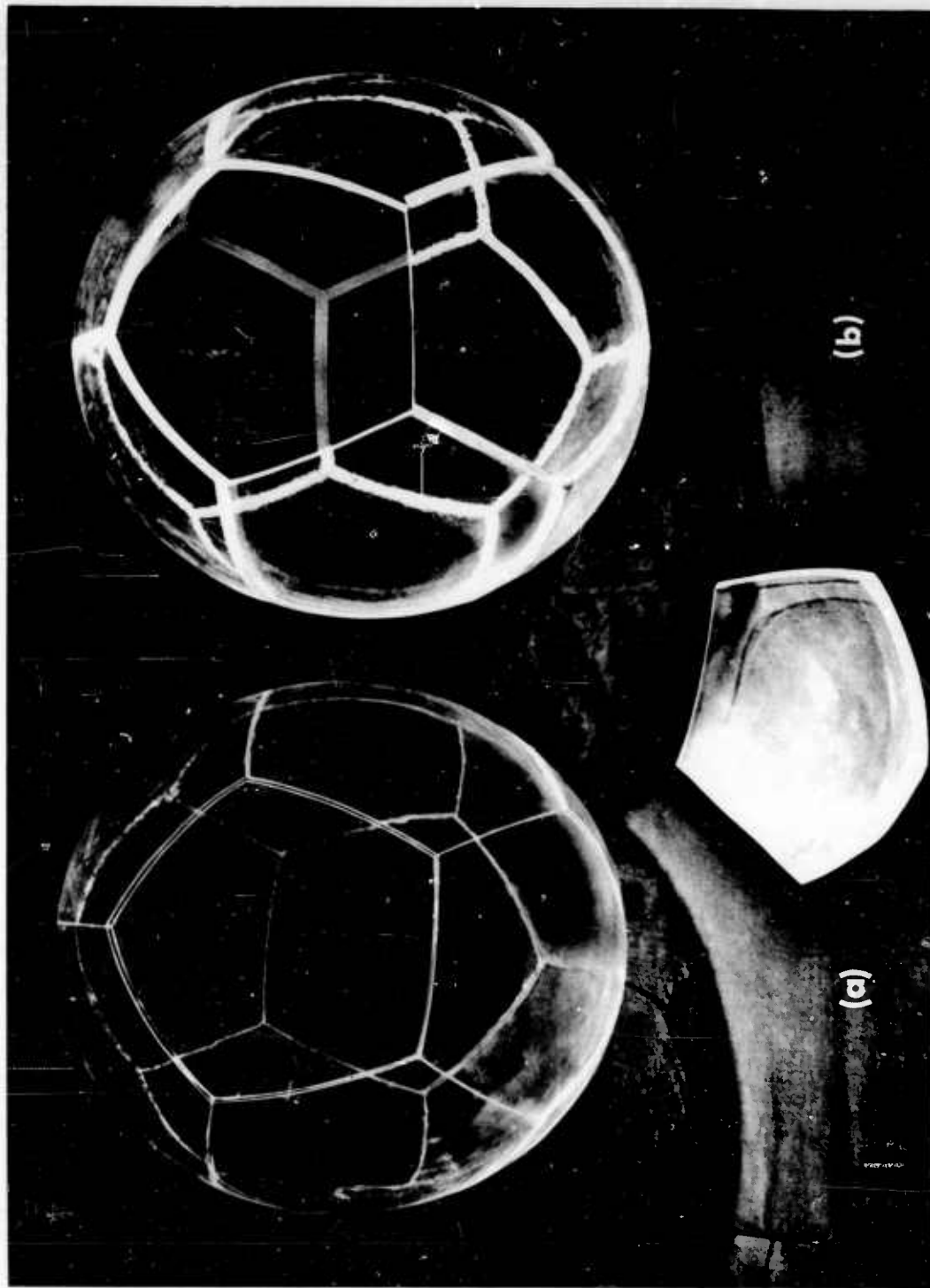


Fig. 14 - Segmented Acrylic Resin Spheres for Tests of Seams: Model MS (a) Has Bonded Seams;  
Model JS (b) Has Taped Seams





Fig. 16 - Components of Pyroceram Model XXX and External Marman Clamp

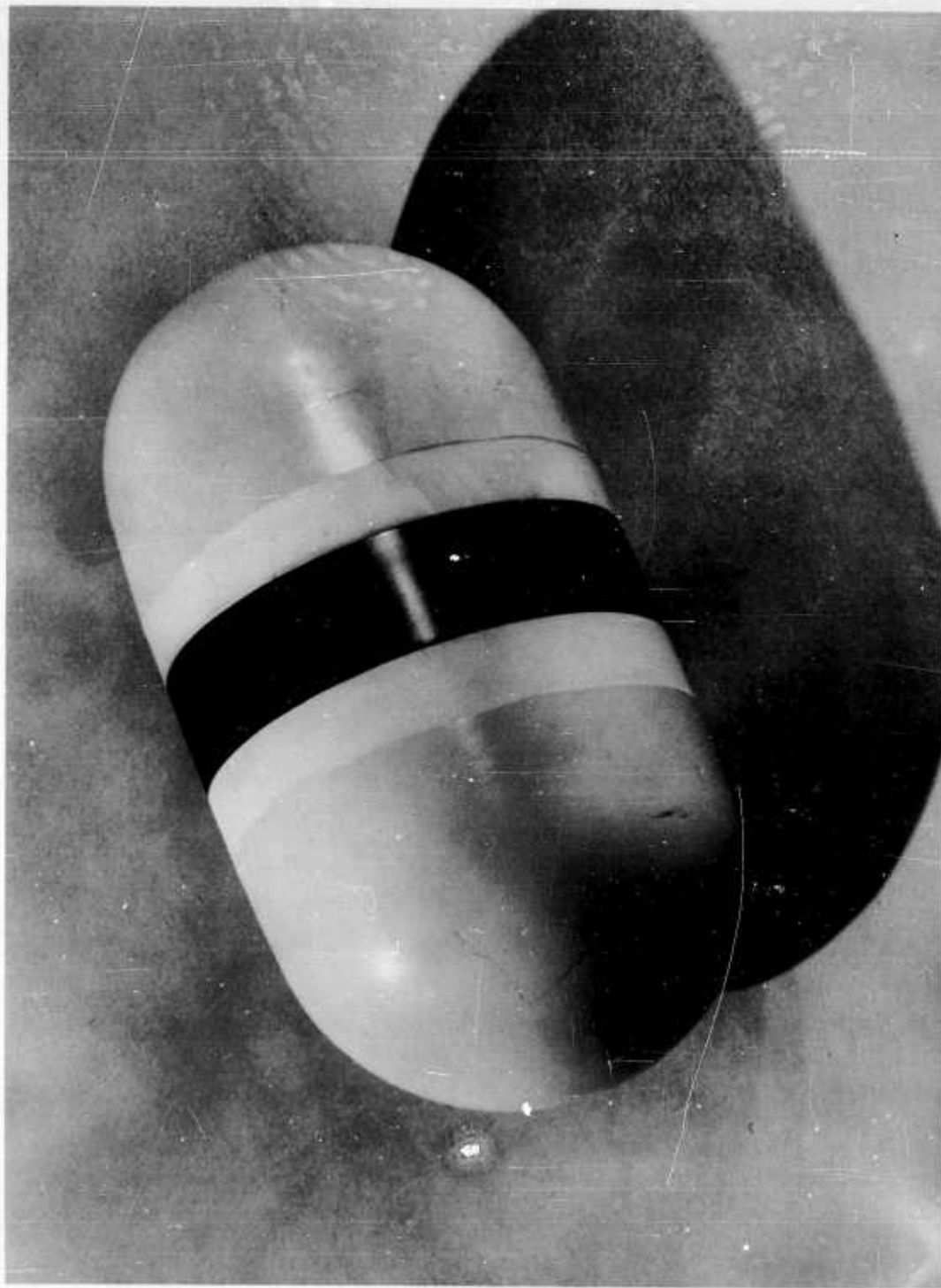


Fig. 17 - Assembled Pyroceram Model XXX

MATERIAL: SHELLS - PYROCERAM NO. 9606  
 JOINT RINGS - 7075-T6 ALUMINUM  
 (all dimensions in inches)

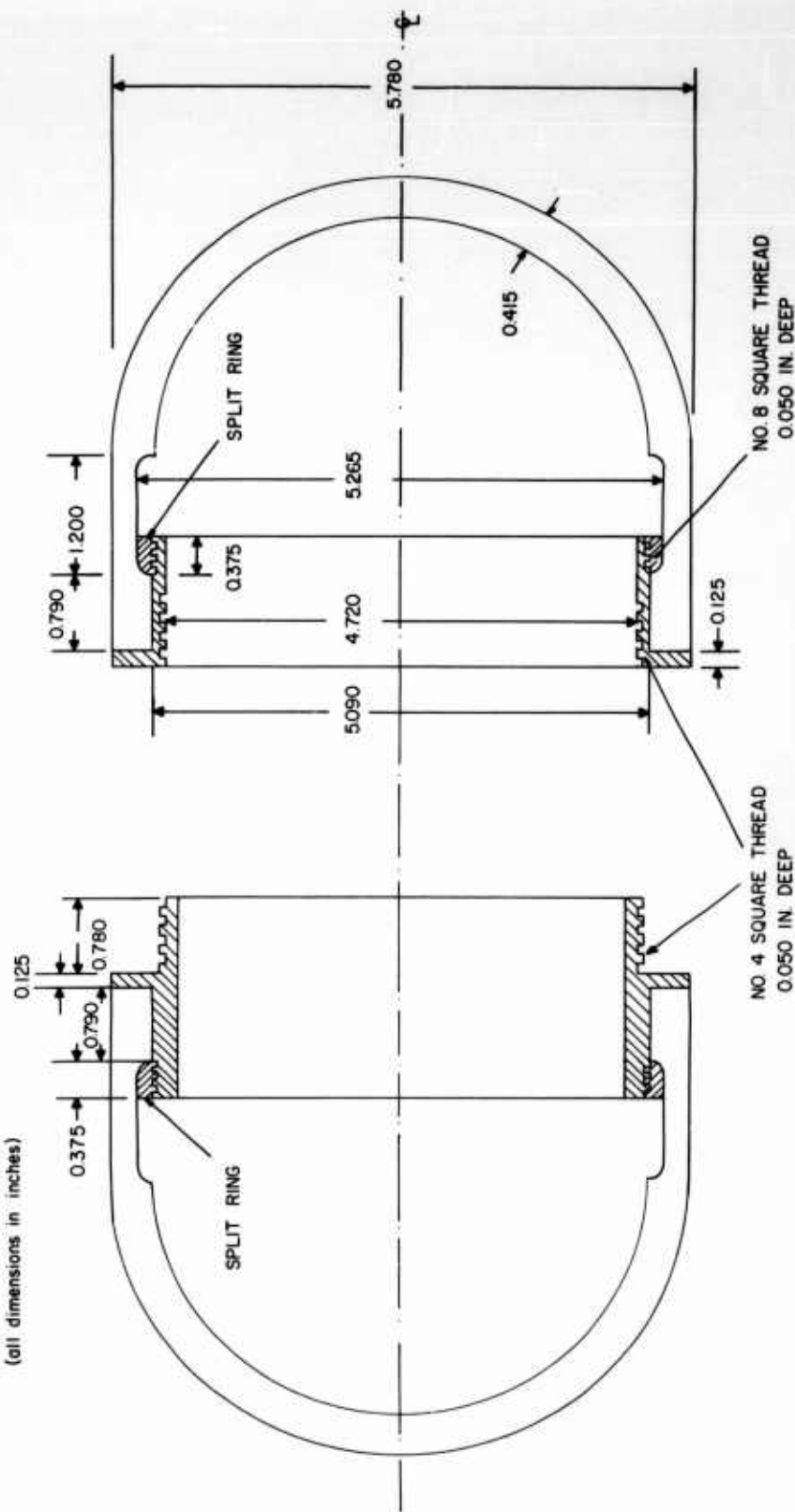


Fig. 18 - Dimensions of Pyroceram Model XXX2 with Breech-Type Joint



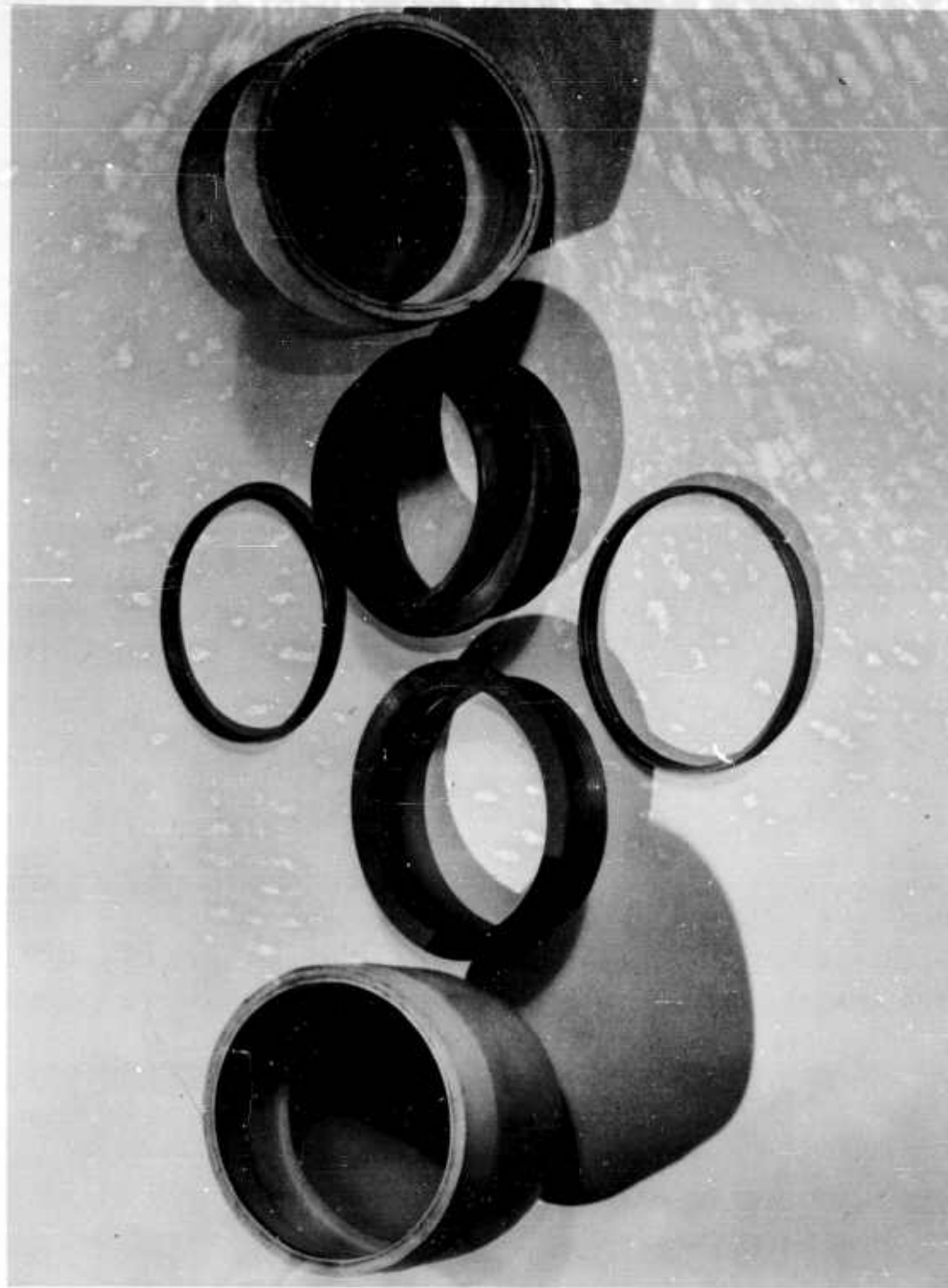


Fig. 19 - Components of Pyroceram Model XXX2

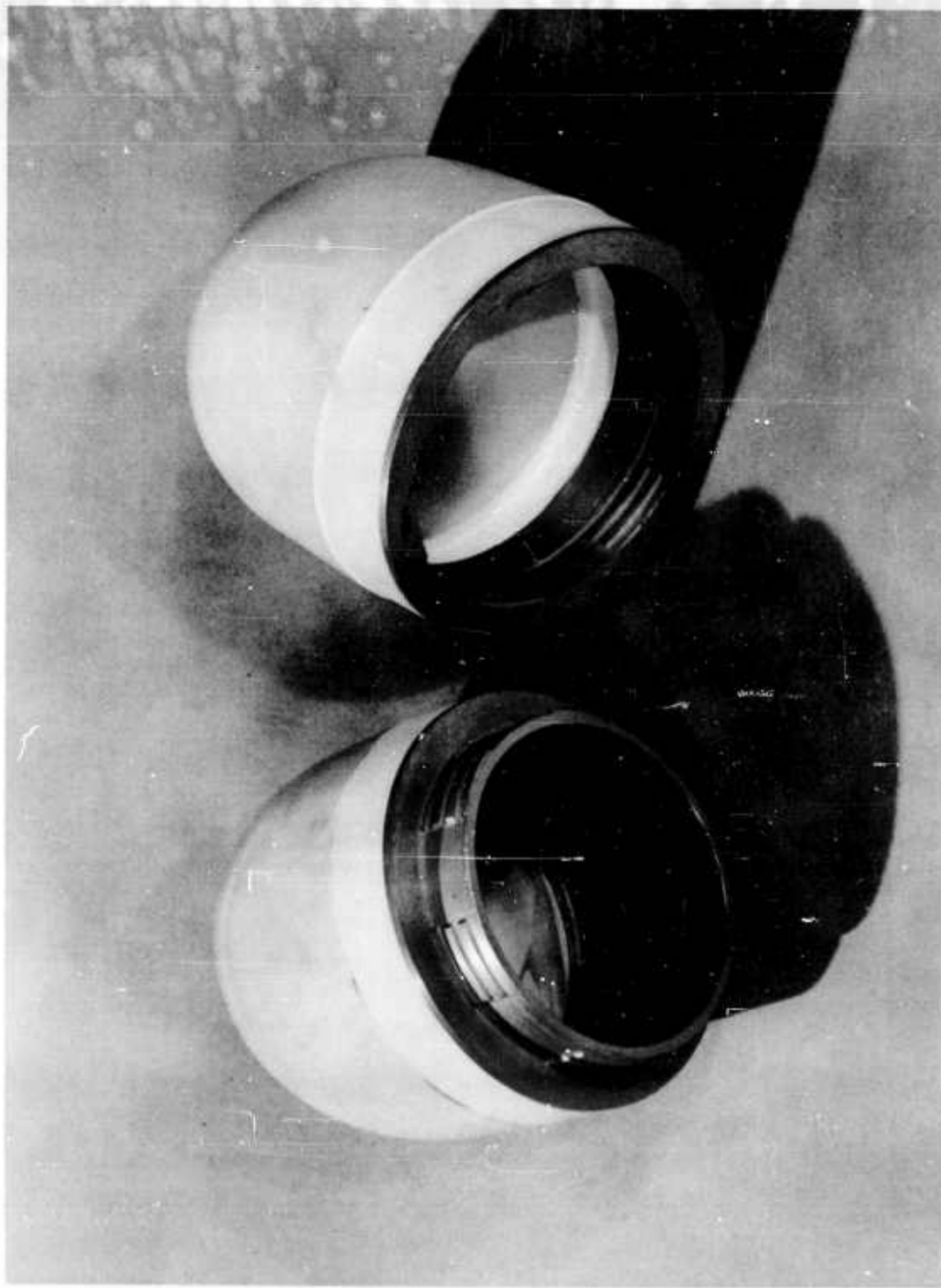


Fig. 20 - Pyroceram Model XXX2 Ready for Assembly



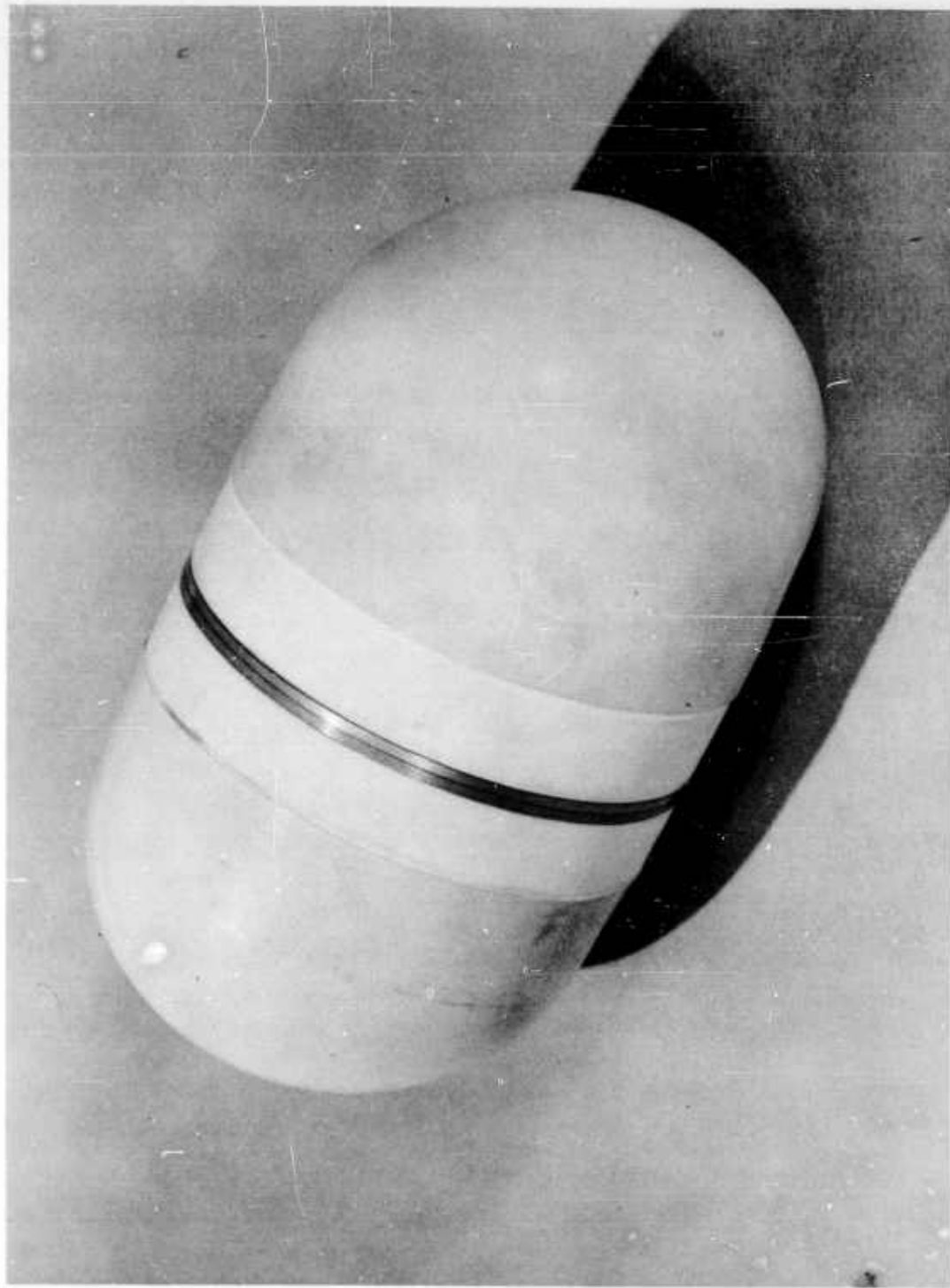


Fig. 21 - Assembled Pyroceram Model XXX2

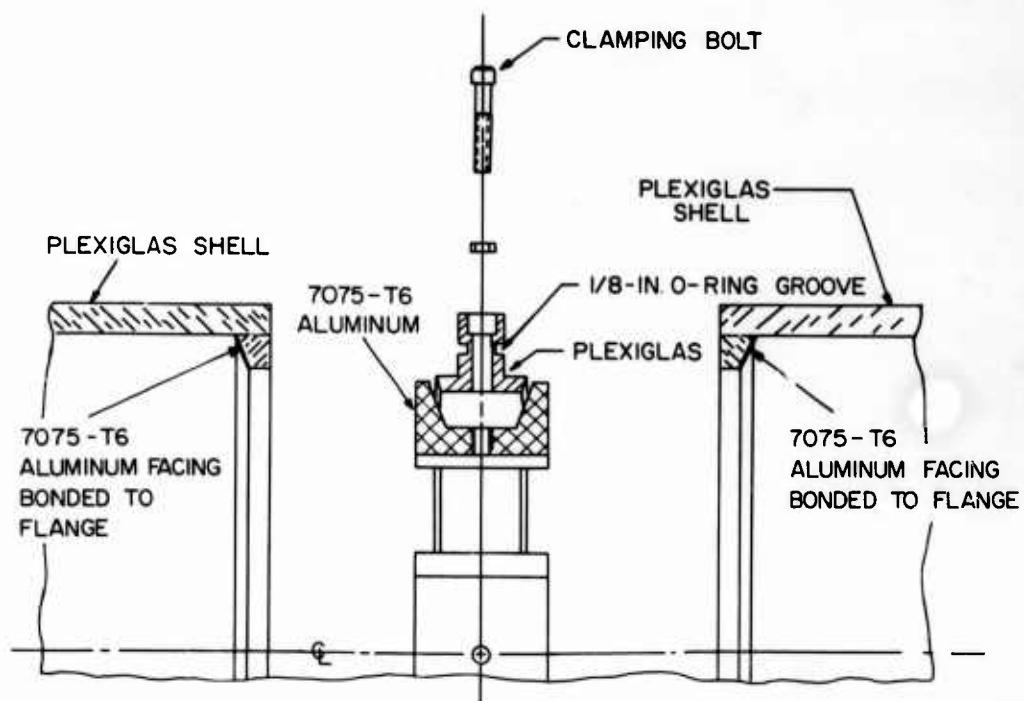


Fig. 22 - Details of Acrylic Resin Model IMC with Internal Marman Clamp

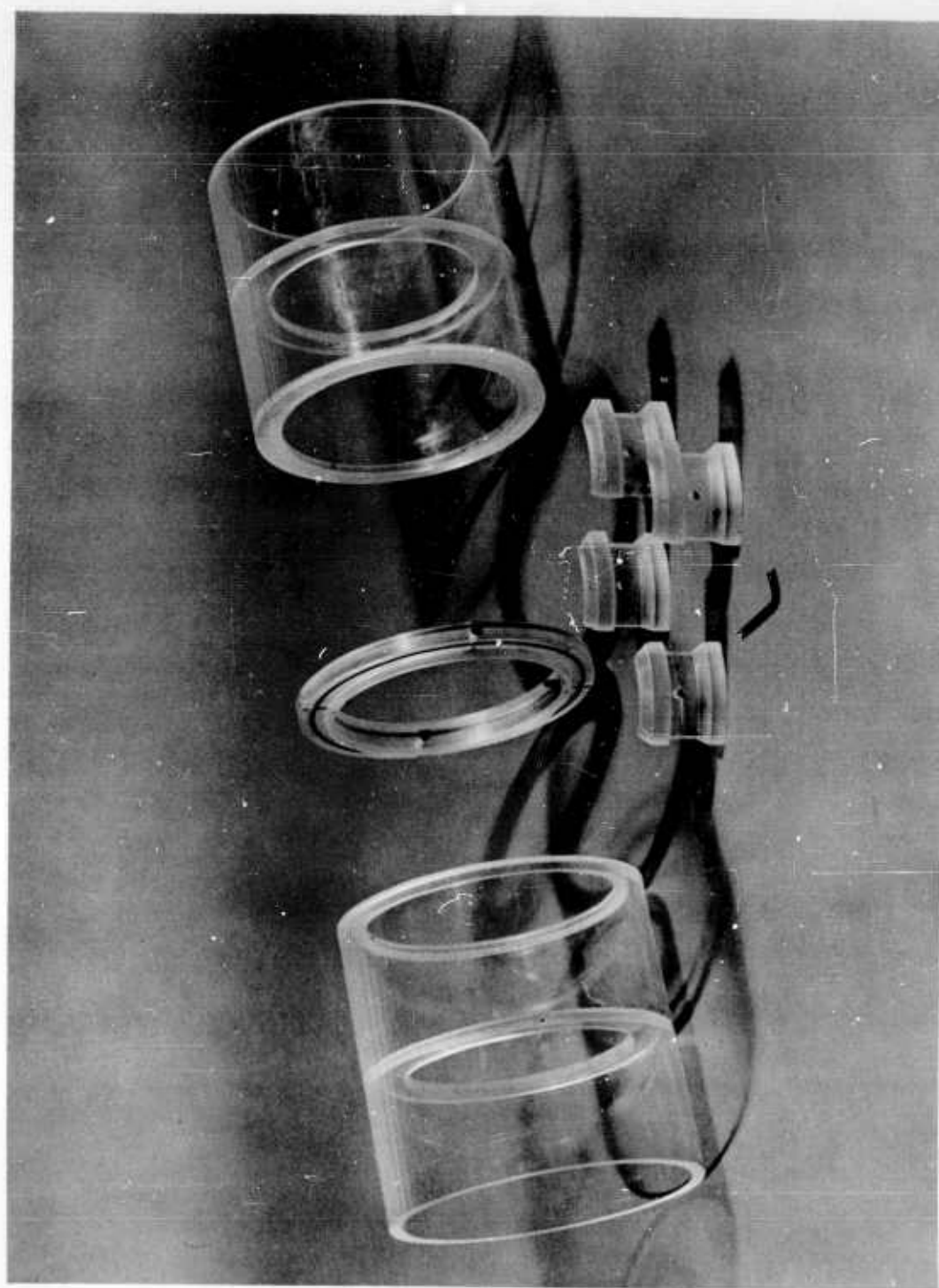


Fig. 23 - Components of Acrylic Resin Model IMC with Internal Marman Clamp

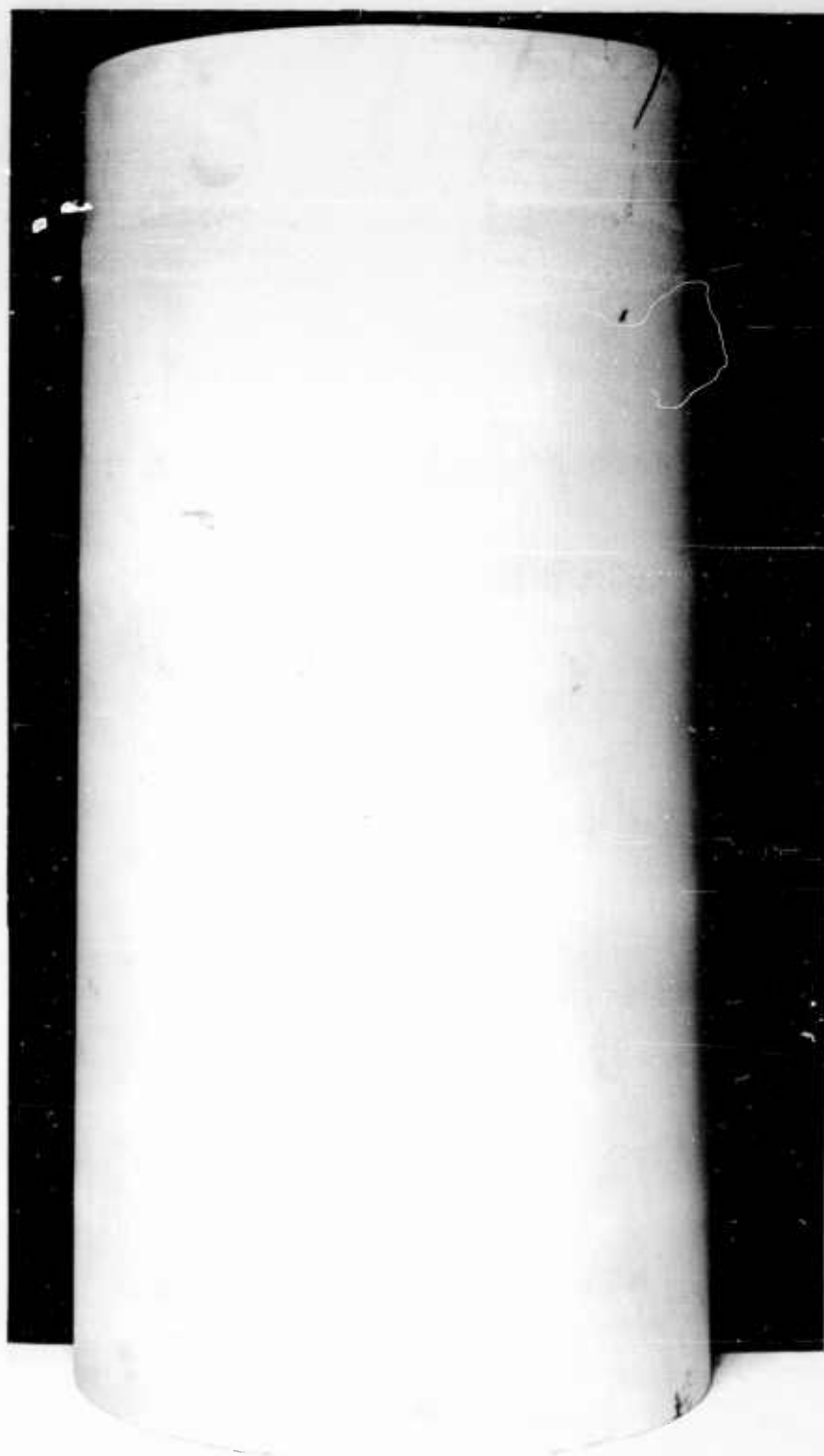


Fig. 24 - Appearance of Outside Surface of Fatigued Cylinder, Model J2

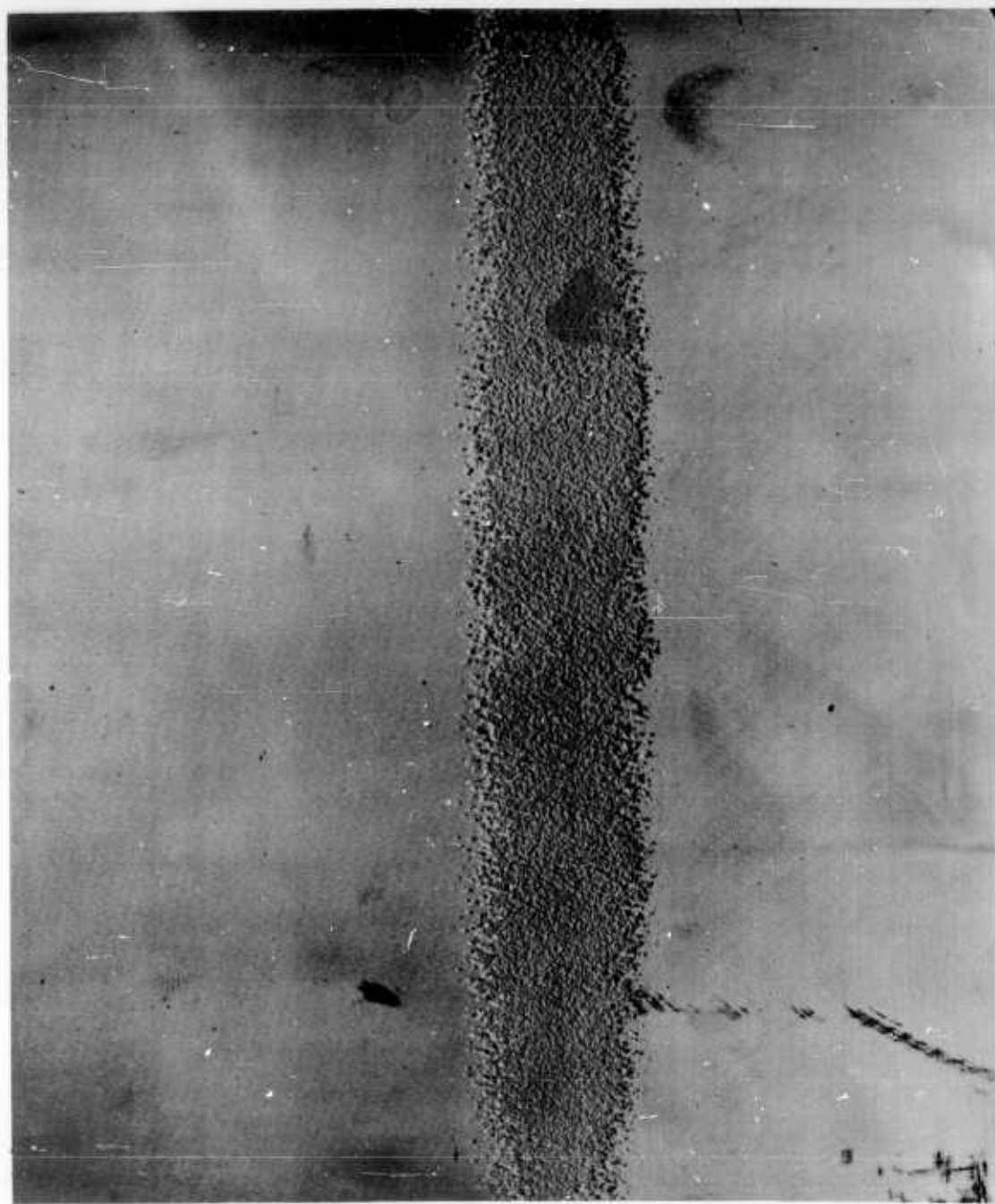


Fig. 25 - Close Up of External Surface of Fatigued Cylinder, Model J<sub>2</sub>



Fig. 26 - Appearance of Inside Surface of Fatigued Cylinder, Model J<sub>2</sub>



Fig. 27 - Close Up of Internal Surface of Fatigued Cylinder, Model J<sub>2</sub>

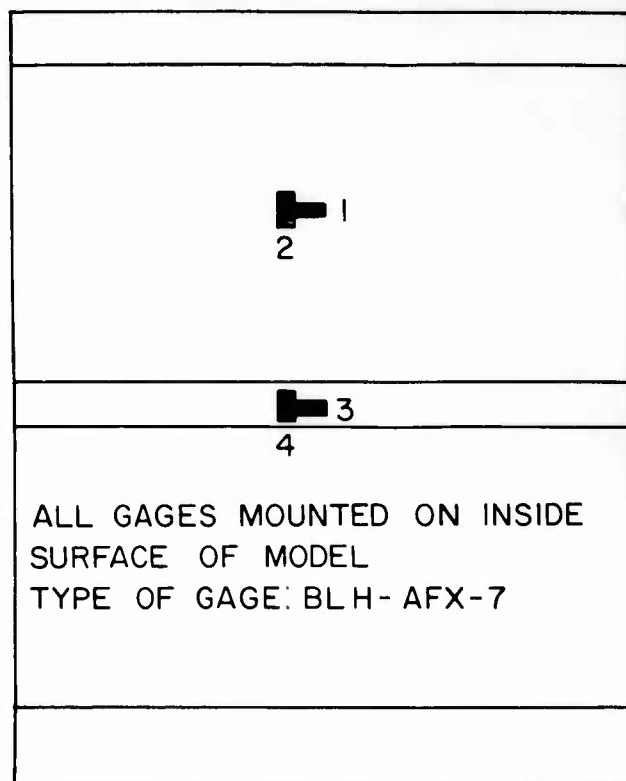


Fig. 28 - Location of Strain Gages inside Model I<sub>1</sub>



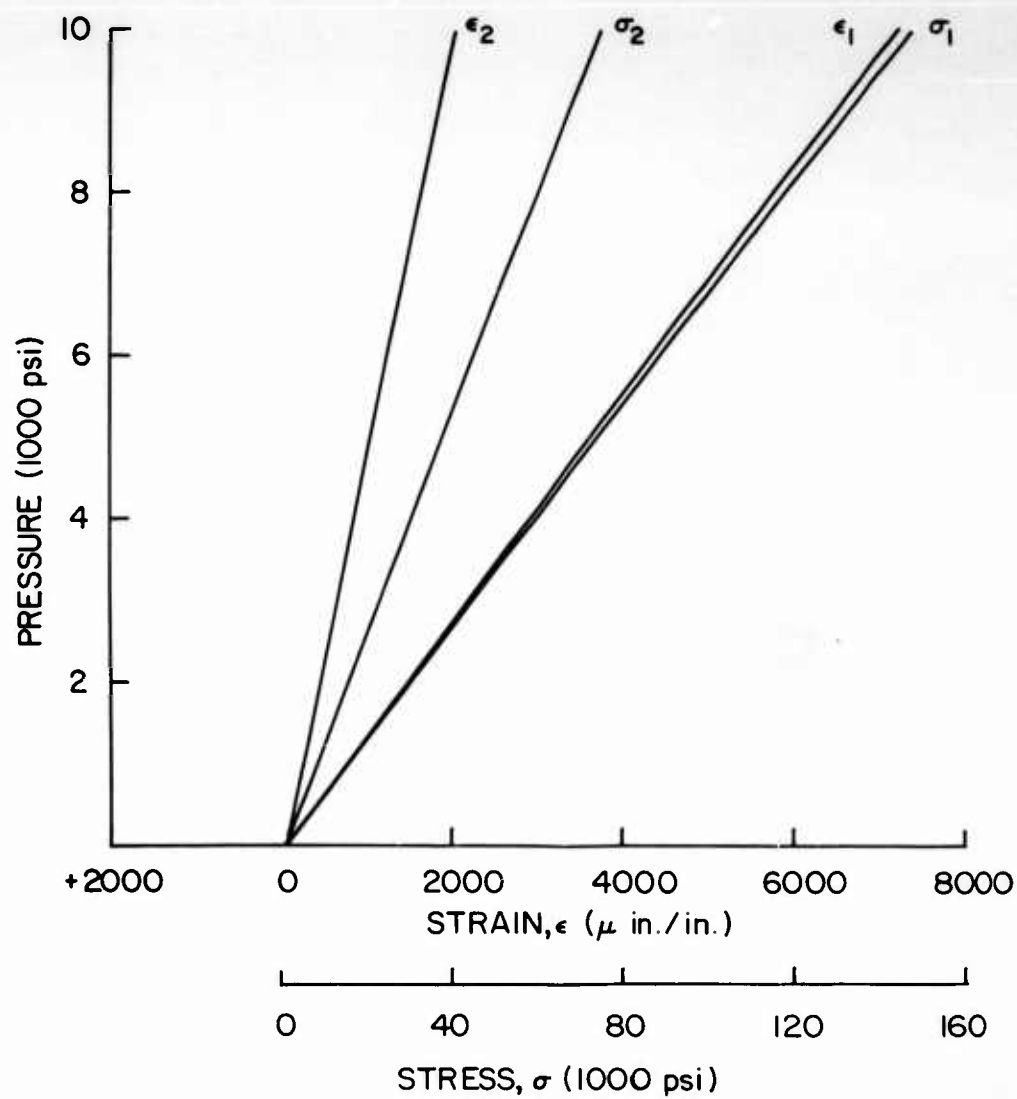


Fig. 29 - Strains and Stresses at Gages 1 and 2 of Model I<sub>1</sub>

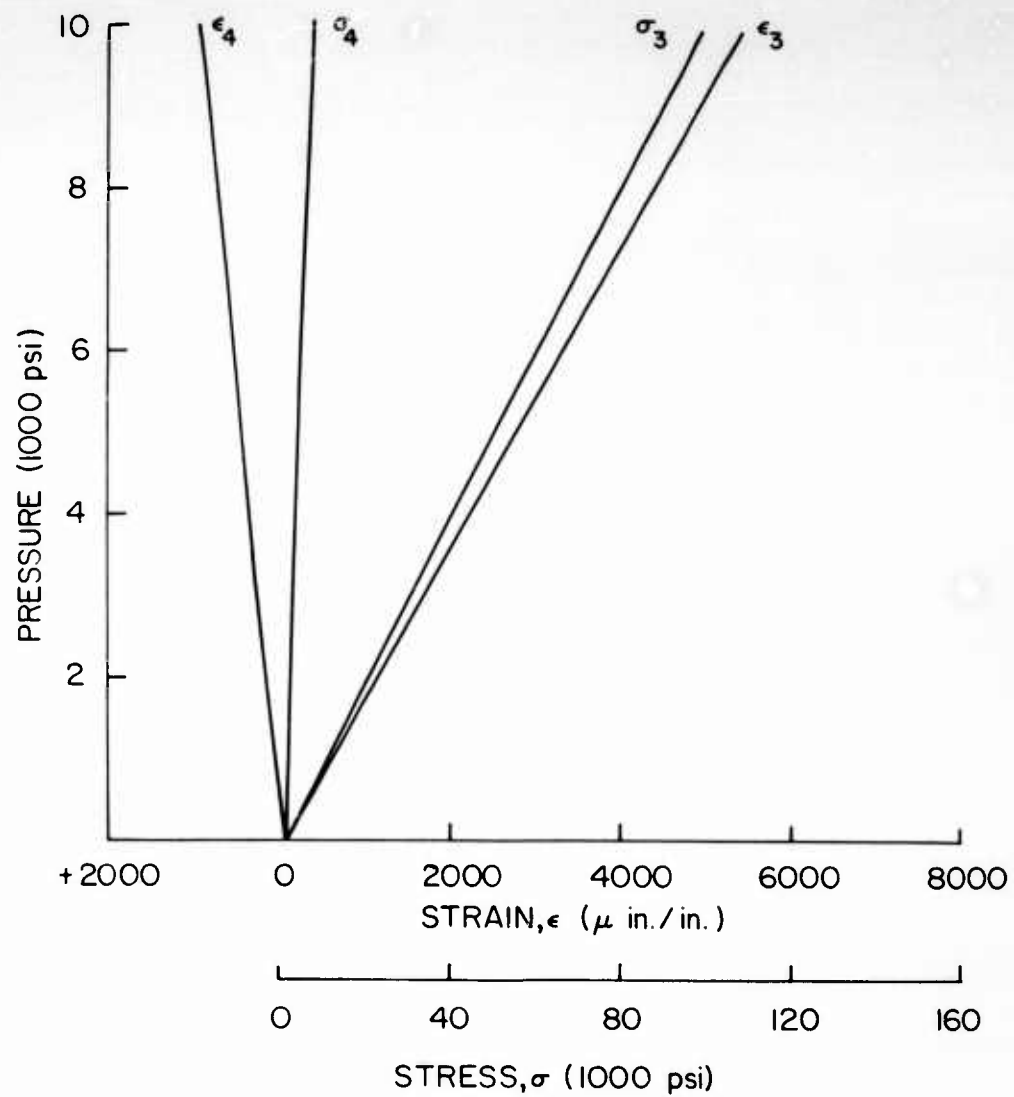


Fig. 30 - Strains and Stresses at Gages 3 and 4 of Mod. 1 I<sub>1</sub>

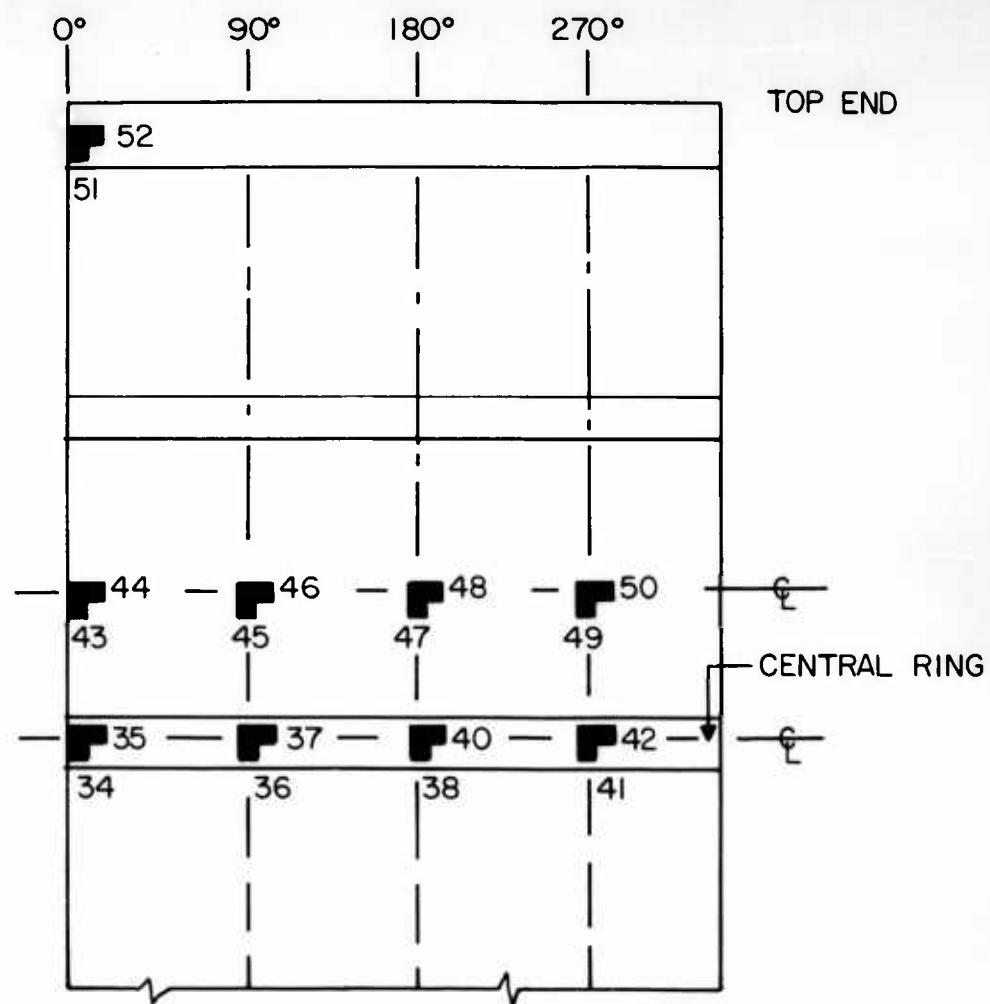


Fig. 31 - Location of Strain Gages inside Model J<sub>1</sub>

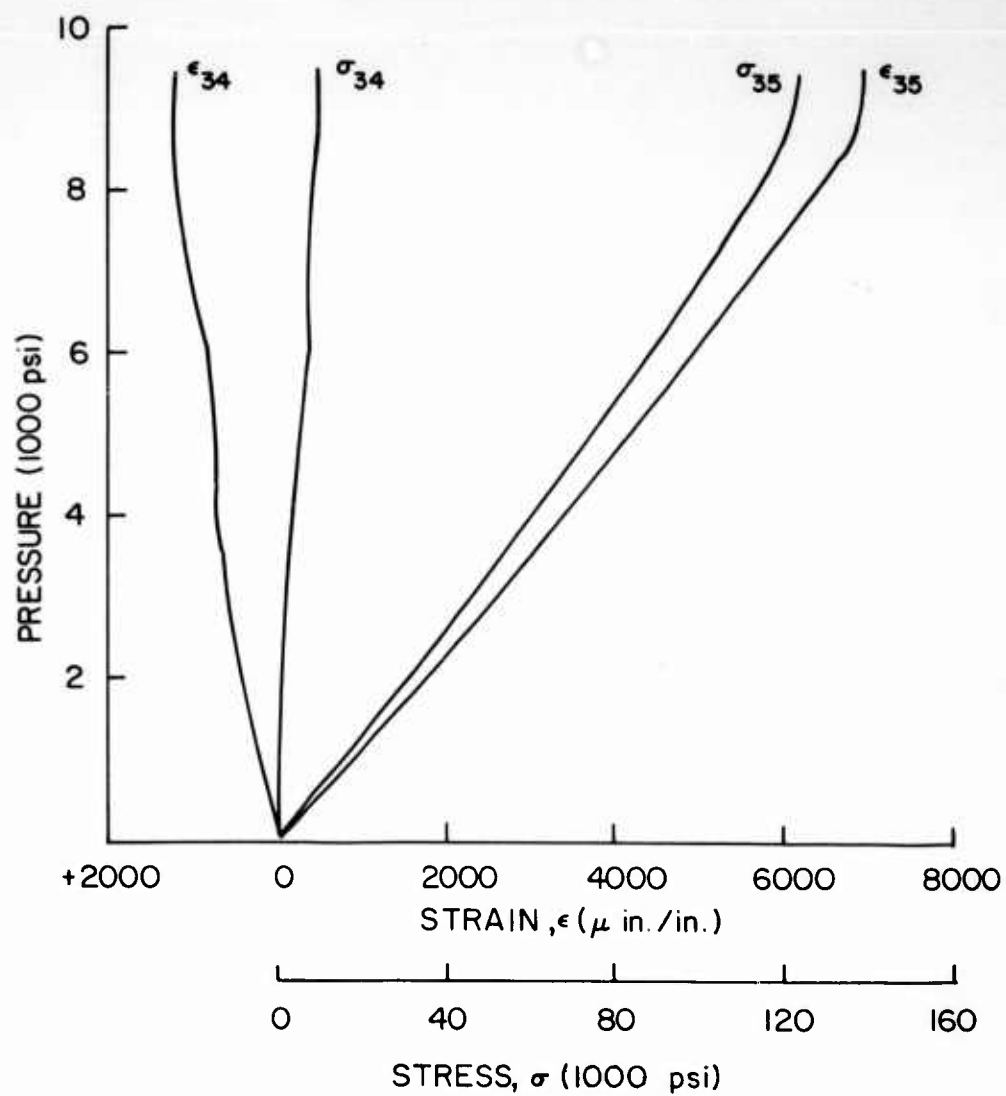


Fig. 32 - Strains and Stresses at Gages 34 and 35 of Model J<sub>1</sub>

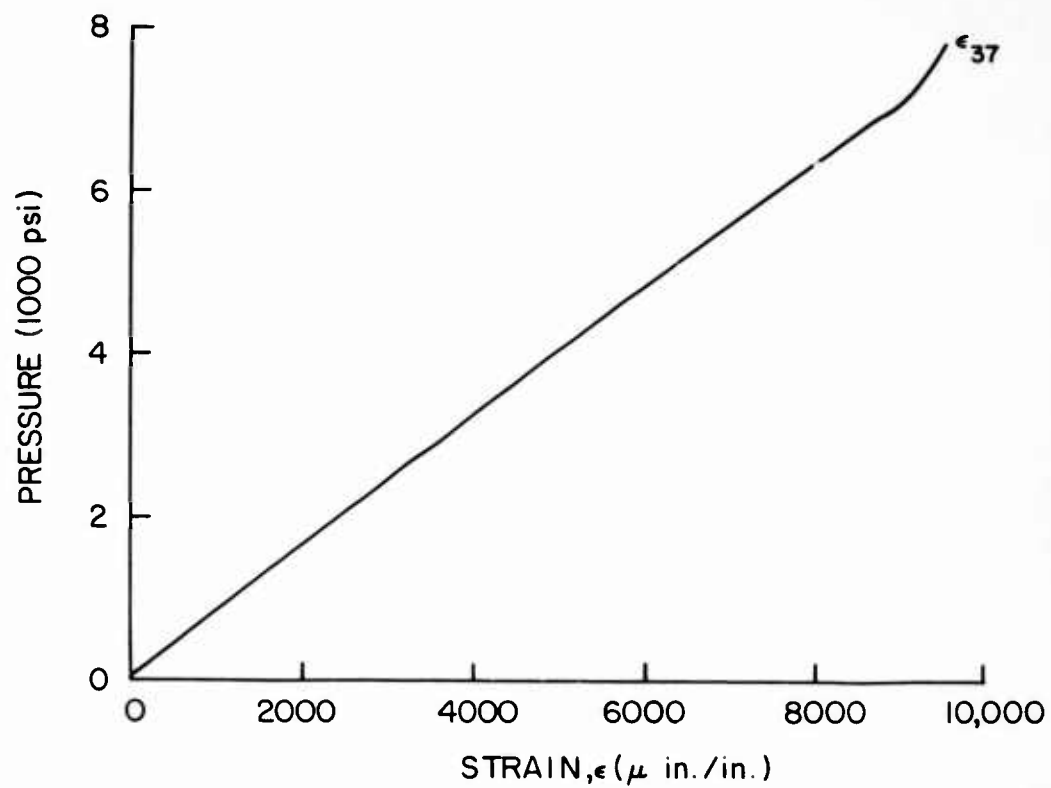


Fig. 33 - Strains at Gage 37 of Model J<sub>1</sub>

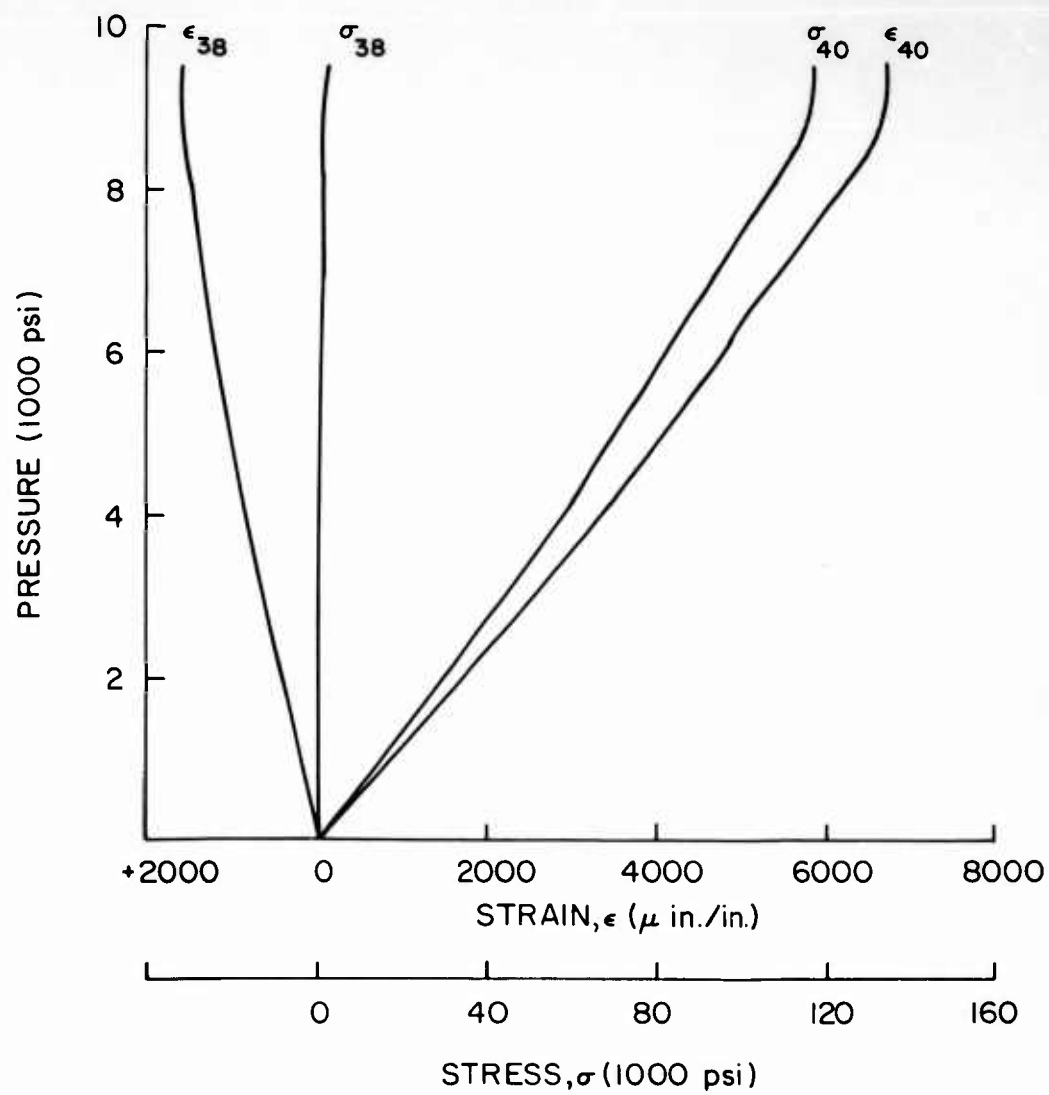


Fig. 34 - Strains and Stresses at Gages 38 and 40 of Model J<sub>1</sub>

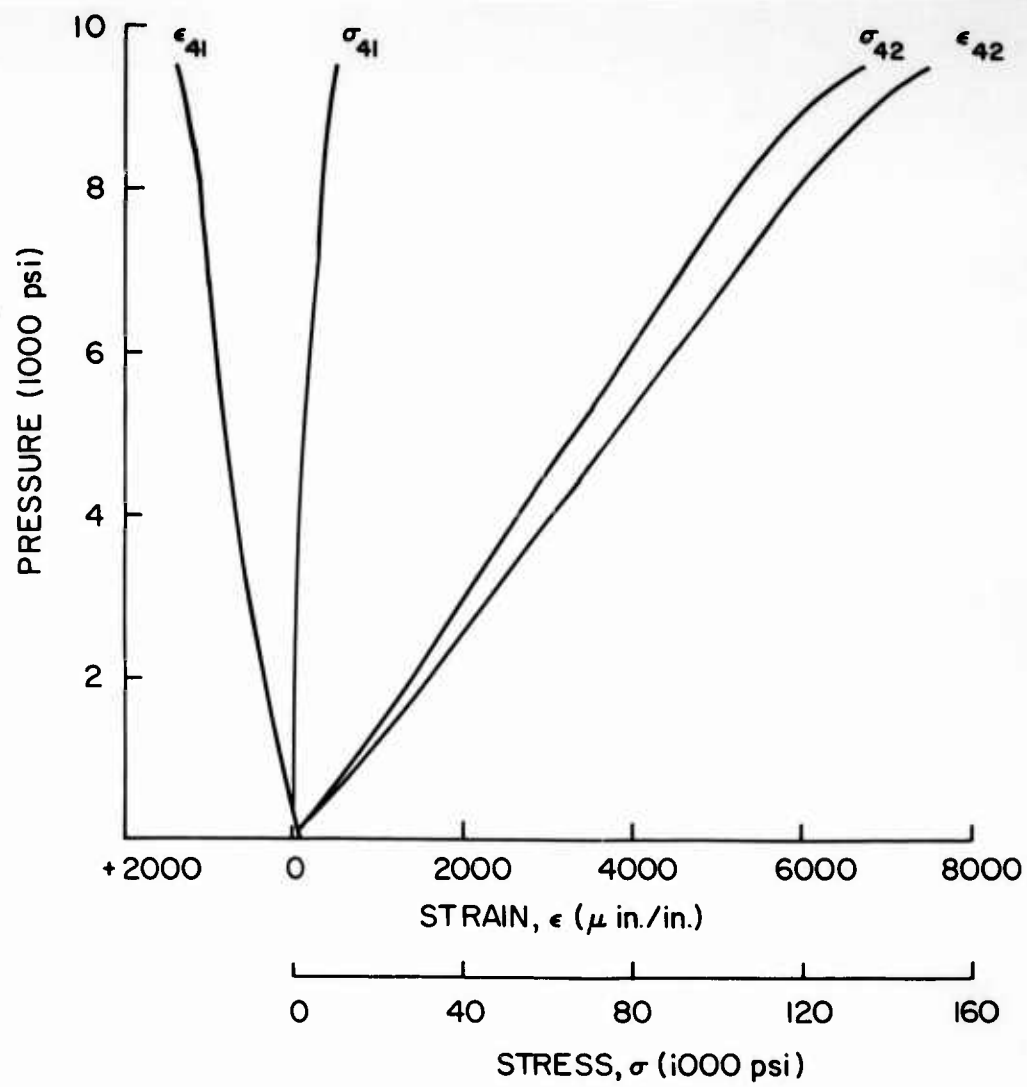


Fig. 35 - Strains and Stresses at Gages 41 and 42 of Model J<sub>1</sub>

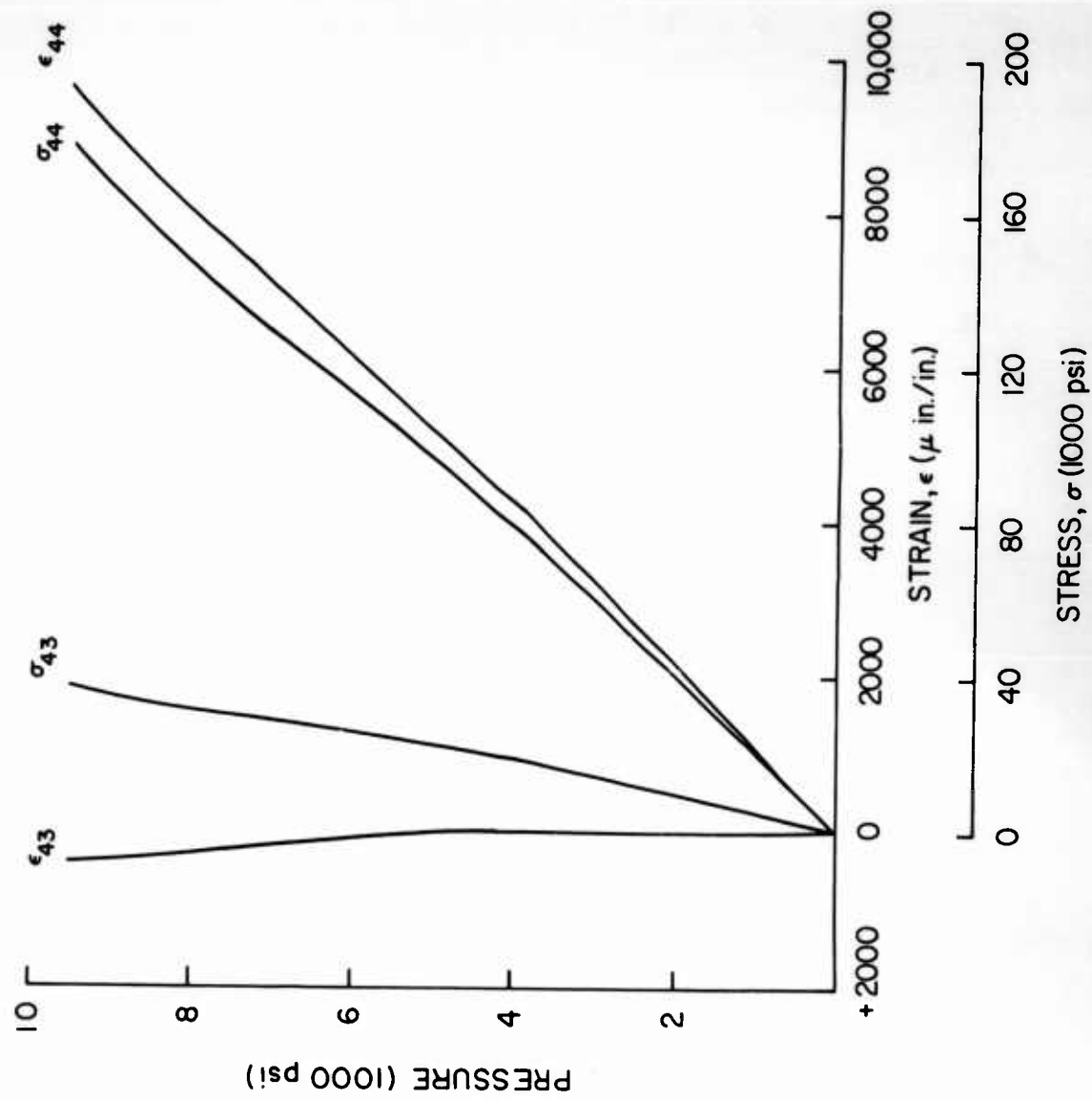


Fig. 36 - Strains and Stresses at Gages 43 and 44 of Model J<sub>1</sub>



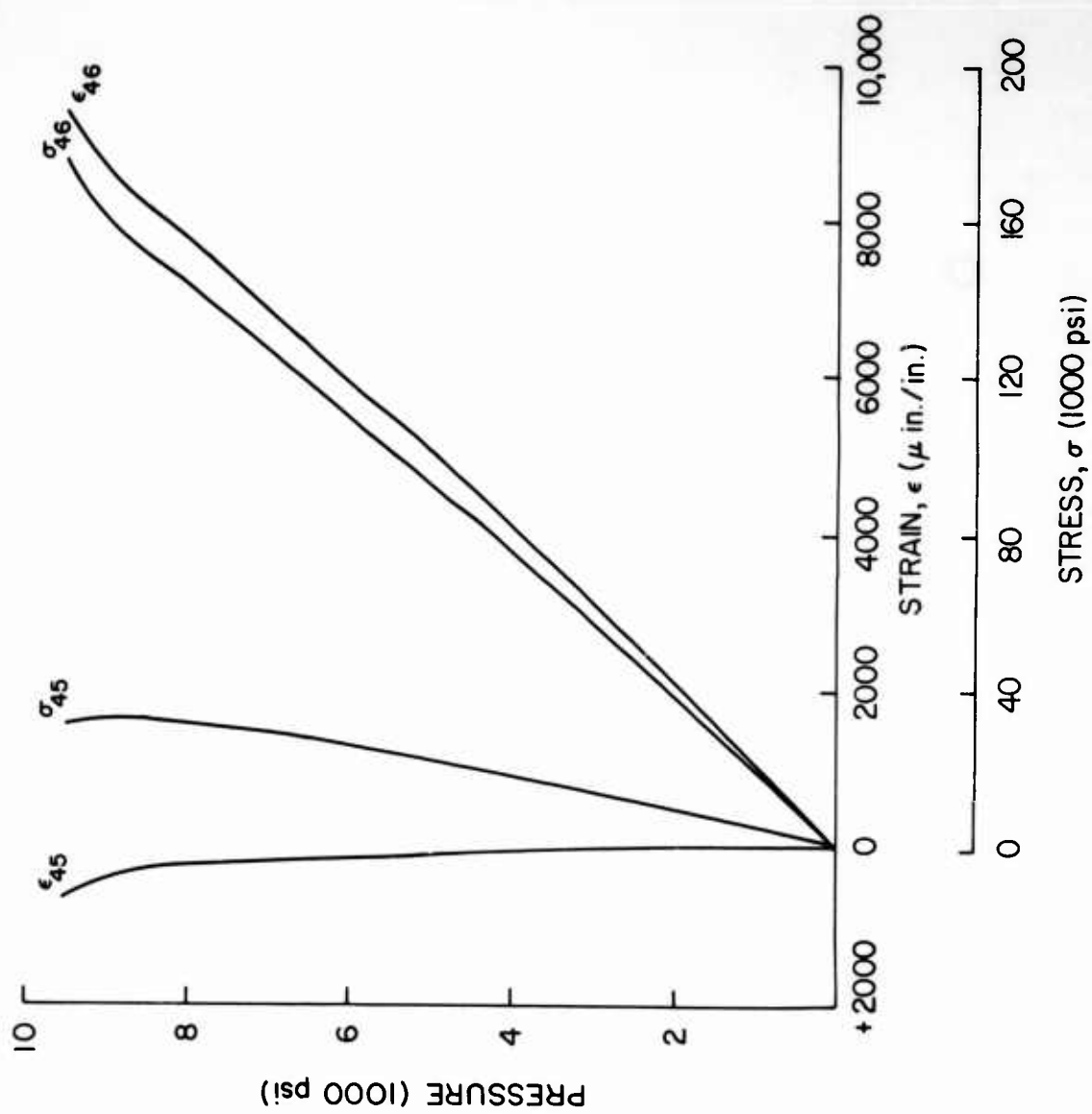


Fig. 37 - Strains and Stresses at Gages 45 and 46 of Model J<sub>1</sub>

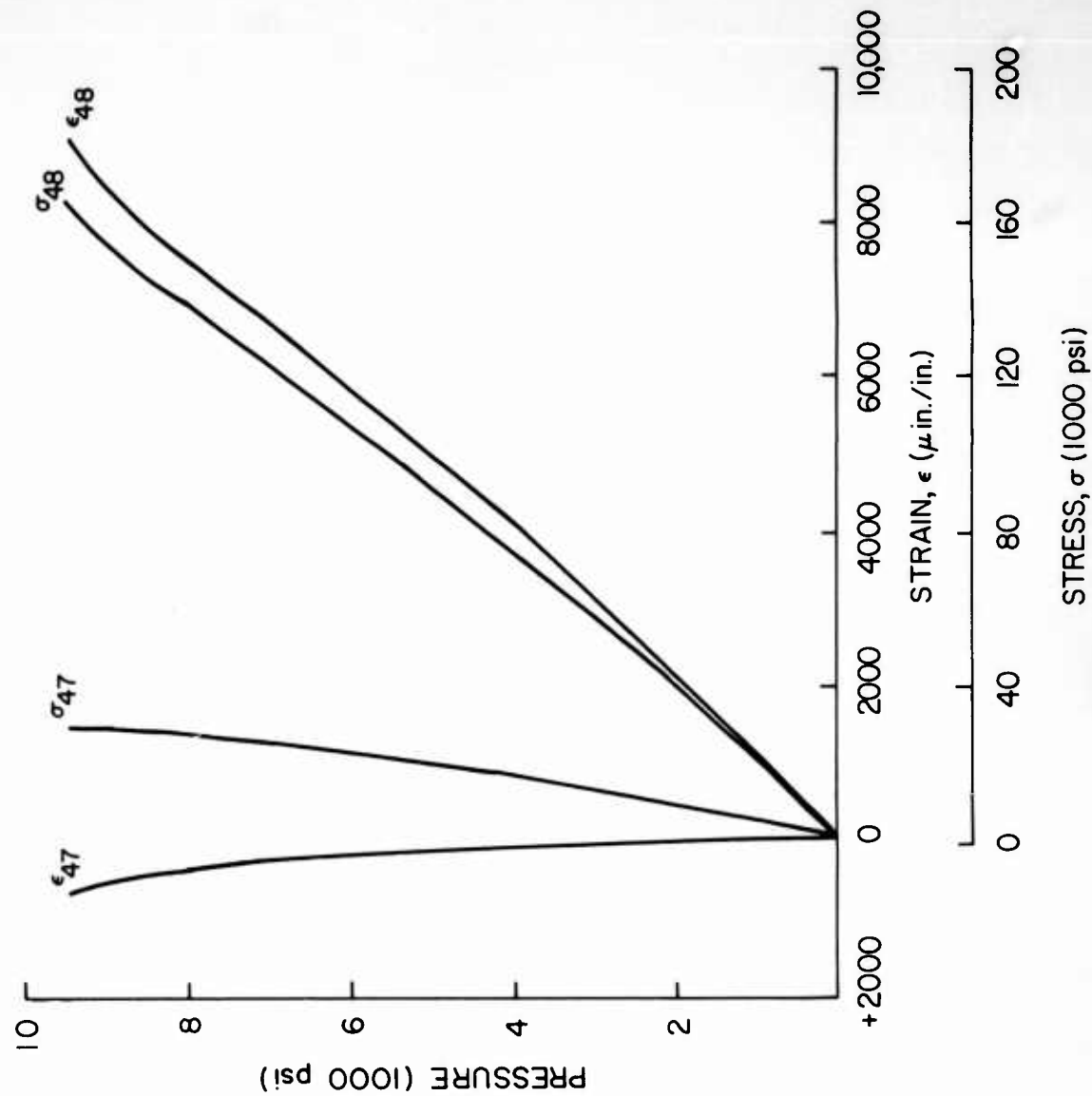


Fig. 38 - Strains and Stresses at Gages 47 and 48 of Model J<sub>1</sub>

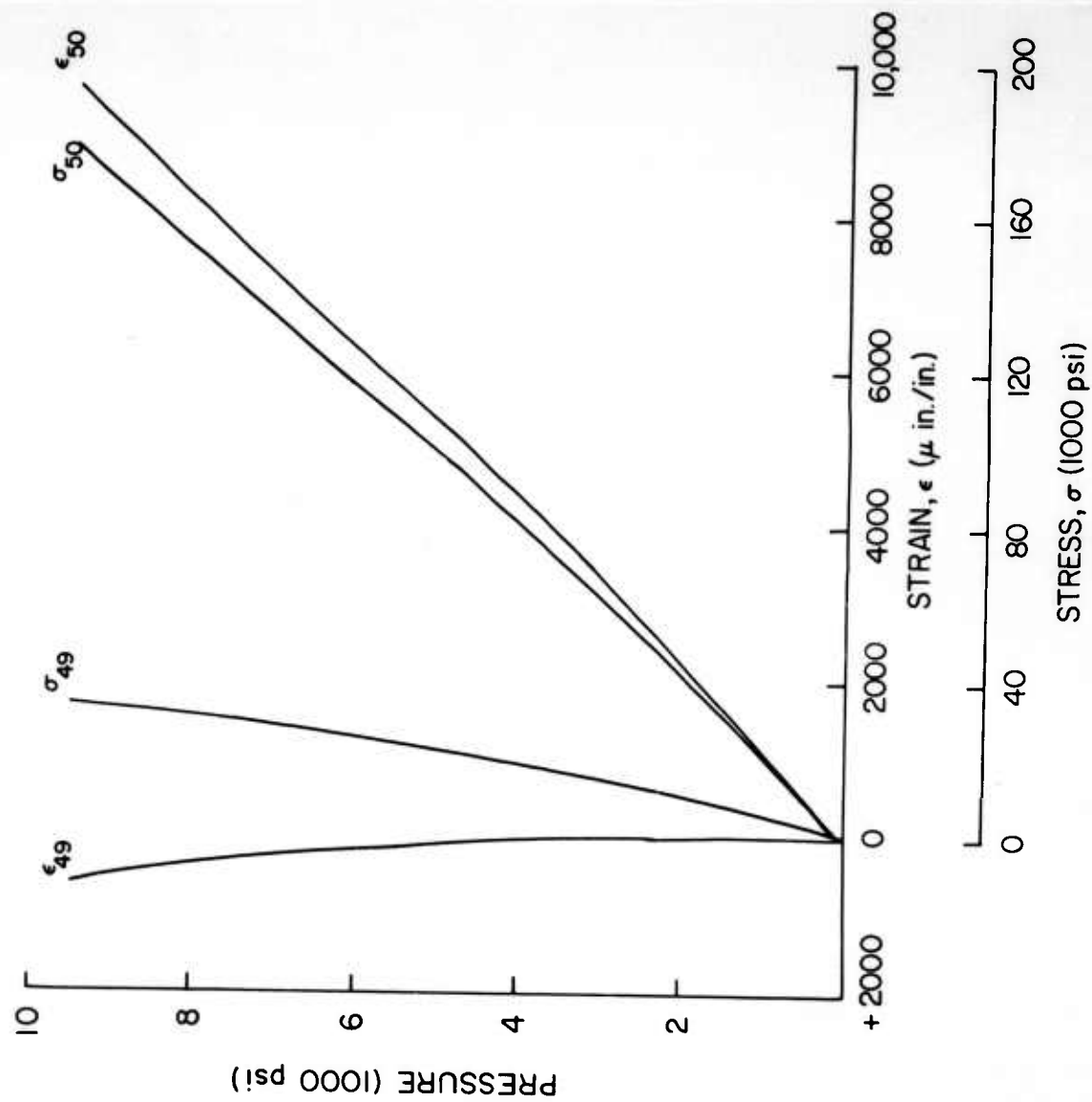


Fig. 39 - Strains and Stresses at Gages 49 and 50 of Model J<sub>1</sub>

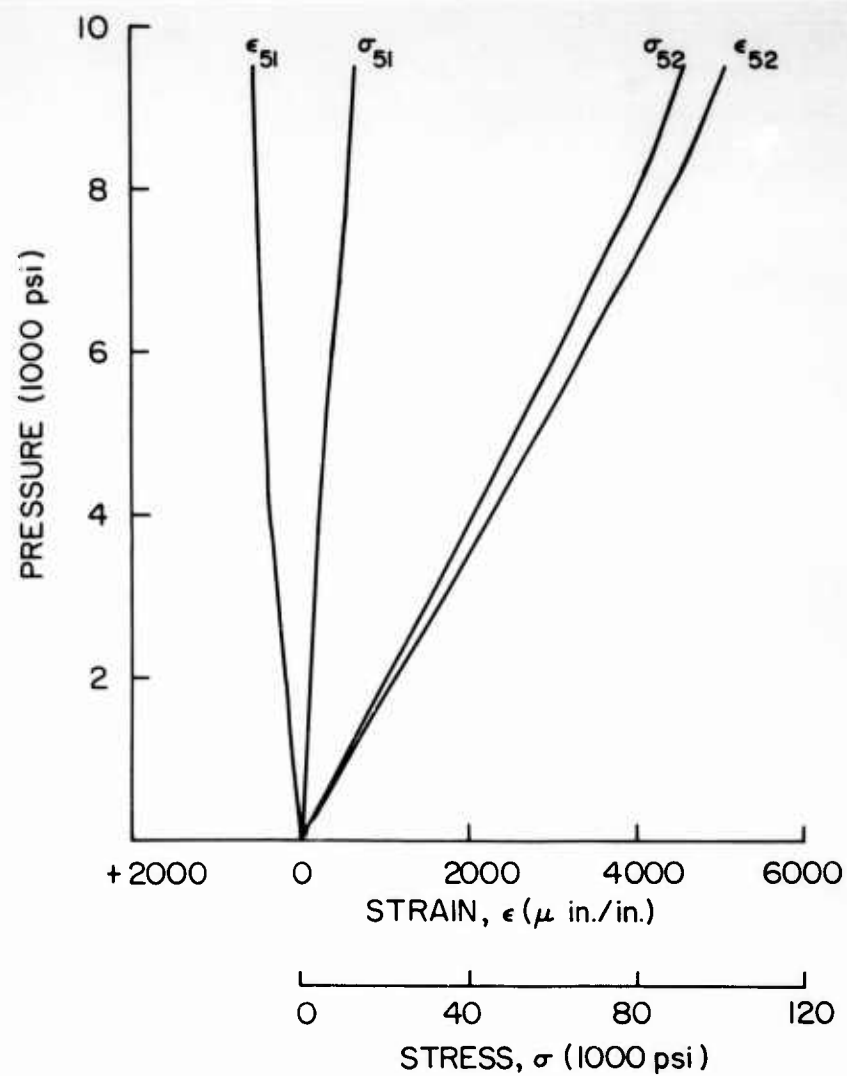


Fig. 40 - Strains and Stresses at Gages 51 and 52 of Model J<sub>1</sub>

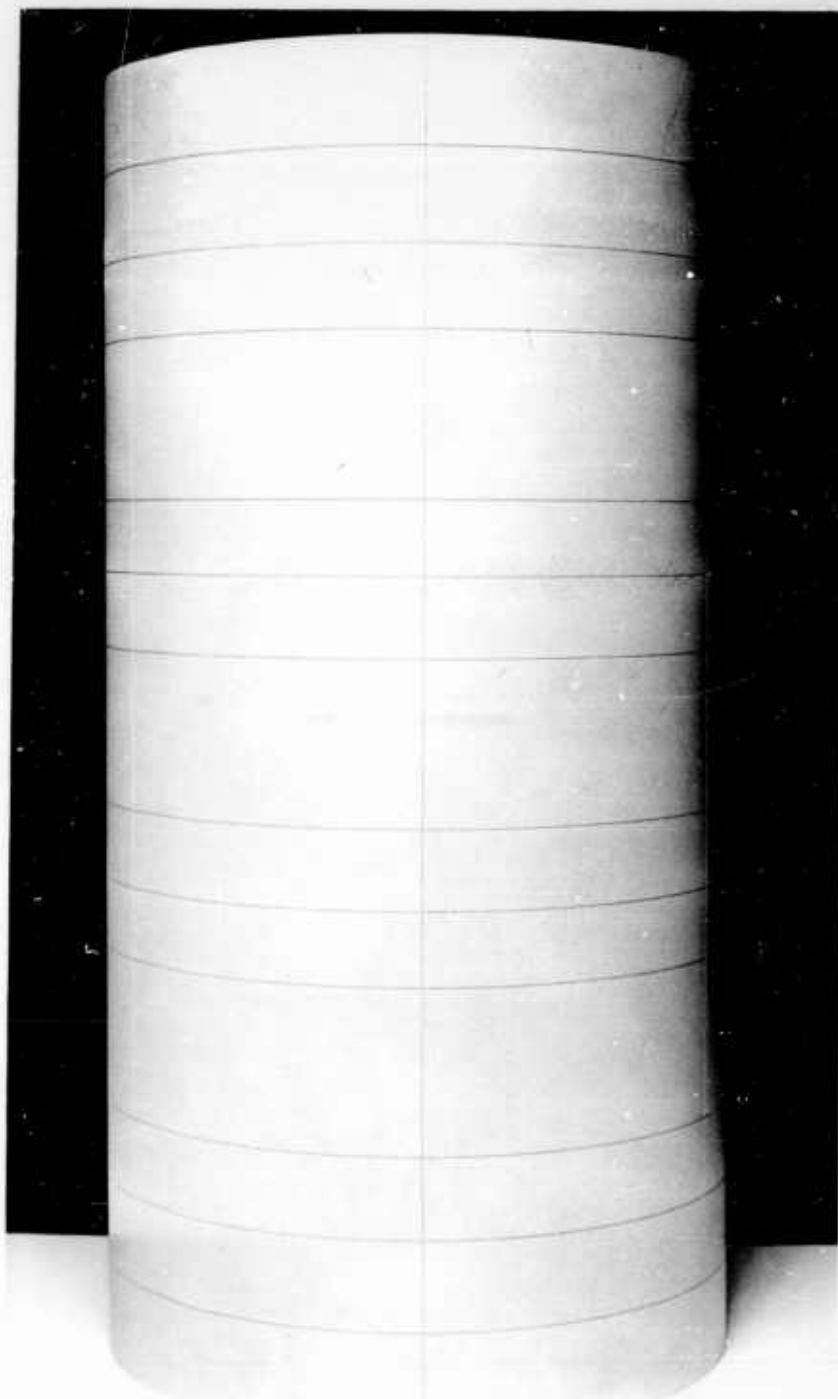


Fig. 41 - Model J<sub>2</sub> Showing Marks Scratched on Surface  
after Fatigue Test and before Implosion

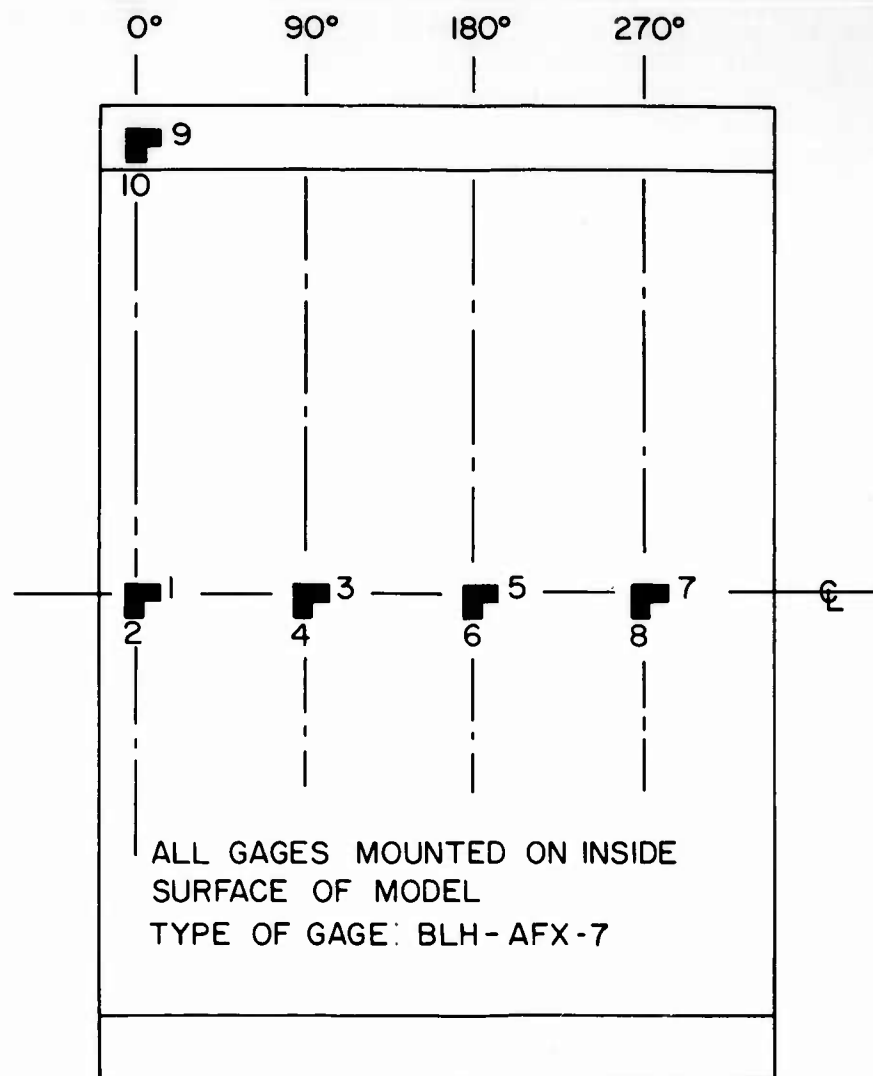


Fig. 42 - Location of Strain Gages inside Models K<sub>1</sub> and K<sub>2</sub>

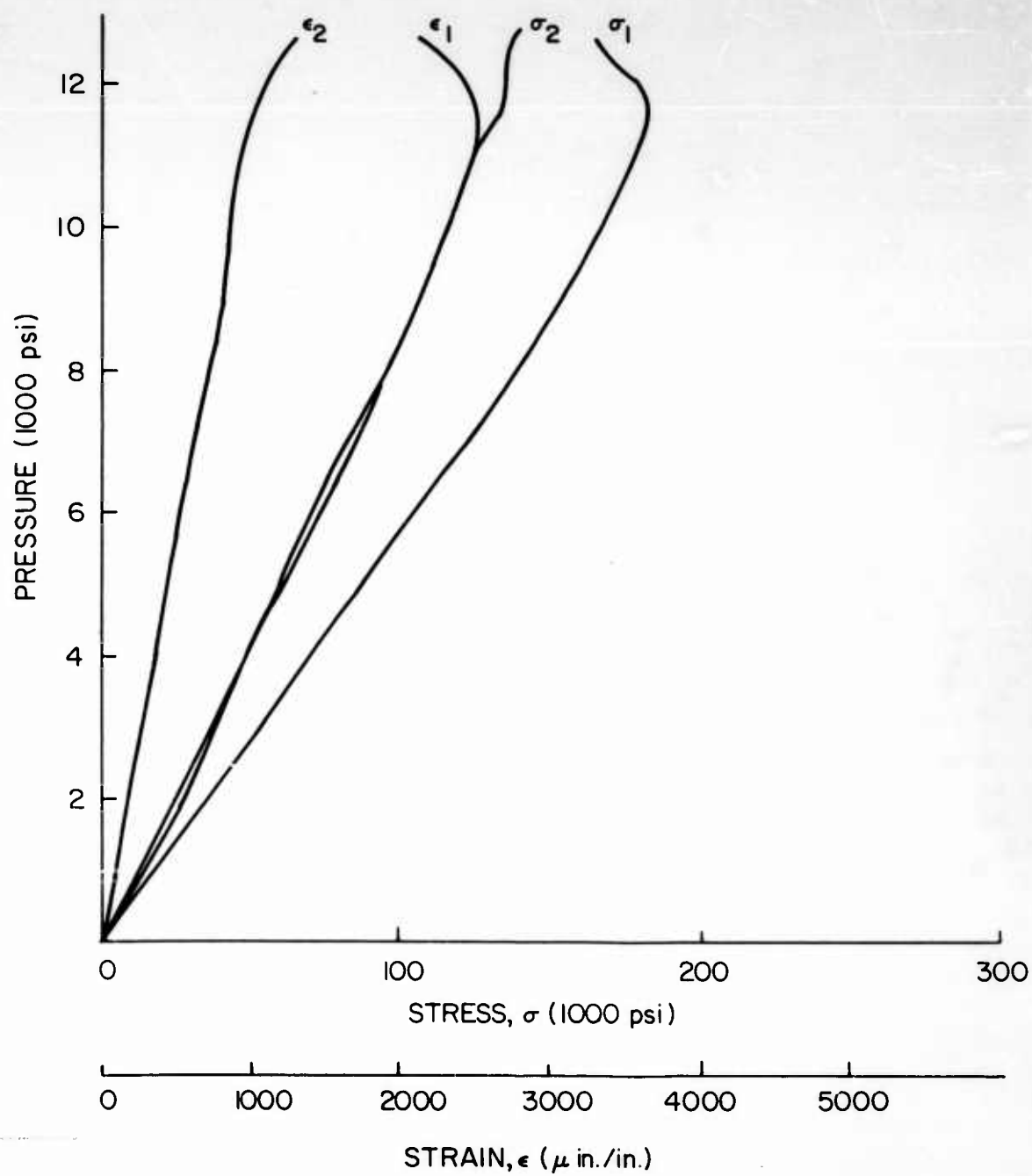


Fig. 43 - Strains and Stresses at Gages 1 and 2 of Model K<sub>1</sub>

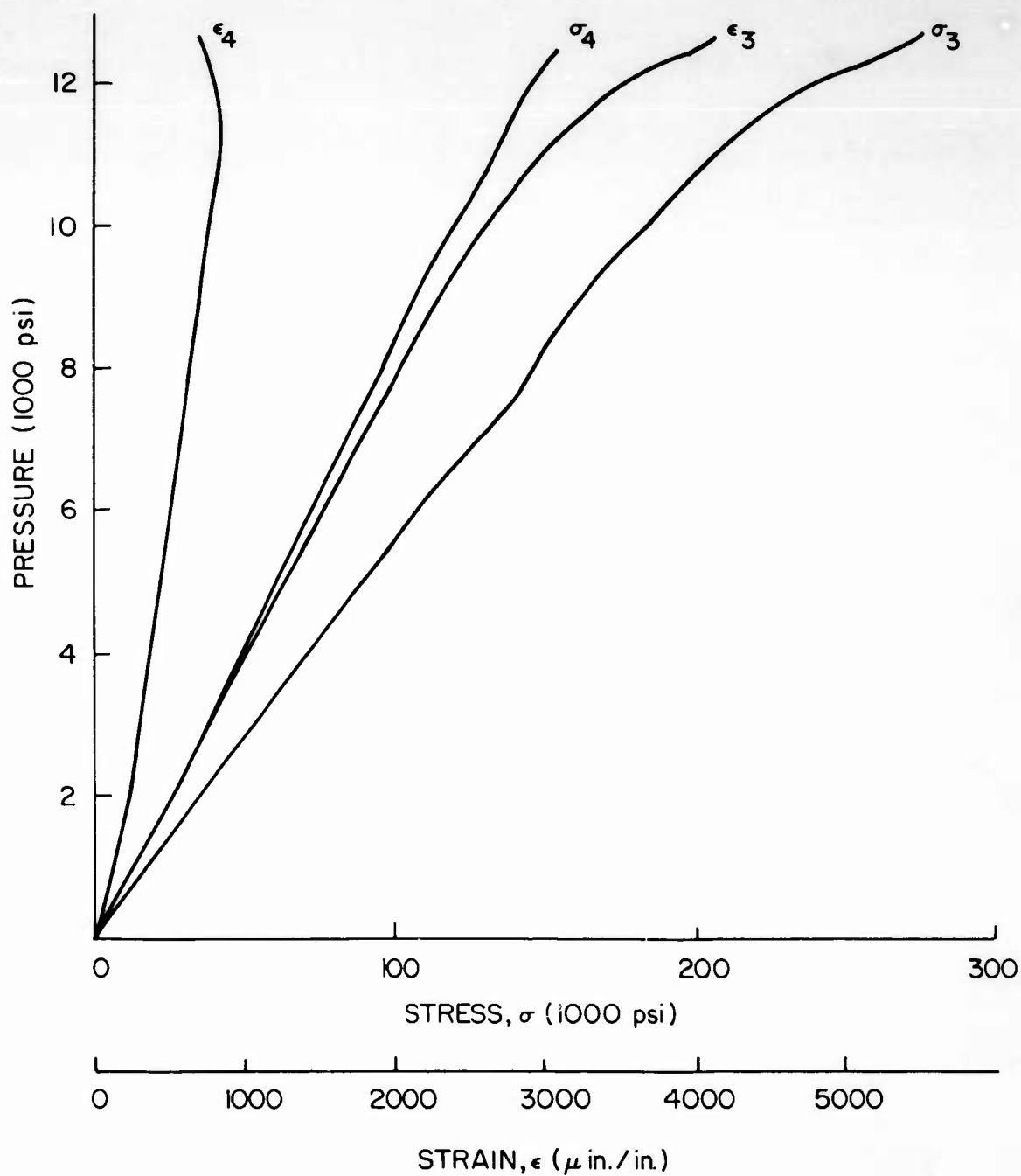


Fig. 44 - Strains and Stresses at Gages 3 and 4 of Model K<sub>1</sub>



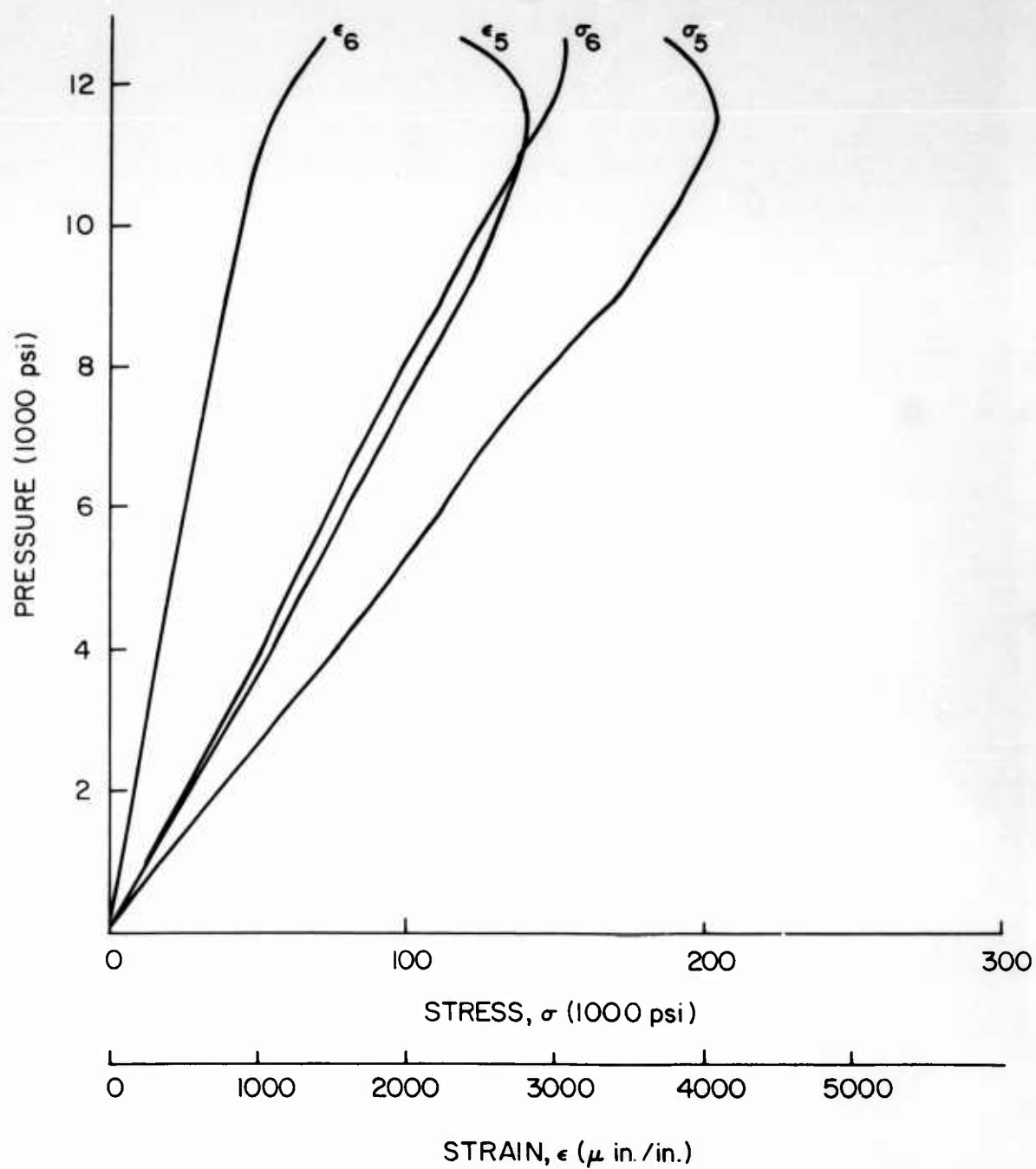


Fig. 45 - Strains and Stresses at Gages 5 and 6 of Model K<sub>1</sub>

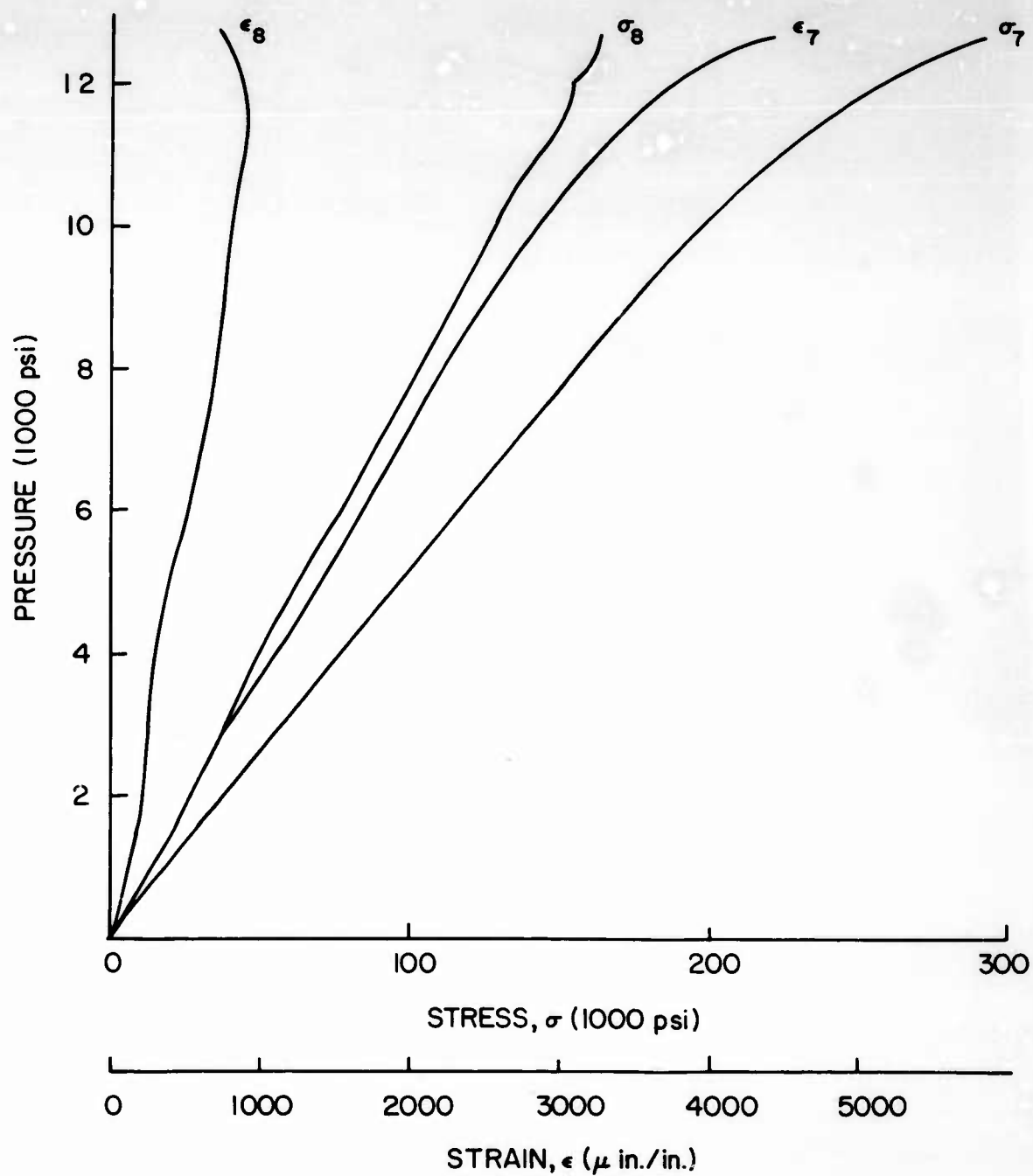


Fig. 46 - Strains and Stresses at Gages 7 and 8 of Model K<sub>1</sub>

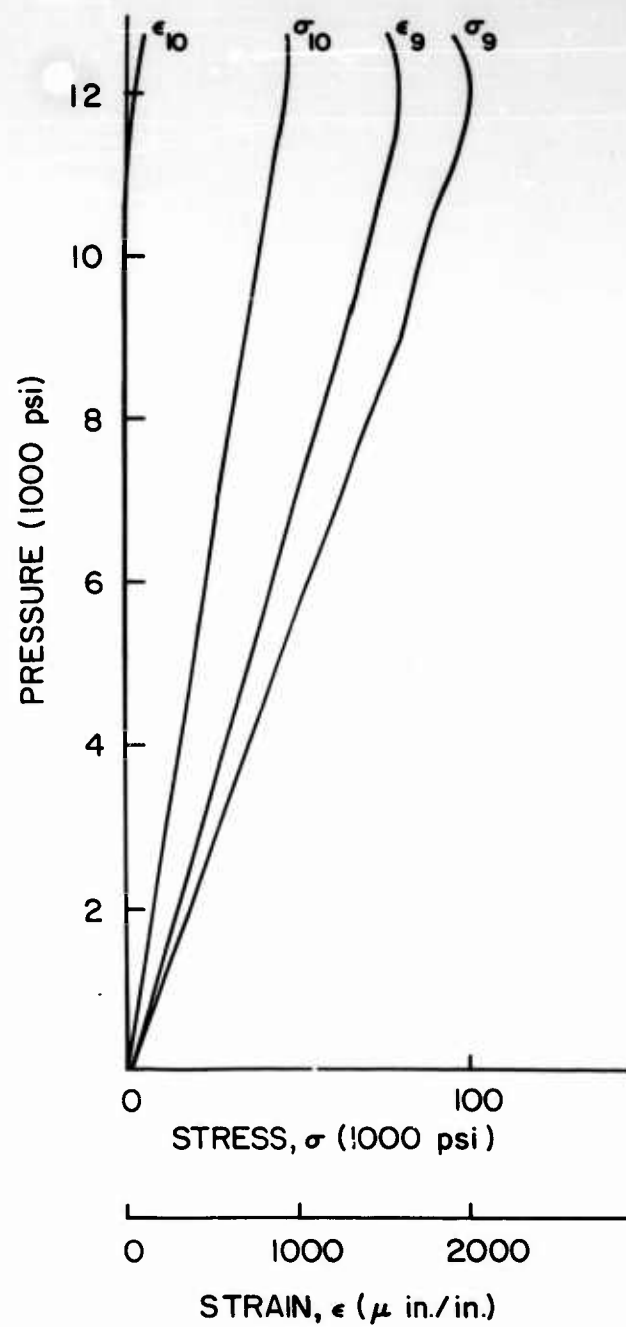


Fig. 47 - Strains and Stresses at Gages 9 and 10 of Model K<sub>1</sub>

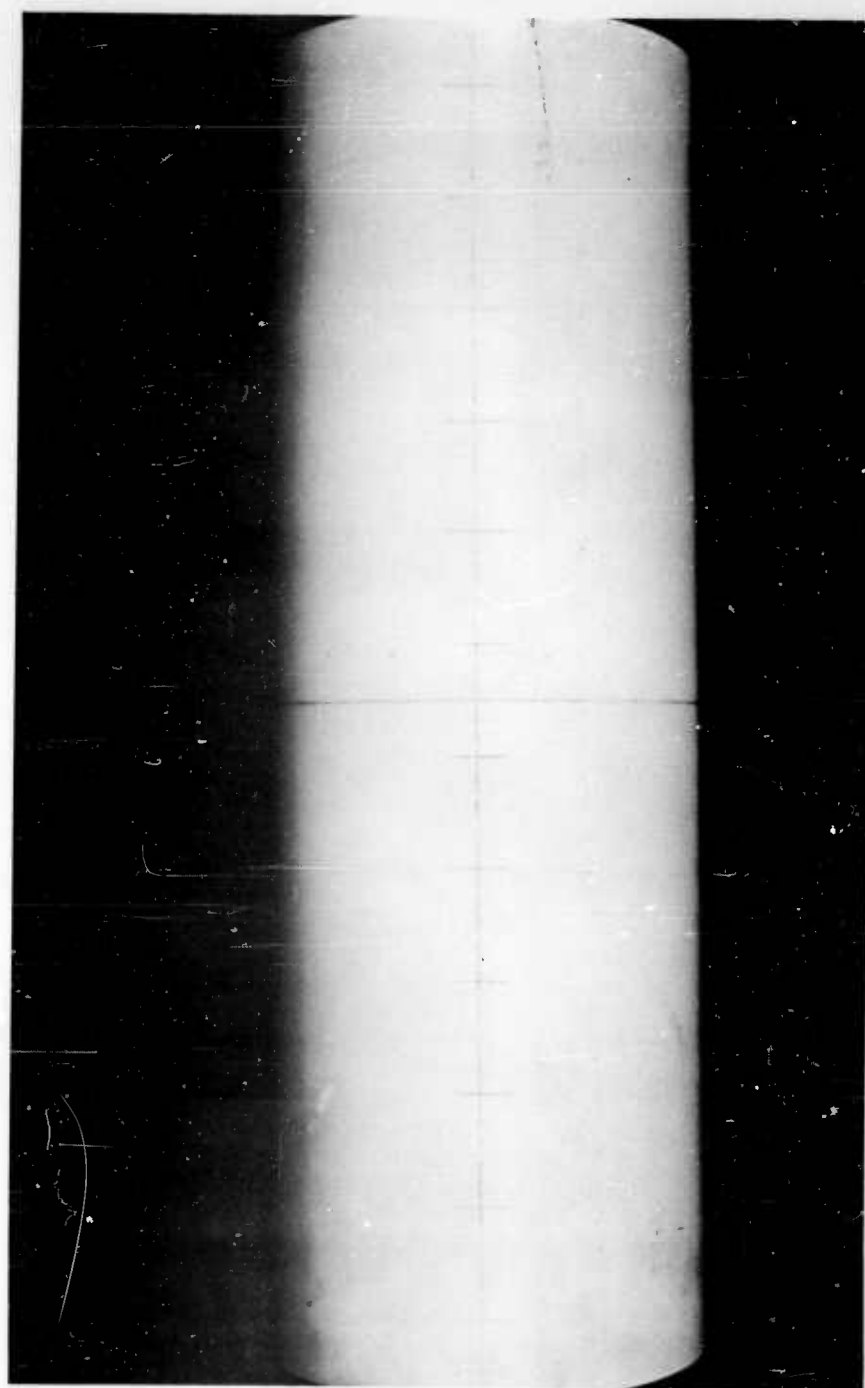


Fig. 48 - Location of Scratches on Model K<sub>2</sub> before Implosion

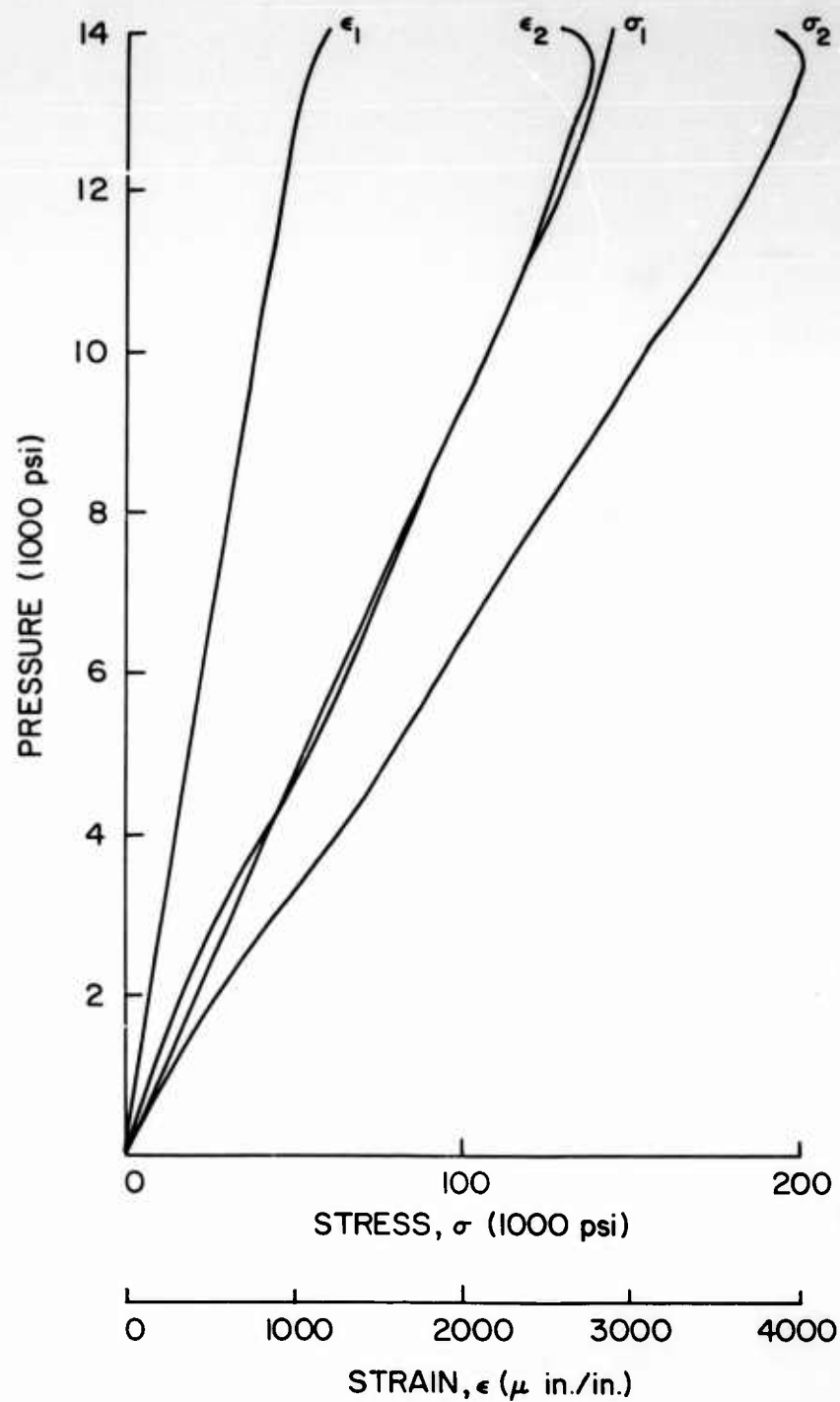


Fig. 49 - Strains and Stresses at Gages 1 and 2 of Model K<sub>2</sub>

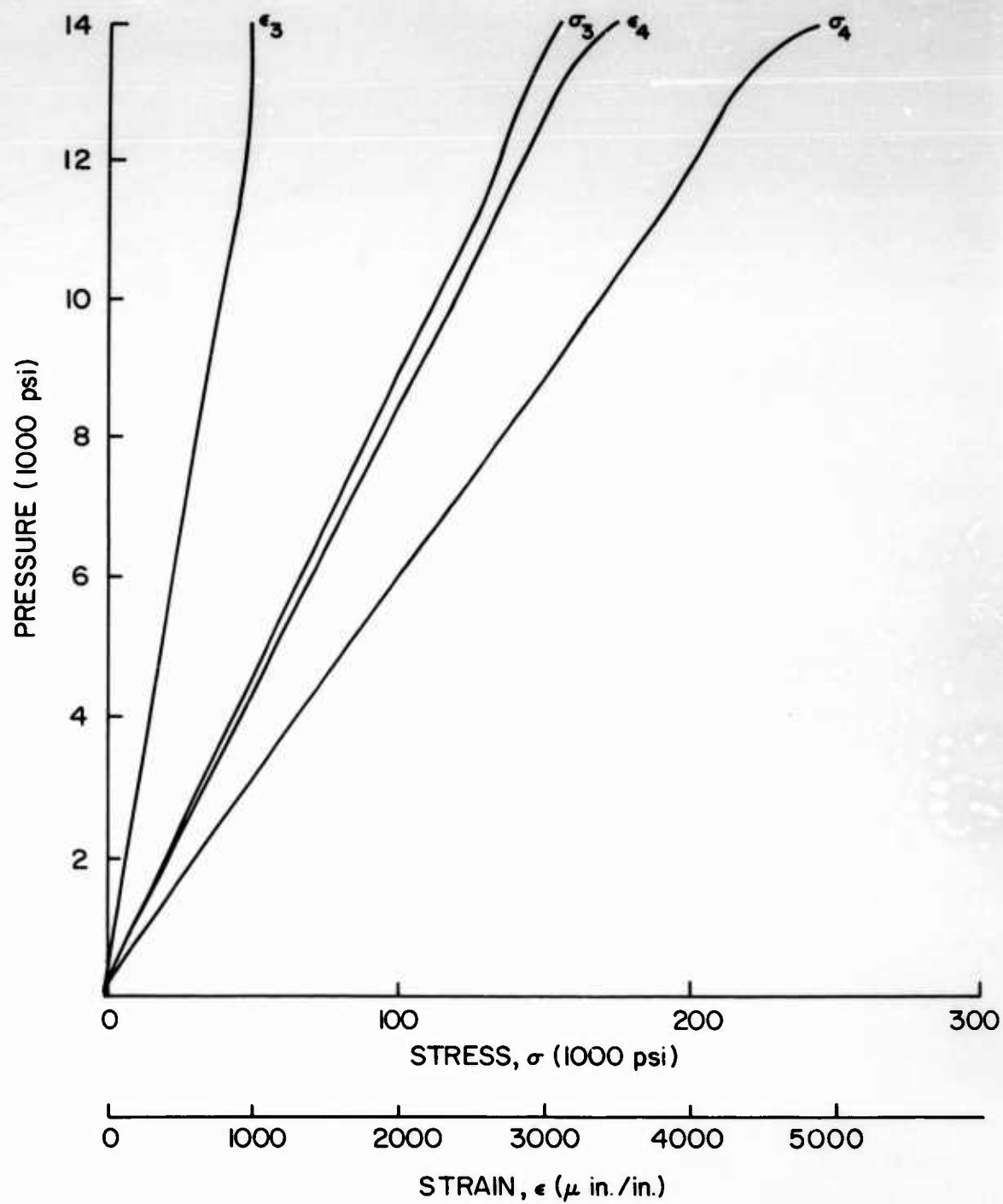


Fig. 50 - Strains and Stresses at Gages 3 and 4 of Model K<sub>2</sub>

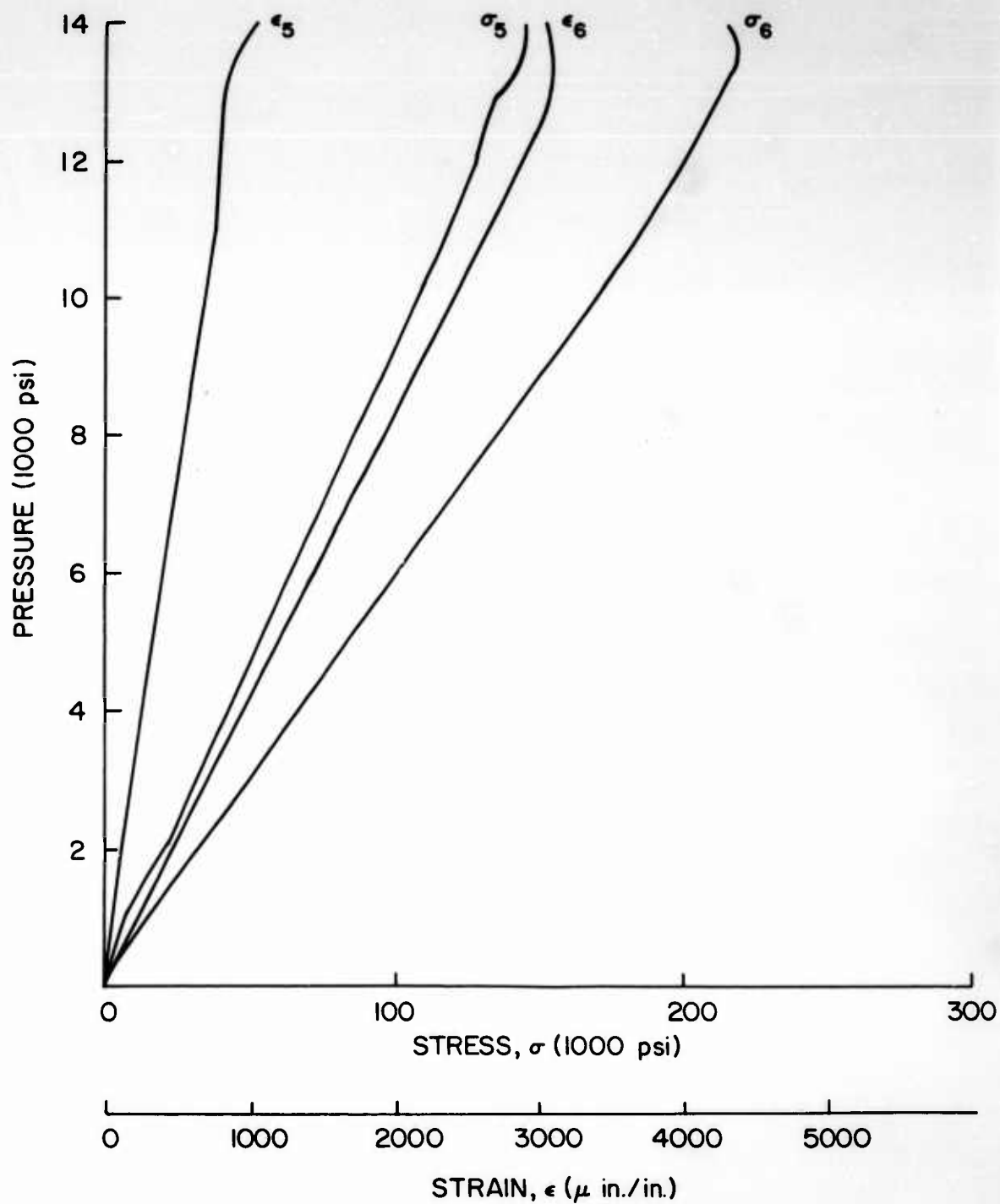


Fig. 51 - Strains and Stresses at Gages 5 and 6 of Model K<sub>2</sub>

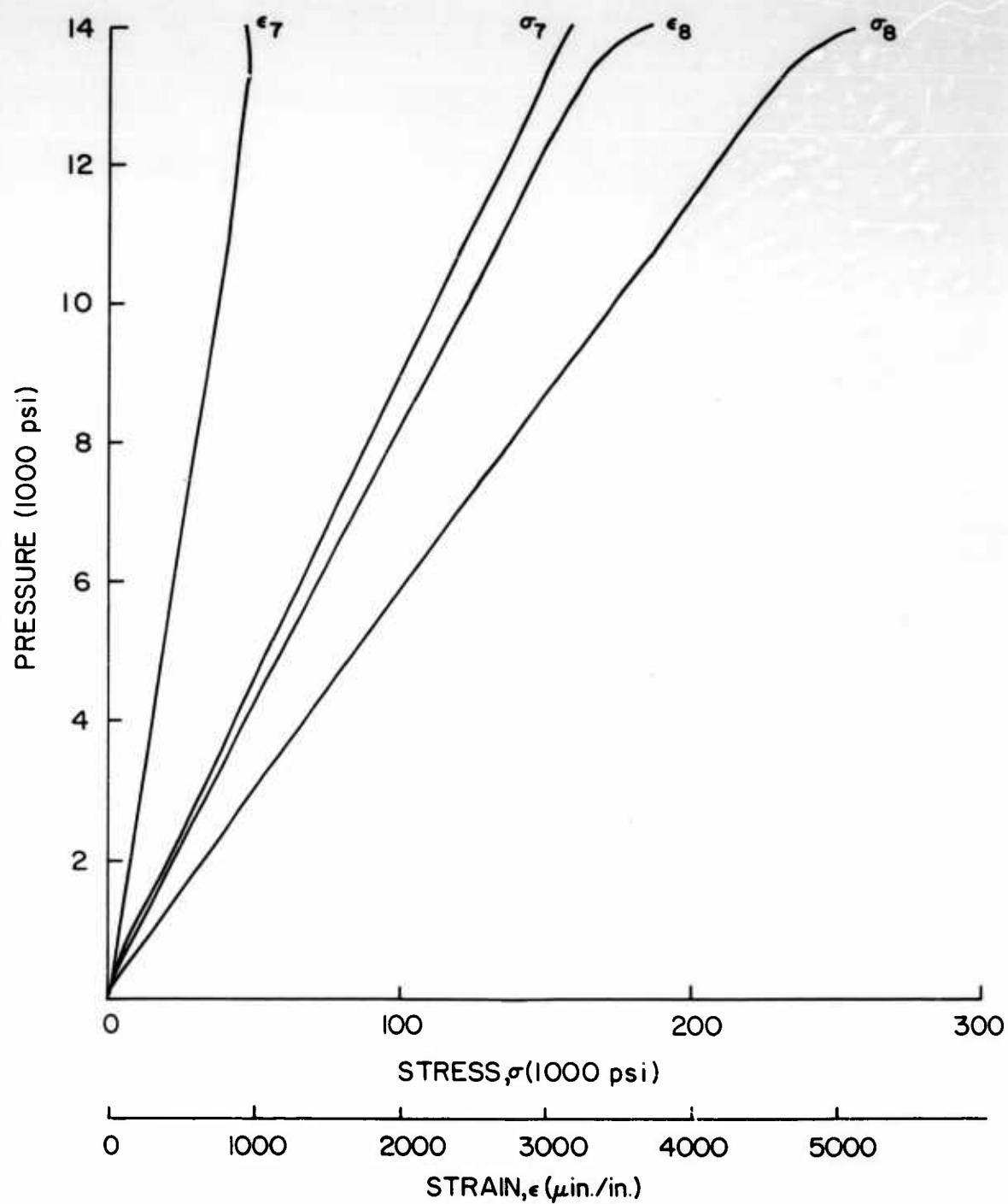


Fig. 52 - Strains and Stresses at Gages 7 and 8 of Model K<sub>2</sub>



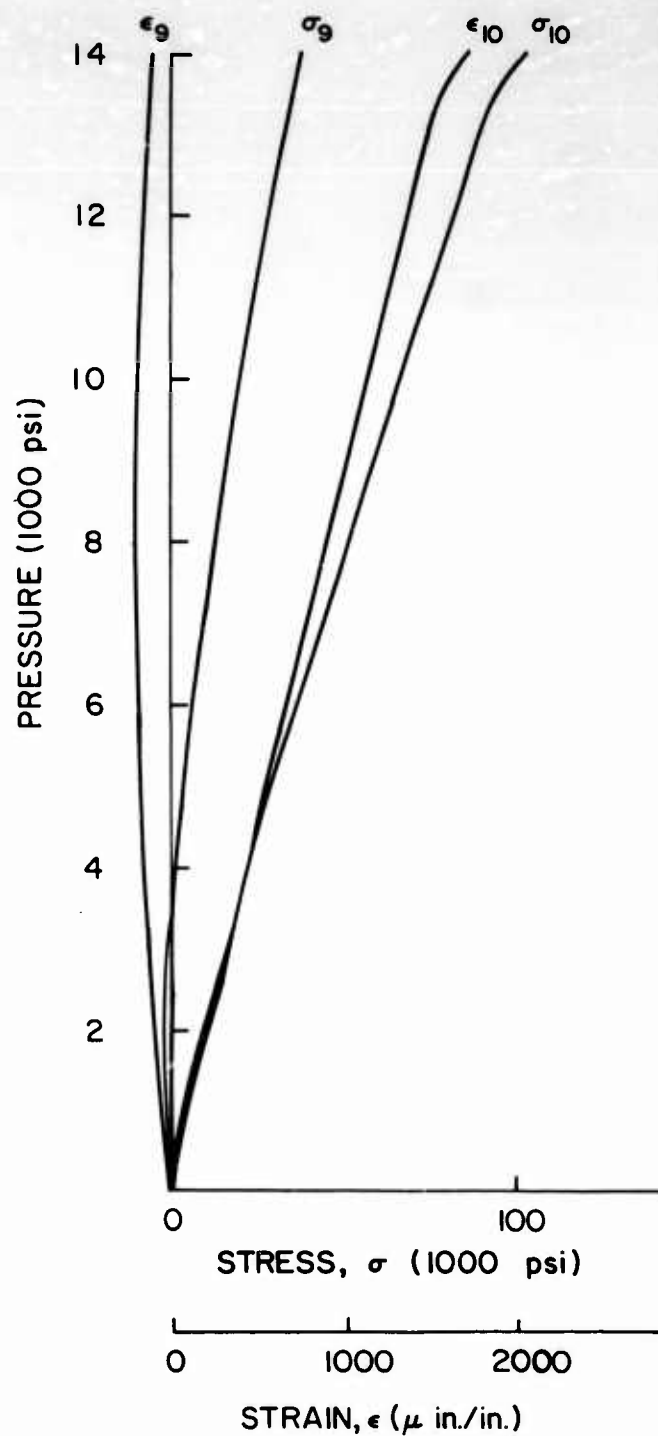


Fig. 53 - Strains and Stresses at Gages 9 and 10 of Model K<sub>2</sub>

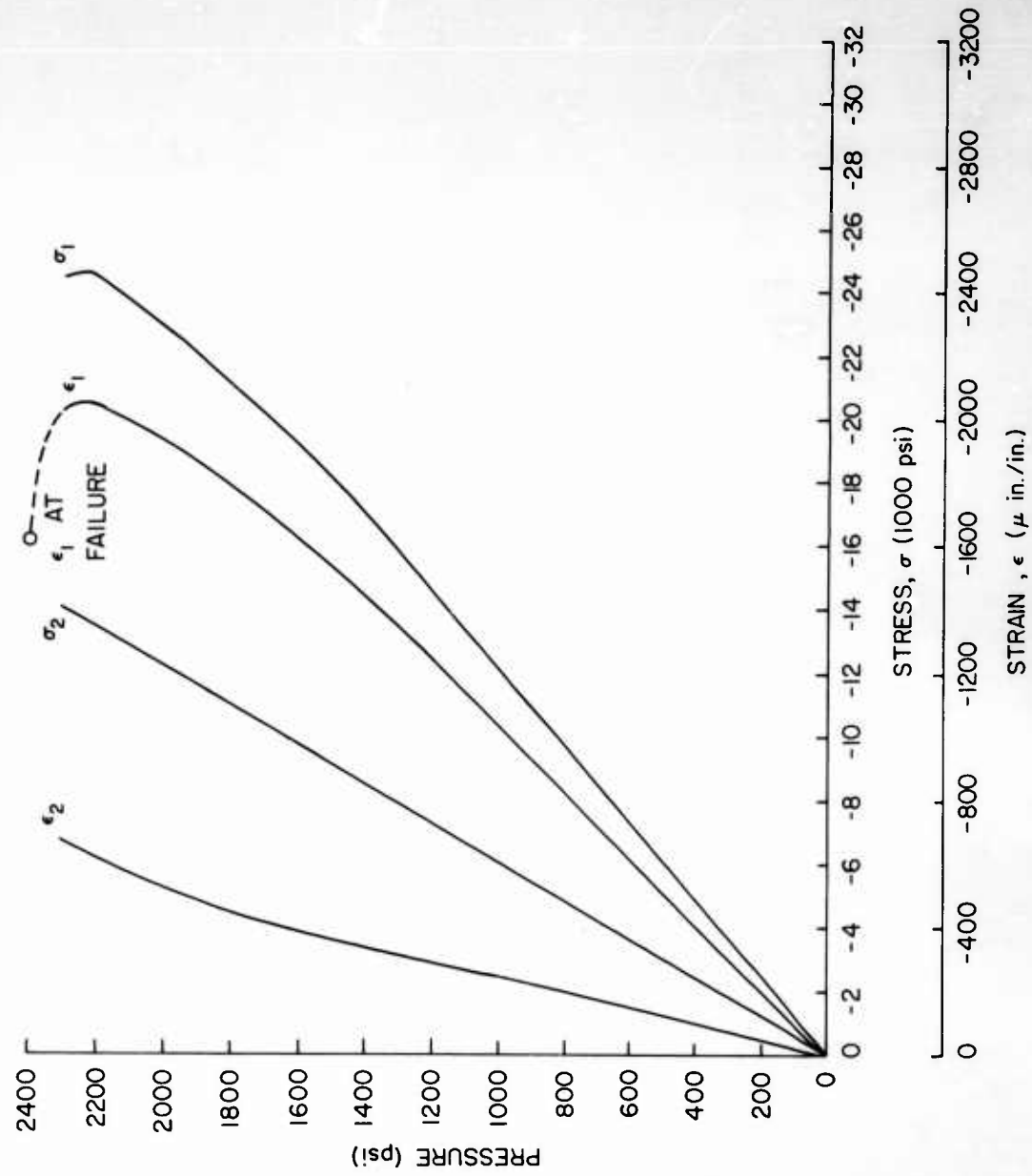


Fig. 54 - Strains and Stresses at Gages 1 and 2 of Model L<sub>1</sub>

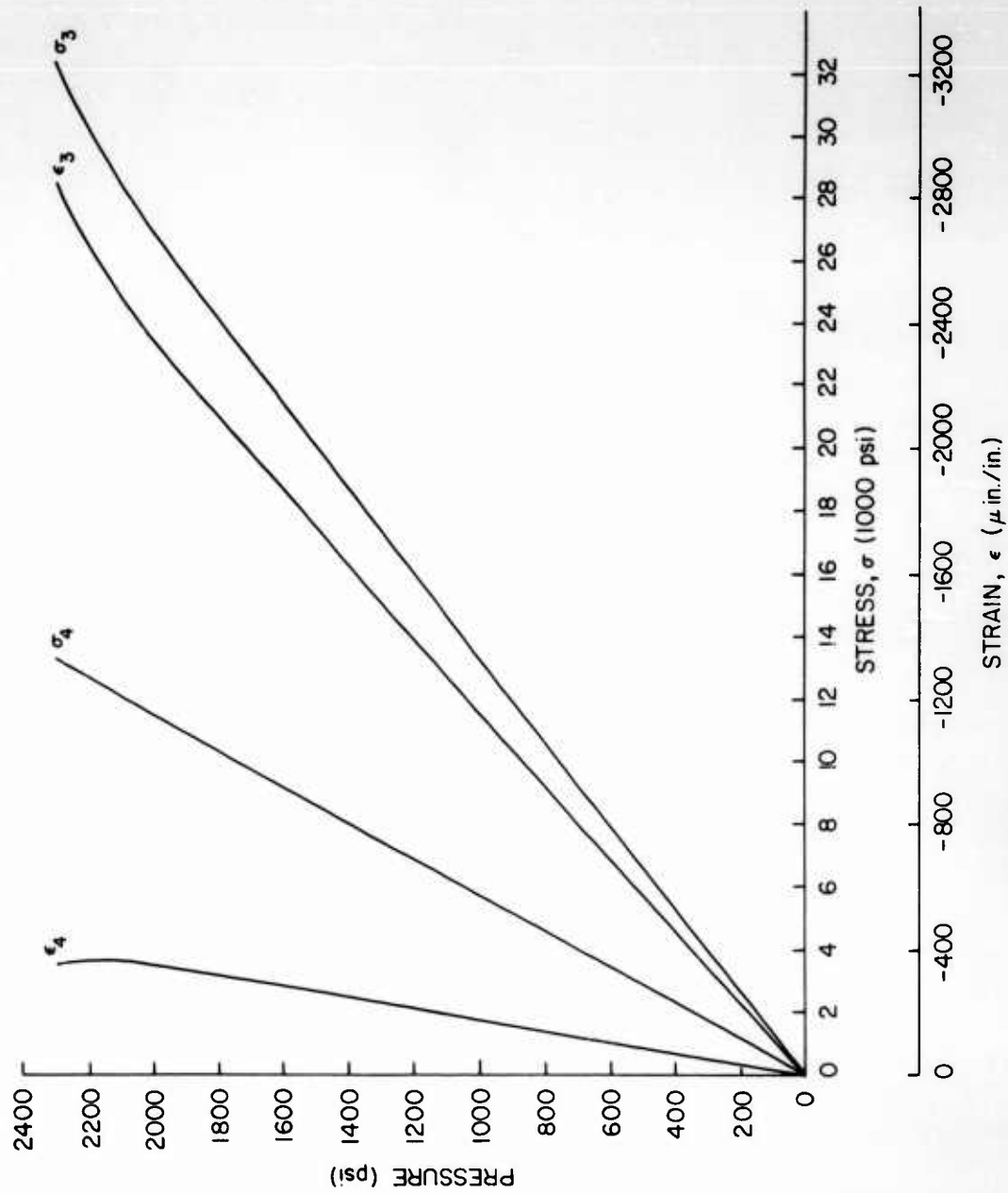


Fig. 55 - Strains and Stresses at Gages 3 and 4 of Model L1

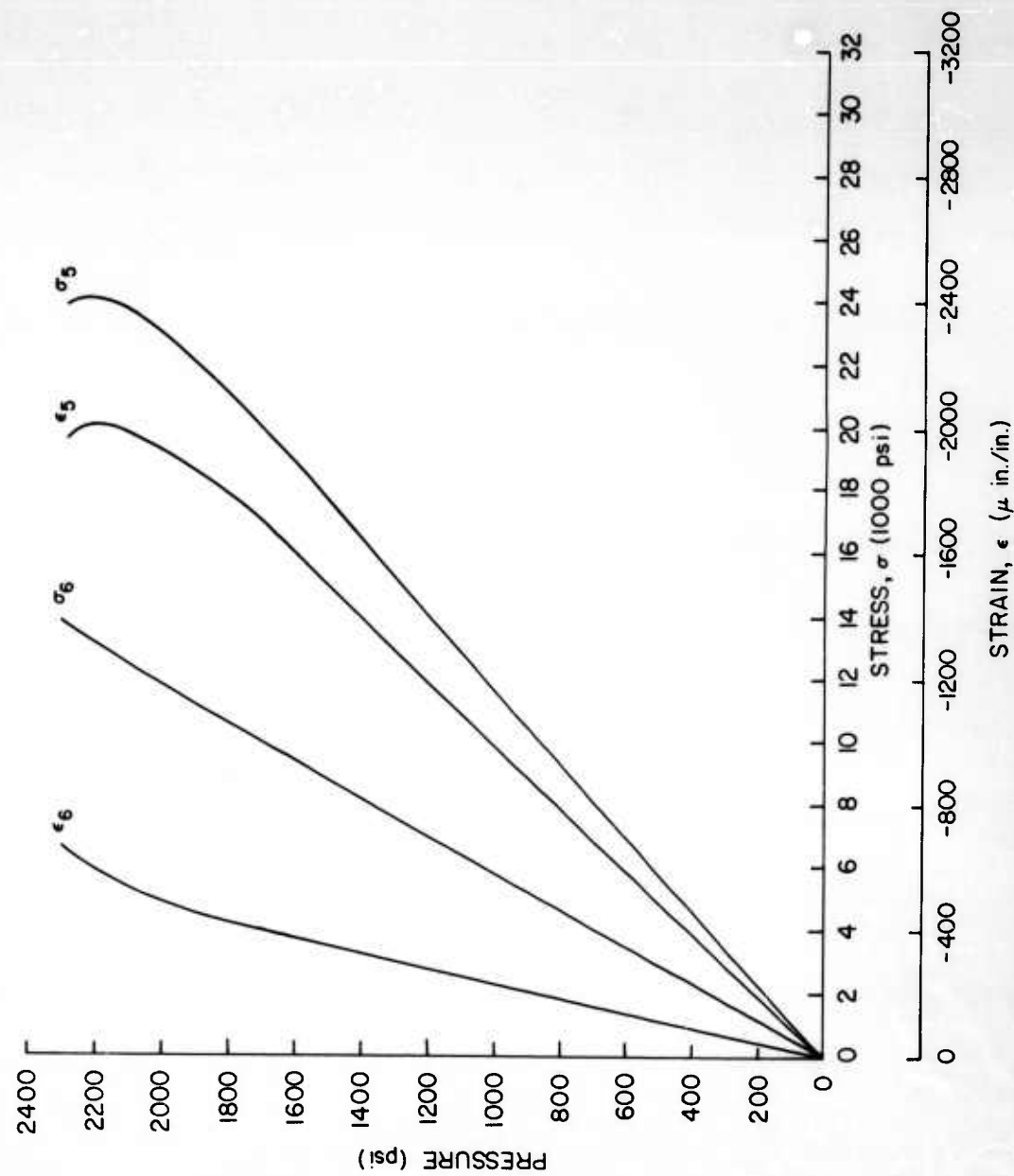


Fig. 56 - Strains and Stresses at Gages 5 and 6 of Model L<sub>1</sub>

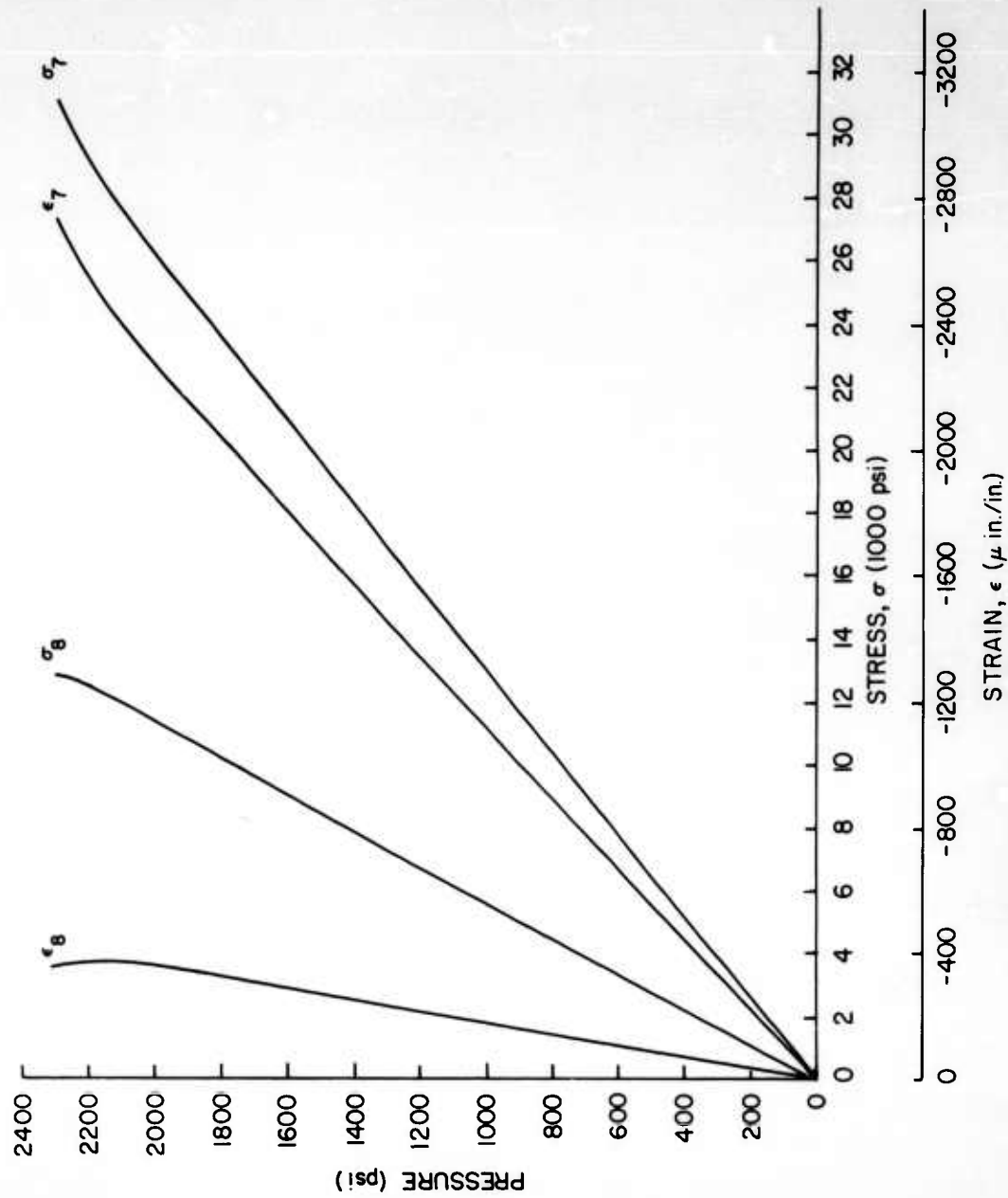


Fig. 57 - Strains and Stresses at Gages 7 and 8 of Model L<sub>1</sub>

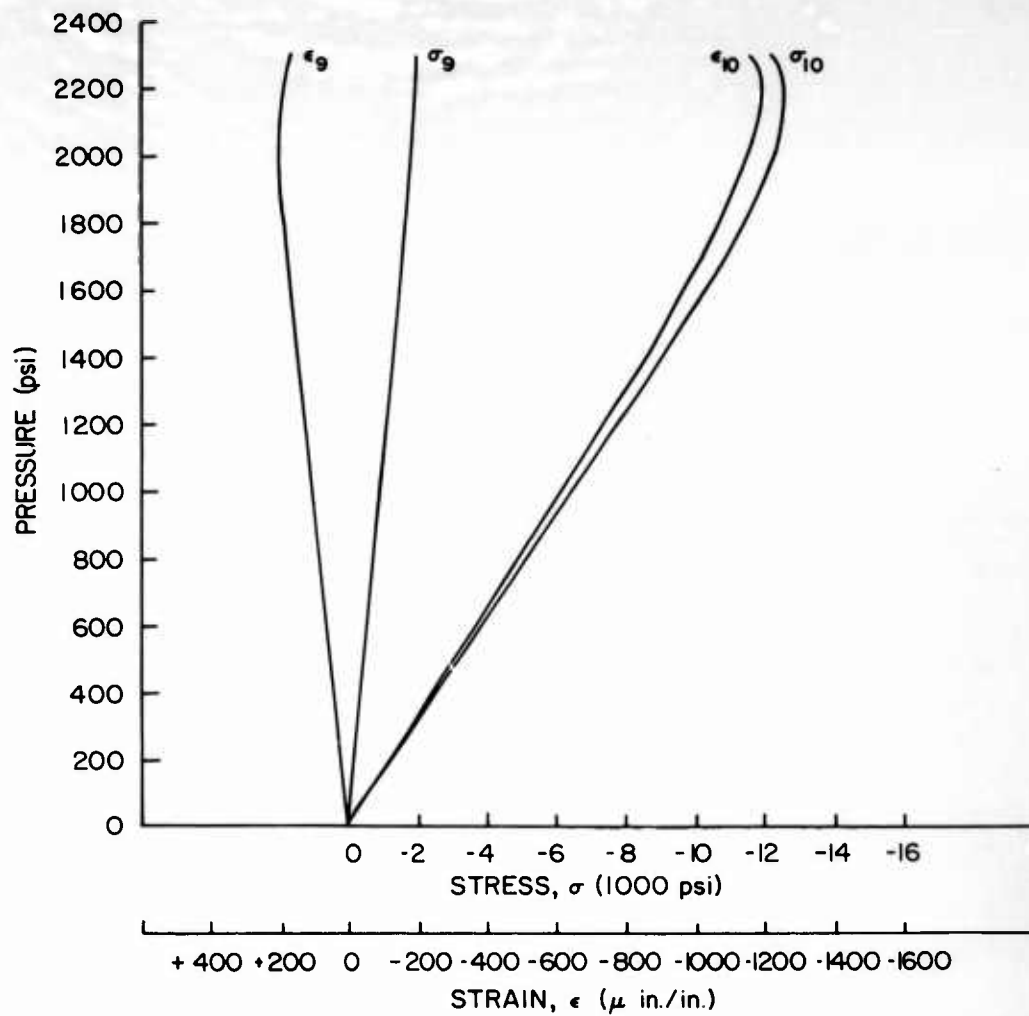


Fig. 58 - Strains and Stresses at Gages 9 and 10 of Model L<sub>1</sub>

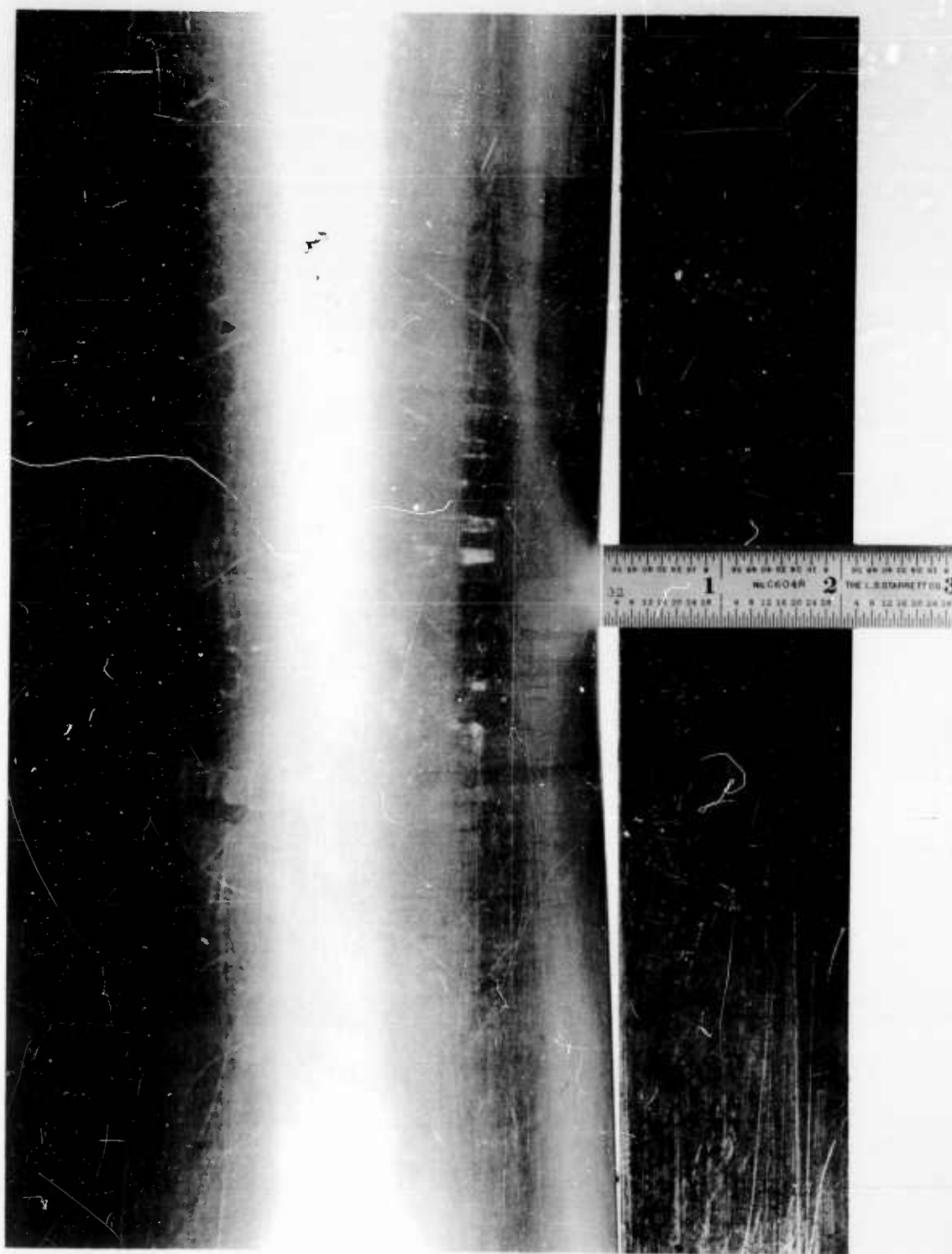


Fig. 59 - Permanent Deformation of Model L<sub>2</sub> Resulting from Shock Test

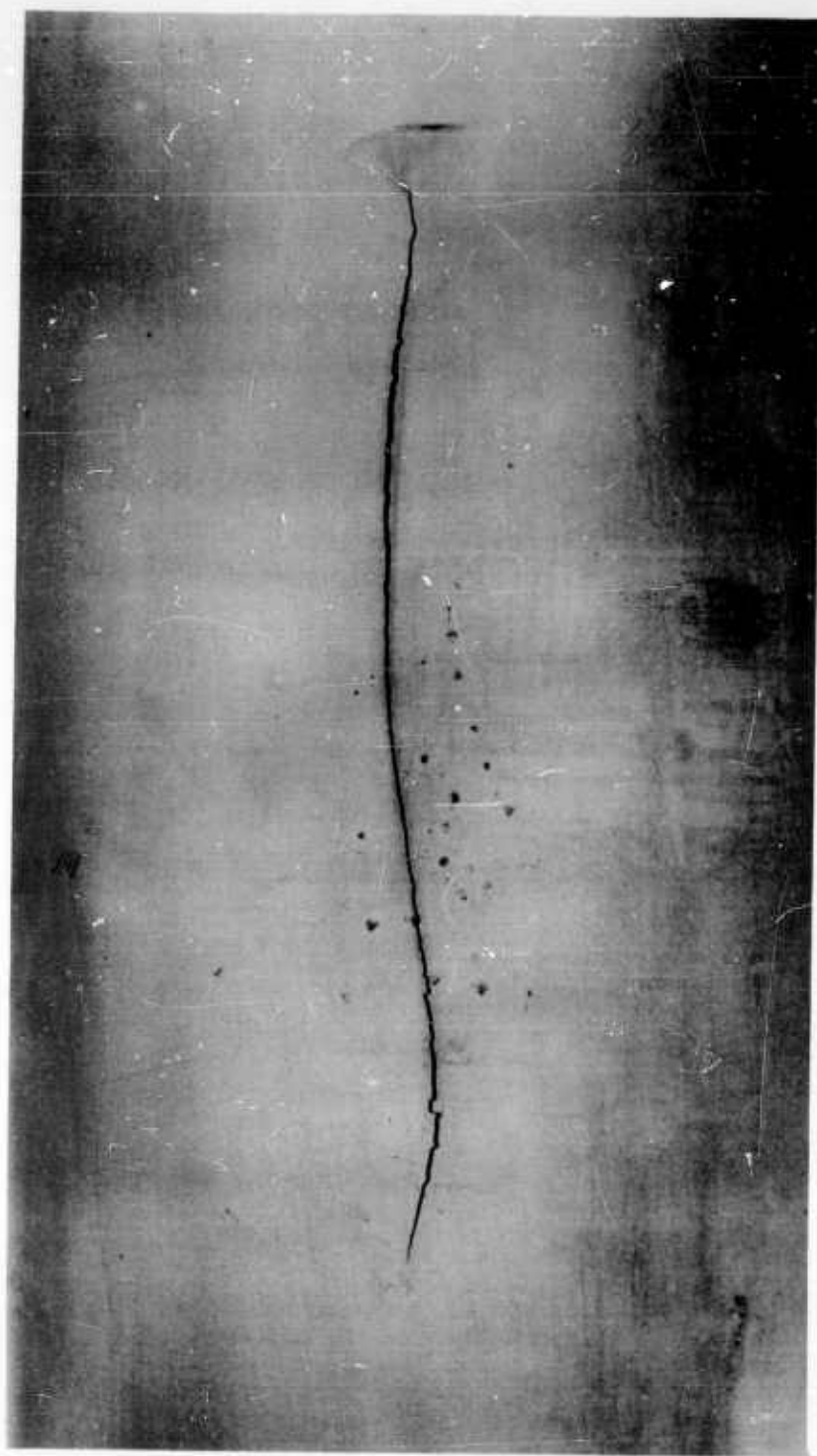


Fig. 60 - Failure of Model L<sub>2</sub> Resulting from Hydrostatic-Pressure Test



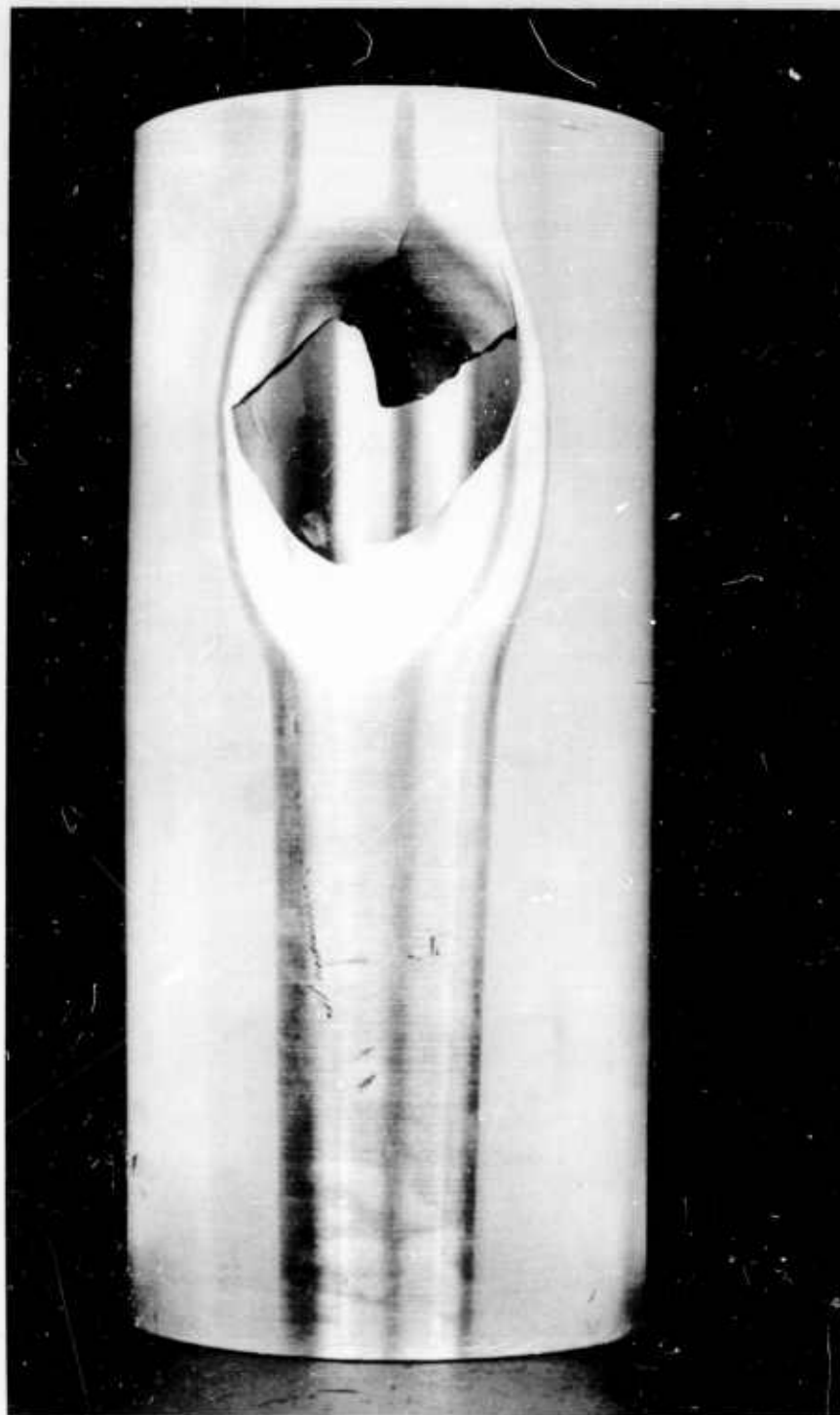


Fig. 61 - Failure of Model M<sub>1</sub> (Model Had Previously Been Severely Damaged by Shock Test)

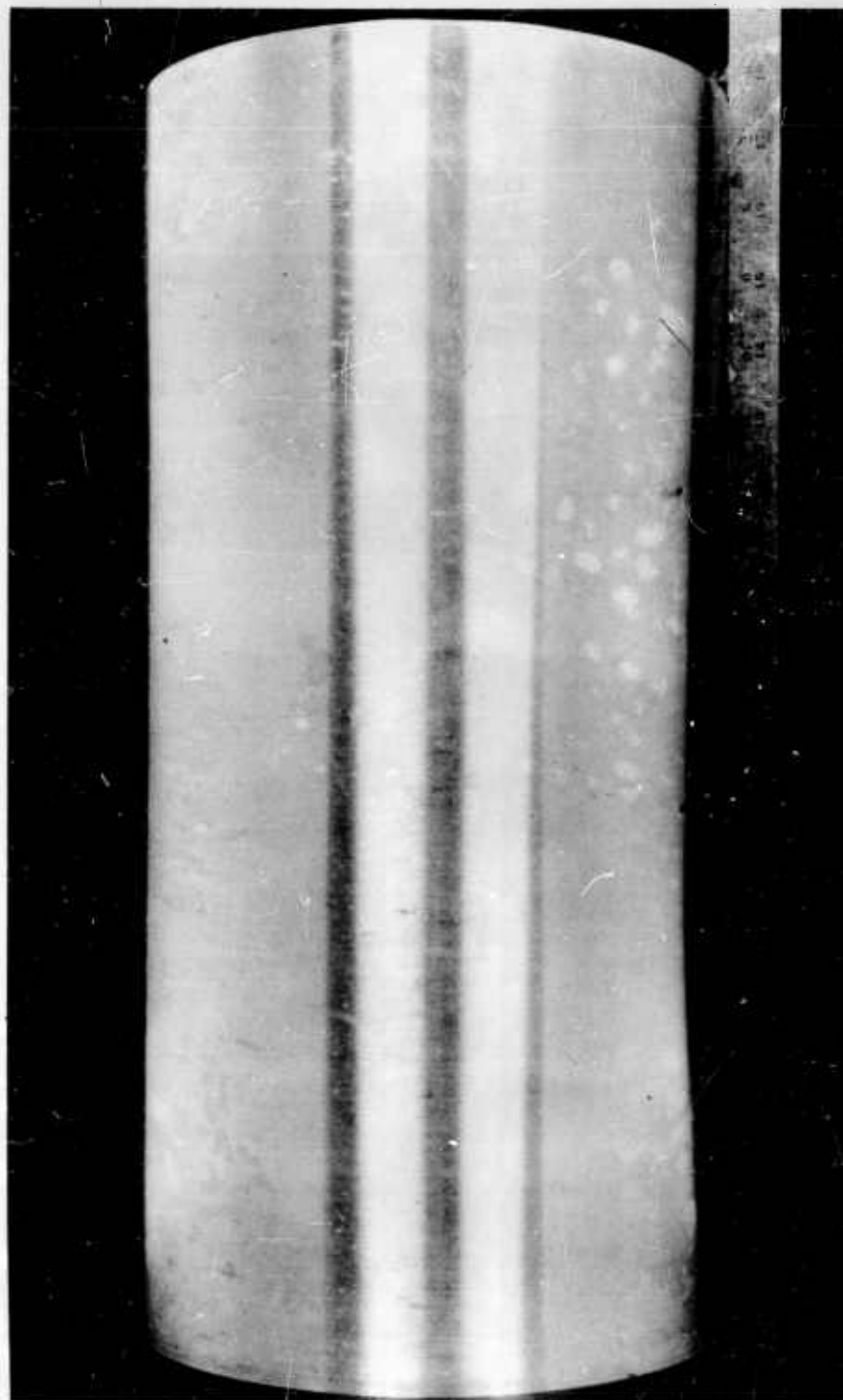


Fig. 62 - Permanent Deformation of Model M<sub>2</sub> Resulting from Shock Test

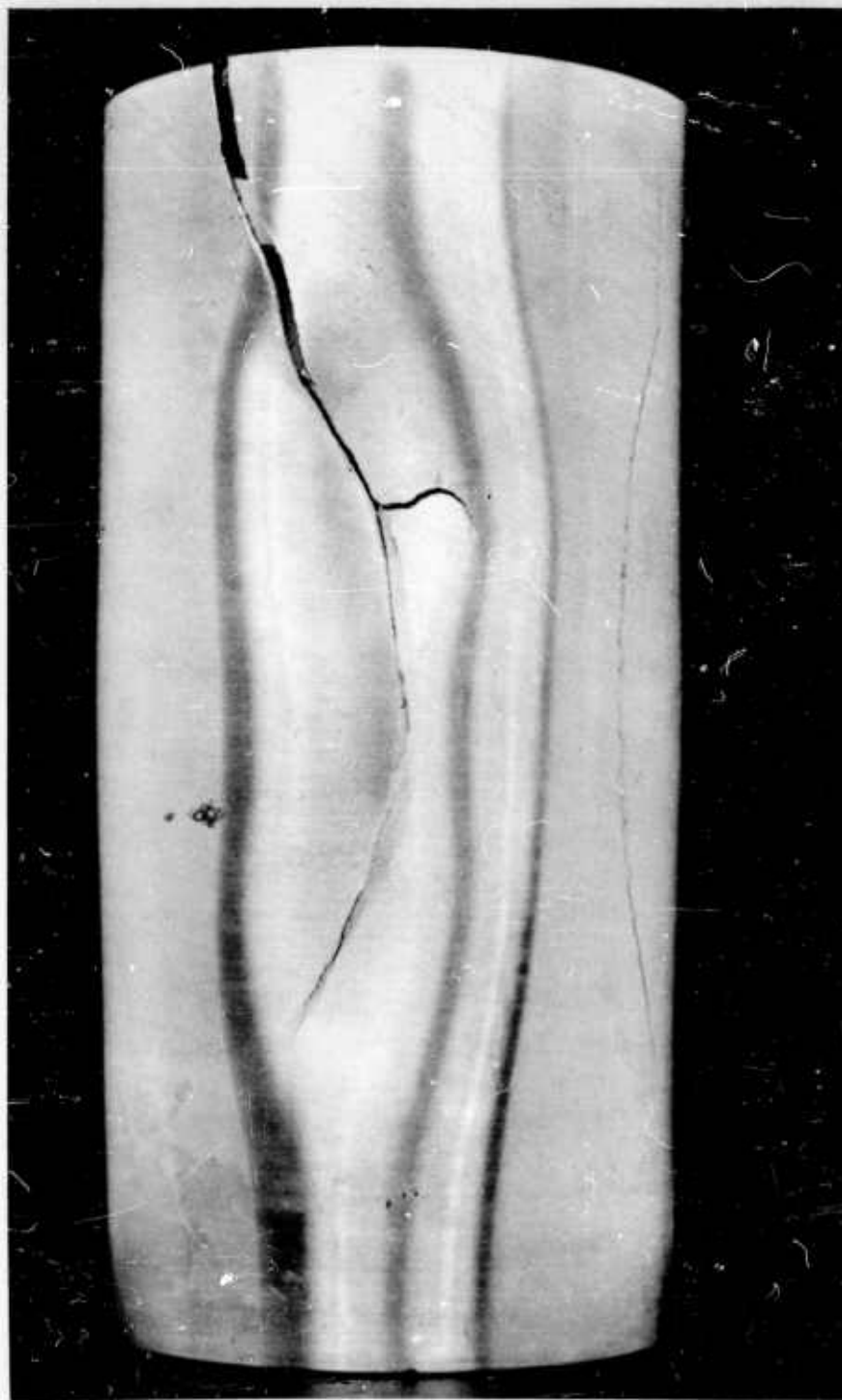


Fig. 63 - Failure of Model M<sub>2</sub> Resulting from Hydrostatic-Pressure Test

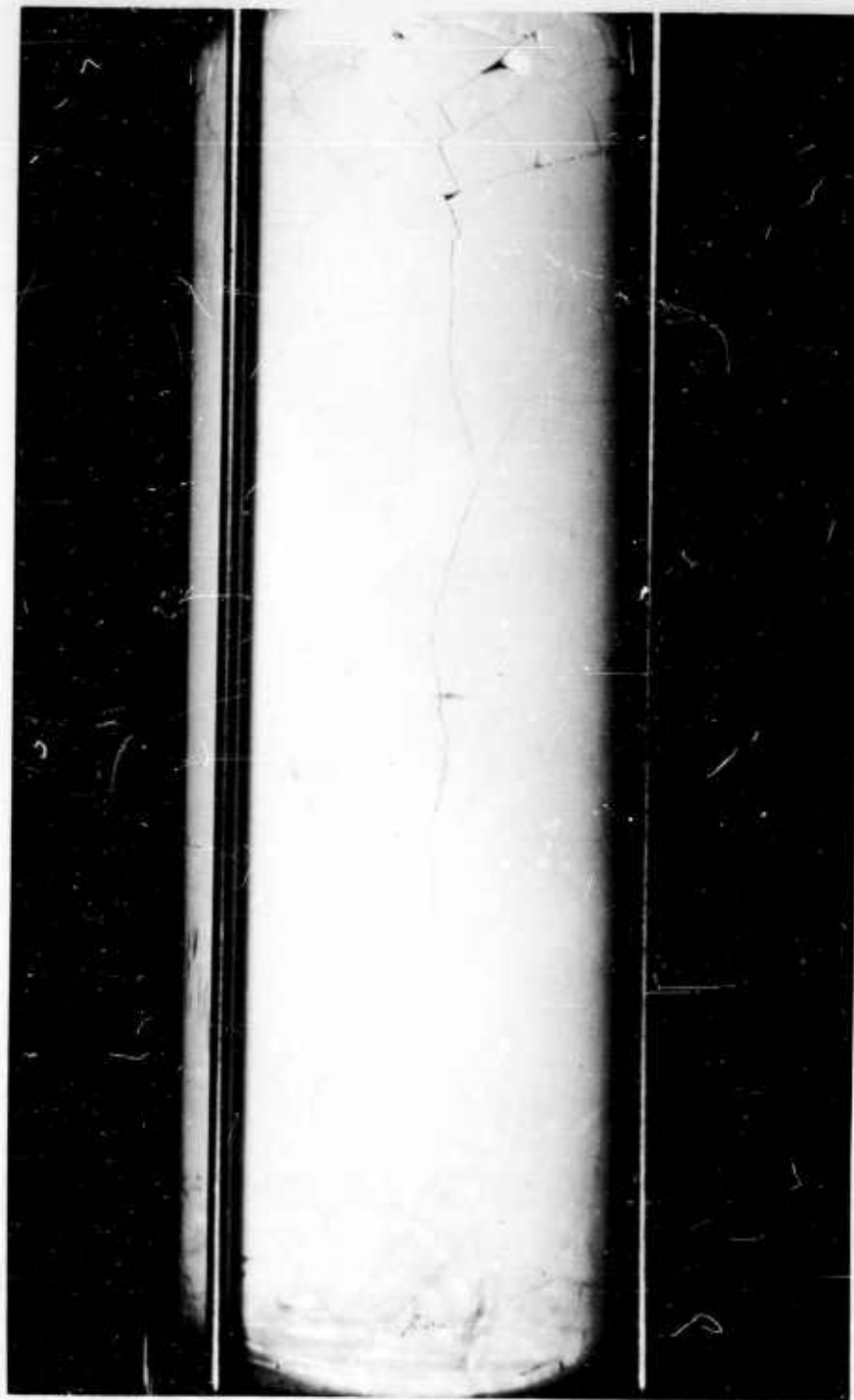


Fig. 64 - Failure of Model K<sub>3</sub> Two-Ribbed Alumina Ceramic Cylinder Resulting  
from Underwater Shock Test

<p>This card is UNCLASSIFIED</p> <p>Ordinance Research Laboratory Report No. NOW 63-0209-c-2 The Pennsylvania State University, University Park, Pa.</p> <p>SOLID GLASS AND CERAMIC EXTERNAL-PRESSURE VESSELS</p> <p>This report is UNCLASSIFIED</p> <p>J. D. Stachiw</p> <p>January 15, 1964; 11 pp. &amp; figs.</p> <p>Solid glass or ceramic hulls provide the maximum buoyancy and internal useful volume for underwater vehicles. This material displays low creep characteristics and withstands external pressure cycling and mild underwater dynamic pressures. Scratches on the exterior surfaces do not decrease appreciably the compressive and elastic strength of such vessels when exposed to either static or cycling pressure. Connectors have been devised that enable glass cylinders to be joined into a monolithic structure that is resistant to both pressure and flexure.</p>	<p>This card is UNCLASSIFIED</p> <p>Ordinance Research Laboratory Report No. NOW 63-0209-c-2 The Pennsylvania State University, University Park, Pa.</p> <p>SOLID GLASS AND CERAMIC EXTERNAL-PRESSURE VESSELS</p> <p>This report is UNCLASSIFIED</p> <p>J. D. Stachiw</p> <p>January 15, 1964; 11 pp. &amp; figs.</p> <p>Solid glass or ceramic hulls provide the maximum buoyancy and internal useful volume for underwater vehicles. This material displays low creep characteristics and withstands external pressure cycling and mild underwater dynamic pressures. Scratches on the exterior surfaces do not decrease appreciably the compressive and elastic strength of such vessels when exposed to either static or cycling pressure. Connectors have been devised that enable glass cylinders to be joined into a monolithic structure that is resistant to both pressure and flexure.</p>
<p>This card is UNCLASSIFIED</p> <p>Ordinance Research Laboratory Report No. NOW 63-0209-c-2 The Pennsylvania State University, University Park, Pa.</p> <p>SOLID GLASS AND CERAMIC EXTERNAL-PRESSURE VESSELS</p> <p>This report is UNCLASSIFIED</p> <p>J. D. Stachiw</p> <p>January 15, 1964; 11 pp. &amp; figs.</p> <p>Solid glass or ceramic hulls provide the maximum buoyancy and internal useful volume for underwater vehicles. This material displays low creep characteristics and withstands external pressure cycling and mild underwater dynamic pressures. Scratches on the exterior surfaces do not decrease appreciably the compressive and elastic strength of such vessels when exposed to either static or cycling pressure. Connectors have been devised that enable glass cylinders to be joined into a monolithic structure that is resistant to both pressure and flexure.</p>	<p>This card is UNCLASSIFIED</p> <p>Ordinance Research Laboratory Report No. NOW 63-0209-c-2 The Pennsylvania State University, University Park, Pa.</p> <p>SOLID GLASS AND CERAMIC EXTERNAL-PRESSURE VESSELS</p> <p>This report is UNCLASSIFIED</p> <p>J. D. Stachiw</p> <p>January 15, 1964; 11 pp. &amp; figs.</p> <p>Solid glass or ceramic hulls provide the maximum buoyancy and internal useful volume for underwater vehicles. This material displays low creep characteristics and withstands external pressure cycling and mild underwater dynamic pressures. Scratches on the exterior surfaces do not decrease appreciably the compressive and elastic strength of such vessels when exposed to either static or cycling pressure. Connectors have been devised that enable glass cylinders to be joined into a monolithic structure that is resistant to both pressure and flexure.</p>

**UNCLASSIFIED**

**UNCLASSIFIED**